

**Effect of heat input on the mechanical properties of butt-  
welded steel joints**

Tensile and hardness test



Bachelor's thesis

Visamäki, Construction Engineering

Autumn, 2018

Vu Pham Nguyen

Degree Programme in Construction Engineering  
Campus Visamäki

---

<b>Author</b>	Vu Pham Nguyen	<b>Year</b> 2018
<b>Title</b>	Effect of heat input on the mechanical properties of butt-welded steel joints	
<b>Supervisor(s)</b>	Ari Saastamoinen	

---

ABSTRACT

The purpose of this Bachelor thesis was to study the effects of heat input on the mechanical properties of butt welded steel joints. The effects of heat during the cooling period on the microstructure of the steel have not been extensively researched. The aim of this research was to provide information that can be used as a resource for further research and also to give recommendations on how to optimize and preserve the strength of steel during butt welding.

Four steel types were chosen (S420, S500, S700 and S960). They were welded with varied heat input and different numbers of weld runs. The temperature and cooling time of the HAZ (Heat affected zone) were recorded through an infrared camera. A reference model was made with thermocouple and infrared camera to accurately calculate the cooling time of each specimen. After the correlation between the temperature recorded through infrared camera and thermocouple was established, the steel plates were welded. Tensile and hardness tests were conducted on the welded specimens.

The results showed the effects of heat input and cooling time on the mechanical properties of the welded joints. Different heat input has a direct correlation on the reduction of the strength of the HAZ. It also showed that improper welding technique can affect the strength of the specimens. The research gives a recommendation on how the setting up of the future researches should be done and identifies the areas that need further study.

**Keywords** Weld, heat input, HAZ (Heat affected zone)

**Pages** 54 pages + appendices 26 pages

# CONTENTS

1	INTRODUCTION .....	1
1.1	Background.....	1
1.2	Theoretical input.....	2
2	OBJECTIVE.....	3
3	TESTING .....	4
3.1	Test preparation and test specimens.....	4
3.2	Welding process and heat input recording.....	5
3.3	Heat input measurements and analysis.....	6
3.4	Cooling time measurements .....	7
3.5	Tensile test .....	13
3.6	Hardness test.....	16
4	RESULTS AND ANALYSIS .....	19
4.1	S420 series analysis .....	20
4.1.1	S420 specimens tensile test results.....	20
4.1.2	S420 specimens hardness test results.....	22
4.2	S500 series analysis .....	27
4.2.1	S500 specimens tensile test results.....	27
4.2.2	S500 specimens hardness test results.....	29
4.3	S700 series analysis .....	33
4.3.1	S700 specimens tensile test results.....	33
4.3.2	S700 specimens hardness test results.....	36
4.4	S960 series analysis .....	41
4.4.1	S960 specimens tensile test results.....	41
4.4.2	S960 specimens hardness test results.....	43
4.5	Comparing all steel types and analysis .....	47
5	CONCLUSION .....	52
	REFERENCES.....	53

## Appendices

Appendix 1 COOLING TIME GRAPHS FROM INFRARED CAMERA

Appendix 2 TENSILE TEST GRAPHS

Appendix 3 FAILURE MODE PHOTOGRAPHS

# 1 INTRODUCTION

Structural steel has been widely used for decades in various construction projects. The knowledge of the mechanical properties of steel allows for manipulation of the strength and toughness for various applications through a thermomechanical controlled process and optimization of chemical compositions. However, there are still some uncertainties about the properties of the material, especially in the behaviour of high strength steel (HSS) products. Due to being relatively new in the industry, high strength steel is not sufficiently researched and covered in standards or building codes. The concern becomes apparent regarding welding. The intensive heating and uneven cooling time of the process change the microstructure of the material, making it more susceptible to cracking and lowering the strength of the material. The aim of this study is to determine the effects of heat input and cooling time on the mechanical properties (tensile strength of the welded joint, hardness and impact) of various steel grades.

## 1.1 Background

During the welding process, the surfaces of the components are raised locally to the melting point by a source of heat by a variety of welding methods based on an electric arc, electrical resistance or a flame. (Croft 2016, 1.) The amount of heat during welding is called the heat input which is the ratio of the total energy expended per unit length of the weld. The heat from the welding process and subsequent re-cooling change the microstructure and thus, the physical properties of the area close to the weld. This area is called the heat affected zone (HAZ). The welded joint then becomes homogenous, consisting of the parent material, the welded joint and the heat affected zone (HAZ). The change of physical properties, which depends largely on heat input and cooling time affects directly the performance of the joint. High heat input leads to a longer cooling time, thus increasing the size of the HAZ and prolonging the decline of the joint quality. However, too rapid cooling time from inadequate heat input also results in defective or weak joints because of the insufficient penetration and incomplete material fusion. Consequently, it is important to regulate closely the heat input and the cooling time during welding to achieve the best quality of the joint.

## 1.2 Theoretical input

The heat input cannot be measured directly, but it can be calculated using formula (1) (EN 1011-2/2001, 44.)

$$Q = \epsilon * \frac{U * I * 60}{V * 1000} \quad (1)$$

Where  $U$  is voltage [V],  $I$  is current [A] and  $V$  is the welding speed [mm/min]. These values are measured through the welding machine. The coefficient  $\epsilon$  is the thermal efficiency of welding procedure, taken as 0.85 for MAG welding, as specified in EN 1011-2. Using the formula, the heat input can be controlled through changing the voltage, the current and the welding speed.

Another crucial aspect of managing the joint strength is the cooling time. After reaching the desired temperature for the weld, the steel is left to cool down. The crystal structure of the steel alloy experiences changes. From 912 to 1,394 °C, the iron in steel undergoes a phase transition into Austenite steel that dissolves a considerable amount of carbon. As the temperature drops, depending on the carbon content, the alloy can ideally form Pearlite, a layering of carbon rich cementite and carbon poor ferrite is formed. Pearlite is one of the strongest bulk materials on Earth (Raabe, Choi, Li, Kostka, Sauvage, Lecouturier, Hono, Kirchheim, Pippin & Embury. 2010, 982.) However, if the cooling time is not sufficient enough for the carbon to diffuse, the trapped carbon will combine with iron and form martensite, which cracks at a lower strain (Ashby & Hunkin-Jones 2005, 89.) As the result, the rate of cooling determines the percentage of different crystal structures of the alloy, and therefore determines the mechanical properties of the resulting steel, such as hardness and tensile strength. Figure 1 below shows the Iron-carbon phase diagram in different temperature.

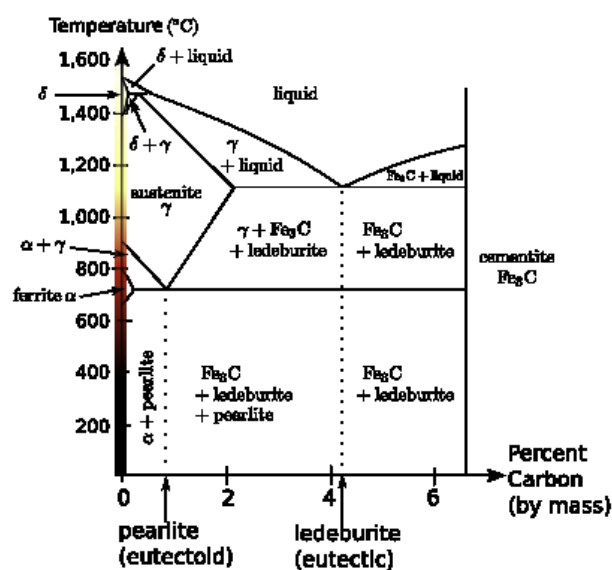


Figure 1. Iron-carbon phase diagram

The most important period is the cooling time from 800°C to 500 °C ( $t_{8/5}$ ) because the critical change occurs in the microstructure of the steel. This time period can be calculated by these formulas; (2) for two-dimensional cooling time and formula (3) for three dimensional cooling time given in equations (2) and (3) (EN 1011-2/2001, 43.)

$$t_{8/5} = (4300 - 4.3 * T_0) * 10^5 * \left(\frac{Q^2}{d^2}\right) * \left[\left(\frac{1}{500 - T_0}\right)^2 - \left(\frac{1}{800 - T_0}\right)^2\right] * F_2 \quad (2)$$

$$t_{8/5} = (6700 - 5 * T_0) * Q * \left[\left(\frac{1}{500 - T_0}\right) - \left(\frac{1}{800 - T_0}\right)\right] * F_3 \quad (3)$$

Where  $T_0$  is working temperature [°C],  $Q$  is heat input [kJ/mm], and  $d$  is thickness of the samples [mm]. Shape factors  $F_2$  and  $F_3$  are taken as 0.9 from EN 1011-2, Table D.1 which is shown below in Figure 2.

**Table D.1 — Influence of the form of weld on the cooling time,  $t_{8/5}$**





Form of weld		Shape factor	
		$F_2$ two-dimensional heat flow	$F_3$ three-dimensional heat flow
Run on plate		1	1
Between runs in butt welds		0,9	0,9
Single run fillet weld on a corner-joint		0,9 to 0,67	0,67
Single run fillet weld on a T-joint		0,45 to 0,67	0,67

Figure 2. Shape factor of the weld form

Calculations were done by both formulas and the longer time was chosen. With both the heat input and cooling time calculated, the tensile tests were then set up to confirm the predictions.

## 2 OBJECTIVE

The aim of this research is to find out the relation between the heat input/cooling time and the tensile strength, hardness of the weld specimens. The tests are carried out between several steel grades to achieve a thorough comparison of the effect input has on different steel grades. The purpose of the tests is to gain data about how much the strength of the specimens

is lost after different welding speeds. Based on the information, suitable welding parameters which would minimize the change in the steel properties can be found. Altogether, this research aims to provide valuable information which could be used to optimize the welds in high strength steels.

### 3 TESTING

To understand the effect of heat input on the joints, samples of steel are welded with different heat input (different run numbers), during which the temperature of different areas are recorded. Tests (tensile, hardness and impact) are then carried out to determine the strength of the specimens. Data is then gathered to create graphs that show the capacity of each steel grade versus different weld run times.

#### 3.1 Test preparation and test specimens

Specimens with different steel grades (S420, S500, S700 and S960) being used in this research are chosen from SSAB catalogue, manufactured from thermomechanical hot-rolled steel. The tensile and hardness tests needs 3 specimens for each weld run. In total for 4 steel grades and 3 types of weld run (1 weld run, 2 weld runs and 3 weld runs), there are 48 steel specimens that need to be prepared. For each number of weld run, 2 steel plates with the dimensions of 200x200x8mm are welded together. The end of each plate is cut at an angle of 60° where they will be welded. Instead of plasma cutting which will result in the loss of strength at the weld joint, water cutting is used to cut the end of the plates. The plates and their dimensions are shown in Figure 3.

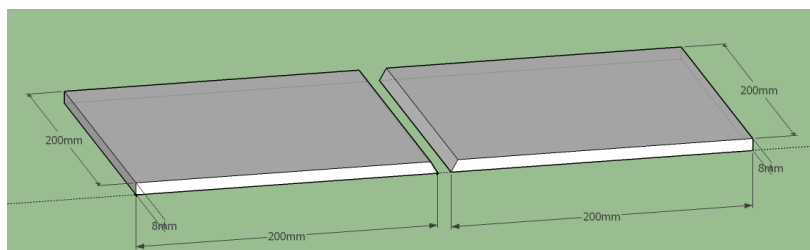


Figure 3. Two steel plates with the dimensions of 200x200x8 mm

The steel plates are welded using a MAG machine, the weld type is Butt weld "V" with the gap of approximate 2mm between the plates. The filler material is 1.2mm ESAB x69 grade wire chosen according to the classification (EN ISO 16834-A/2012, 10.) During the welding process, the plates are heated to the peak temperature, then they are left to cool down. The heat input is recorded by the welding machine. The cooling time  $t_{8/5}$  from 800 °C to 500 °C is recorded through infrared camera.

The thermocouple records the inner temperature and the infrared camera records the surface temperature. A mathematical correlation can then be made between the surface and inner temperature after welding. Subsequent welding session uses only the infrared camera because from the surface temperature, the inner temperature can be accurately calculated. Figure 4 below shows the infrared camera used to measure the surface temperature and cooling time.



Figure 4. The infrared camera used to measure the surface temperature and cooling time

### 3.2 Welding process and heat input recording

Each steel grade will have three weld series as the plates are welded using one, two and three weld runs. The welding temperature is controlled. While welding with one weld run, high heat input is used to completely melt the filler material and to allow the full penetration of the steel and the filler material in the groove. On the other hand, welding with two or three runs requires less heat because the first run has already melted the root of the steel plates. The next one or two runs are used to fill the groove, allowing less cooling time as opposed to a single run welding.

The welding processes took place in Tavastia Vocational School, Hämeenlinna by a professional welder Mr. Harri Nieminen to ensure the quality of the weld. The welding procedures followed Kemppi's WPS (welding procedure specification) 135-BW-5 welding instructions



according to standards EN ISO 15609-1/2004 and EN ISO 15612/2004. These instructions apply for steel grades S235, S275 and S355. However, using these instructions to weld HSS S700, it was possible to achieve low cooling times. (Greiçevci, 2016.) After the welding, the steel plates were left to cool down, the heat input for each weld run was recorded by the welding machine. Figure 5 shows the picture of S700 steel plates after two weld runs.

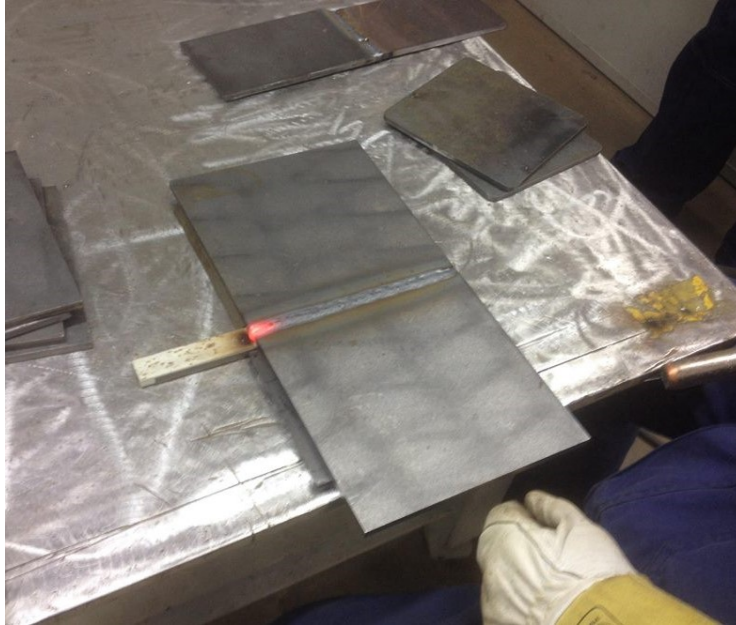


Figure 5. S700 Steel plates after two weld runs

### 3.3 Heat input measurements and analysis

There are three different weld types for each steel grade. The samples made with one weld run have the highest heat input, while the ones with two weld runs have less heat input. The heat input of the samples with three weld runs is the lowest. The welding speed is also one of the factors to determine the level of penetration of the materials, thus the strength of the joints. Data were gathered from the welding machine after each welding session, putting the emphasis on the heat input and welding speed for each run.

Table 1-4 list the heat input of each steel grade.

Table 1. S700 heat input

Sample name <sup>1)</sup>	weld length (mm)	First run		Second run		Third run	
		Welding speed (mm/s)	Heat input (kJ/mm)	Welding speed (mm/s)	Heat input (kJ/mm)	Welding speed (mm/s)	Heat input (kJ/mm)
S700-1R	200	1.87	1.37	-			
S700-2R	200	2.53	0.71	2.85	0.87	-	
S700-3R	200	2.081	0.82	4.347	0.49	4.34	0.51

<sup>1)</sup> Sample name: [Steel grade]-[Number of weld run(R)]

Table 2. S960 heat input

Sample name <sup>1)</sup>	weld length <sup>1)</sup> (mm)	First run		Second run		Third run	
		Welding speed (mm/s)	Heat input (kJ/mm)	Welding speed (mm/s)	Heat input (kJ/mm)	Welding speed (mm/s)	Heat input (kJ/mm)
S960-1R	200	1.9	1.48	-			
S960-2R	200	2.35	0.56	2.71	0.86	-	
S960-3R	200	2.9	0.5	4.84	0.46	4.535	0.52

<sup>1)</sup> Sample name: [Steel grade]-[Number of weld run(R)]

Table 3. S500 heat input

Sample name <sup>1)</sup>	weld length (mm)	First run		Second run		Third run	
		Welding speed (mm/s)	Heat input (kJ/mm)	Welding speed (mm/s)	Heat input (kJ/mm)	Welding speed (mm/s)	Heat input (kJ/mm)
S500-1R	200	1.82	1.47	-			
S500-2R	200	2.82	0.44	2.34	1	-	
S500-3R	200	3.15	0.43	4.048	0.52	4.82	0.49

<sup>1)</sup> Sample name: [Steel grade]-[Number of weld run(R)]

Table 4. S420 heat input

Sample name <sup>1)</sup>	weld length (mm)	First run		Second run		Third run	
		Welding speed (mm/s)	Heat input (kJ/mm)	Welding speed (mm/s)	Heat input (kJ/mm)	Welding speed (mm/s)	Heat input (kJ/mm)
S420-1R	200	2.125	1.48	-			
S420-2R	200	2.628	0.53	2.635	0.82	-	
S420-3R	200	2.789	0.47	4.75	0.46	4.6	0.51

<sup>1)</sup> Sample name: [Steel grade]-[Number of weld run(R)]

### 3.4 Cooling time measurements

During each welding session, the cooling time from 800°C to 500°C was recorded using the FLIR A3 infrared camera. However, the temperatures recorded during the welding sessions were only surface temperatures. Thermocouples were used to accurately record the inner temperatures of the specimens. However, the drawback of using thermocouples was the time needed to drill holes and setting up the test specimens. Since there were 12 steel specimens that needed to be prepared, setting up the thermocouples for each session would take plenty of time.

In order to speed up the process, a model welding session in which both infrared camera and thermocouples were used to achieve the mathematical correlation between the surface temperatures and the inner temperatures. From this data, surface temperatures recorded by the infrared camera could be converted to inner temperatures. The cooling time  $t_{8/5}$  could then be safely calculated without having to use thermocouples in every welding session.

Reference steel plates with the dimension of 100x50x8mm were used. Holes with a diameter of 3mm and depth of 10mm were drilled into the plates. Thermocouples consisted of 2 metal wires serving as temperature sensors for inner temperatures of the specimens were then inserted to the holes. Figure 6 shows how the reference plates looked like before the welding sessions.



Figure 6. The reference plate used to measure surface and inner temperature during welding

The other ends of the sensors were connected to an HBM Data Logger that measured and recorded the temperatures. The data was analysed by Catman software. The setup is demonstrated by Figure 7 below.



Figure 7. Thermocouples connected to HBM Data Logger and analysed by Catman software.

The thermocouples were attached using tapes. Before the measurement session, the thermocouples were spot-welded onto the plates. The weld spots acted as protection against the extreme heat generated during the welding, ensuring the data recorded was accurate.

Below in Figure 8 is the diagram of the thermocouple positions during the welding session.

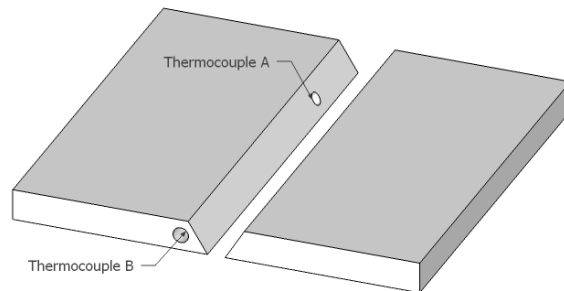


Figure 8. Thermocouples position during reference welding sessions.

An infrared camera was used to record the surface temperature. The measurement points in the infrared camera were set to be as close to the sensor positions as possible. However, during the first reference welding session, it became clear that the thermocouple B position did not fulfil the required accuracy (not reaching 800-500°C threshold or too big temperature fluctuation). A second test was carried out with only the thermocouple A attached to guarantee the results in the first reference test were correct. Figure 9 below shows the comparison of temperature recorded by thermocouples and infrared camera in both sessions. For easier identification,  $t_t$  stands for thermocouples temperature and  $t_i$  represents Infrared camera temperature.

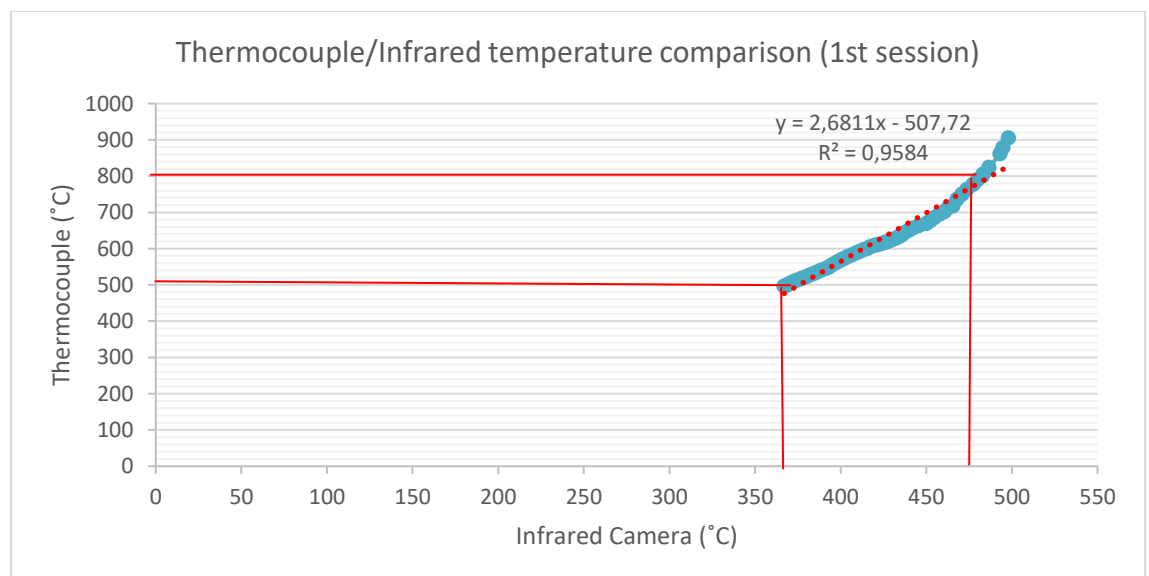


Figure 9. Comparison of temperature recorded using thermocouples and infrared camera in the 1<sup>st</sup> session

The graph shows that as the material cools down after reaching peak temperature, the ratio of  $t_t$  over  $t_i$  decreases linearly, especially during the  $t_{8/5}$  period.

The graph for second session can be seen in figure 10 below, showing a similar relationship between  $t_t$  and  $t_l$  during the cooling time  $t_{8/5}$ .

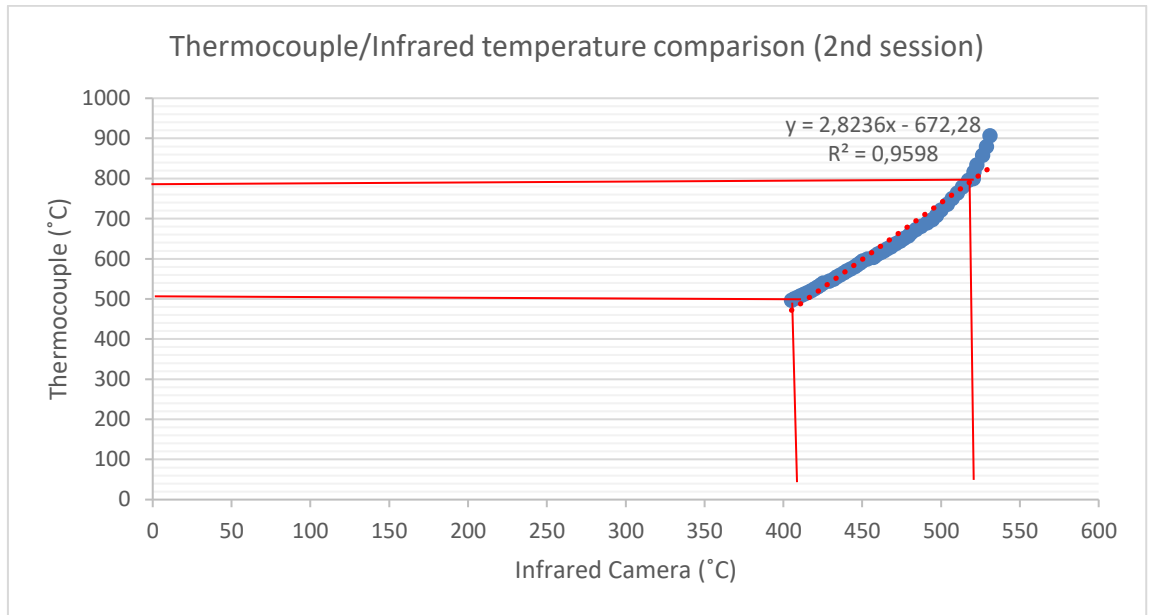


Figure 10. Comparison of temperature recorded using thermocouples and infrared camera in 2<sup>nd</sup> session

The two sessions showed that the  $t_t : t_l$  (thermocouple temperature over infrared temperature) ratio during the cooling down period could be calculated quite accurately using the formula  $y=ax+b$ , where  $y$  is the thermocouple temperature and  $x$  is the infrared camera temperature. The two session gave two different equations shown below:

$$y = 2.6811x - 507.72 \tag{4}$$

$$y = 2.8326x - 672.28 \tag{5}$$

The first session had the  $t_{8/5}$  equalled to 24.88 seconds, while the second session had the  $t_{8/5}$  of 22.08 seconds. The equations showed that differences during the welding sessions (welding speed, heat input, welding technique...) could affect the  $t_t : t_l$  ratio and the cooling time itself. A way to combine these results is to create a line of symmetry between these two lines. The line of symmetry can be seen as the average of the two trend lines in each session, having the formula:

$$y = 2.75x - 587 \tag{6}$$

In table 5 below is the conversion table of  $t_t : t_l$  during the 800°C to 500°C period

Table 5.  $t_t$  and  $t_l$  calculated from the new formula

	New formula	
$t_t$ (°C)	800	500
$t_l$ (°C)	504.36	395.27

To confirm if the formula can be used for the other sessions,  $t_i$  calculated using formula (6) and their corresponding time were checked in another session to see if the  $t_{8/5}$  are similar or not.

Tables 6 and 7 below show the record the time of the first and second session at 504.36 °C and 395.27°C.

Table 6. Time and relative time at 504.36 °C and 395.27°C in session 1

Time	Milliseconds	Relative time	Thermocouple A
12:00:40	983	22.3	504.7407532
12:00:41	0	22.317	504.4759216
12:00:41	16	22.333	504.3796082
12:00:41	33	22.35	504.2832947
12:00:41	50	22.367	503.9702148
0:00:00	566	44.883	395.4176025
0:00:00	583	44.9	395.3907471
0:00:00	600	44.917	395.2833252
0:00:00	616	44.933	395.0684204
0:00:00	633	44.95	394.960968

Table 7. Time and relative time at 504.36 °C and 395.27°C in session 2

Time	Milliseconds	Relative time	Thermocouple A
10.59.39	783	20.917	504.8370361
10.59.39	800	20.934	504.6925964
10.59.39	816	20.95	504.4036865
10.59.39	833	20.967	504.2592163
10.59.39	850	20.984	504.1147156
11.00.02	750	43.884	395.3907471
11.00.02	766	43.9	395.3907471
11.00.02	783	43.917	395.2295837
11.00.02	800	43.934	395.2027283
11.00.02	816	43.95	395.1490173

In the 1<sup>st</sup> session the total time is 22.584 seconds while the 2<sup>nd</sup> session is 22.967 seconds. The relative time between 504.36 °C and 395.27°C in two sessions is compared to their respective  $T_{8/5}$  in table 8 below to check for accuracy of the result.

Table 8. Comparison of relative time at 504.36 °C and 395.27°C in two sessions

	Session 1	Session 2
Time at 504.36°	22.333	20.95
Time at 395.27	44.917	43.917
Total	22.584	22.967
T8/5	24.88	22.08
Differences	-2.296	0.887

Because the results are very close, it is confirmed that formula (6) accurately represents formula (4) and (5). It can now be used to convert the infrared camera temperatures gathered during the specimen welding sessions to the inner temperatures needed for analysis.

It is recommended that the thermocouples and infrared camera be set up in a future test again and the thermocouple-to-infrared temperature ratio be recalculated because different test and set up can have different results and ratio. It is also recommended that more thermocouples should be installed along the edge of the weld to improve the accuracy of the temperature recorded, as the welding speed is not uniform. This could result in the cooling time at the start of the weld be different than the cooling time at the end of the weld. It is suggested that robot welding is used in this kind of research to achieve a uniform welding speed.

The welding sessions were then carried out using only an infrared camera as a temperature recorder because the results can be accurately converted to inner temperatures during the analysis phase. Table 9 below list the cooling time  $t_{8/5}$  of all steel specimens.

Table 9. Cooling time  $t_{8/5}$  of all steel specimens

Sample name <sup>1)</sup>	Average working temperature	First run		Average working temperature	Second run		Average working temperature	Third run	
	(°C)	$t_{8/5}$ calculated (s)	$t_{8/5}$ measured (s)	(°C)	$t_{8/5}$ calculated (s)	$t_{8/5}$ measured (s)	(°C)	$t_{8/5}$ calculated (s)	$t_{8/5}$ measured (s)
700-1R	21.30	30.15	20.70	-	-	-	-	-	-
700-2R	21.30	8.10	10.57	100.00	12.16	6.35	-	-	-
700-3R	21.30	10.80	5.28	100.00	3.86	8.65	100.00	4.18	4.43
S960-1R	21.30	35.19	33.47	-	-	-	-	-	-
S960-2R	21.30	5.04	7.61	100.00	11.88	12.27	-	-	-
S960-3R	21.30	4.02	5.03	100.00	3.40	11.40	100.00	4.34	5.07
S500-1R	21.30	34.72	32.60	-	-	-	-	-	-
S500-2R	21.30	3.11	7.48	100.00	16.07	8.50	-	-	-
S500-3R	21.30	2.97	2.98	100.00	4.34	10.18	100.00	3.86	3.48
S420-1R	21.30	35.19	36.12	-	-	-	-	-	-
S420-2R	21.30	4.51	4.67	100.00	10.80	9.95	-	-	-
S420-3R	21.30	3.55	4.20	100.00	3.40	8.82	100.00	4.18	4.17

<sup>1)</sup> Sample name: [Steel grade]-[Number of weld run(R)]

With the gathered heat input from the welding sessions, the cooling times were calculated using formula (2) and (3) (see page 3). The measured cooling time was converted from formula (7) (see page 10). It can be seen

that the measured cooling times  $t_{8/5}$  are close to the calculated  $t_{8/5}$ , confirming the accuracy of the conversion formula. The one-weld runs used the highest heat input, thus the longest cooling time. The two-weld runs operated with a medium heat input and had shorter cooling times. The three weld runs used the least heat input, hence the shortest cooling times in all four types of steels.

### 3.5 Tensile test

After the welding sessions, tensile tests were performed in order to determine the effect of heat on the strength of steel specimens. The welded samples were water cut into smaller test samples. This guarantees that they are not subjected to further heat treatments and preserve the strength of the materials. The test samples were designed and dimensioned according to SFS-EN ISO 4136. From the cut steel plates, hardness test samples were also prepared. The S700 series were the first specimens to be cut as seen in Figure 11 below.

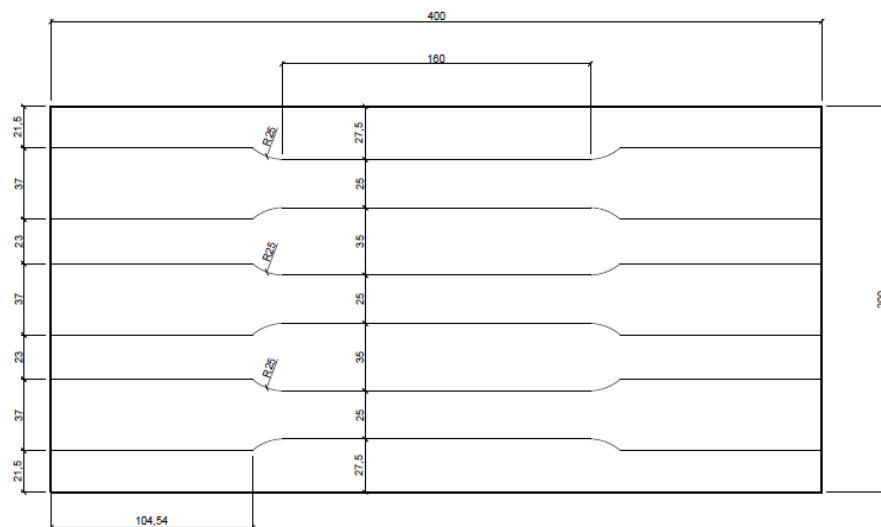


Figure 11. S700 steel series cutting plan for tensile test.

However, after the first tensile test of S700 series, the design length of S420, S500 and S960 specimens were shortened because the extensometer of the tensile machine has the length limit of 80mm.

The revised cutting plan of S420, S500 and S960 can be seen in Figure 12.



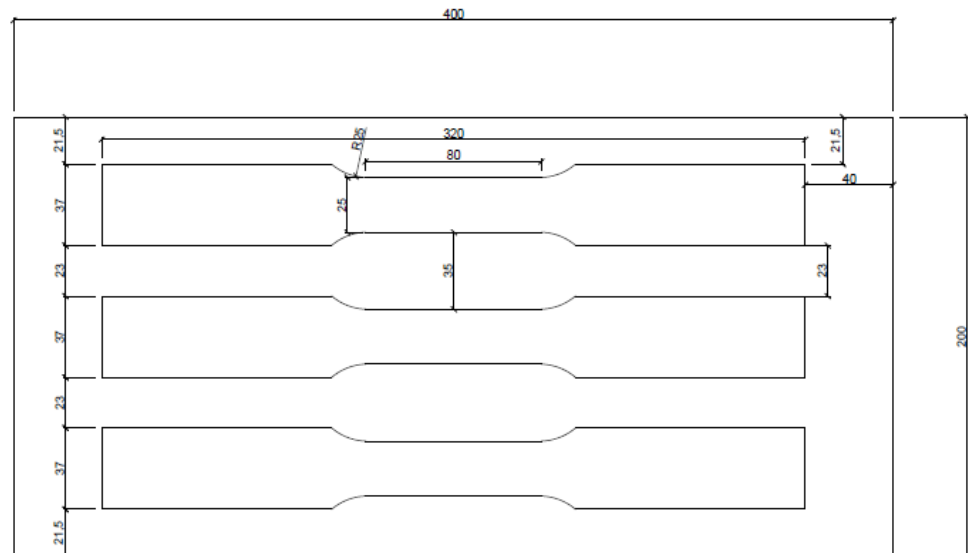


Figure 12. S420, S500 and S960 revised steel series cutting plan for tensile test.

After the specimens were cut, the tensile specimens were ground at the welded area to remove excess material. The grinding was done carefully so that the stresses during the testing would not concentrate on the imperfections of the weld surfaces and the heat produced would be minimal. The grinding of each tensile specimen can be seen in Figure 13 below



Figure 13. The weld area ground to a smooth surface.

Because the grinding took away the materials from the surface, the thickness of the specimens was not the standard 8mm. These deviations

can change the result of the tensile test significantly. The specimens were 3D scanned to check the area of the cross section at the weld. The scans were done using ATOS Compact Scanner. The data was then processed by GOM Inspection software to get the cross sectional area.

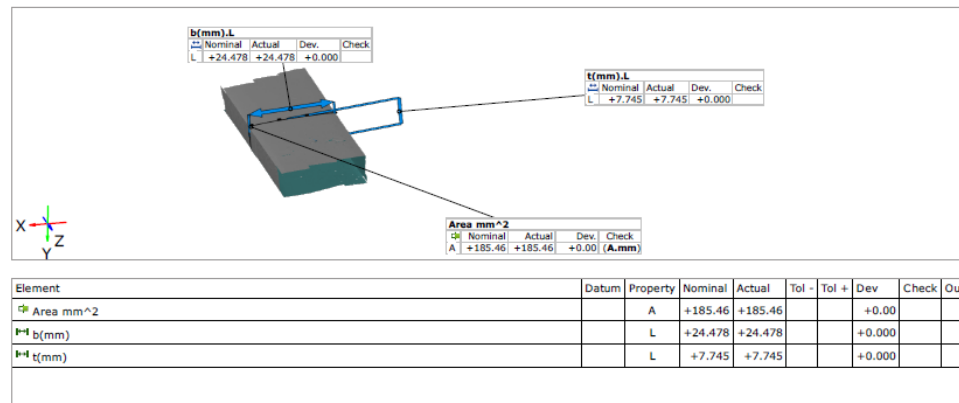


Figure 14. 3D scanning result of the new cross sections.

Finally, the tensile tests were carried out on two over three specimens from each series. One specimen from each series is saved for later tests. The tests were conducted in accordance with EN ISO 6892-1 and EN ISO 5178 to acquire the ultimate strength, the maximum load and yield strength of each specimen. The machine used was Zwick Roell Z250 tensile tester, shown in Figure 15 below.



Figure 15. The Zwick Roell Z250 tensile tester.

The ultimate strength of the specimens were consequently recalculated using the formula:

$$\sigma = \frac{F}{A} \quad (7)$$

Where  $\sigma$  is the ultimate strength of the specimen (MPa),  $F(N)$  is the ultimate load obtained from the tensile test and  $A(\text{mm}^2)$  is the cross sectional area of the weld after grinding.

### 3.6 Hardness test

The tensile tests give the information about the ultimate strength of the steel specimens. However, the results are only reliable if there is no deformation inside the weld that can cause a failure before the ultimate strength of the material is reached. Therefore, hardness tests were required to acquire more data about the strength of the base metal, HAZ and the filler material. Vickers hardness tests were conducted on the leftover pieces of the steel plates. The hardness obtained from the tests could then be converted to ultimate strength to verify if the tensile specimens had deformation or not prior to the tests.

The hardness tests were carried out correspondingly to EN ISO 6507-1. To prepare for the hardness test, three specimens are water cut from each leftover steel plates. The diagram below in figure 16 shows how the hardness test specimens were cut from the left over of the steel plate. The blue areas represent the hardness specimens that were cut out of the plates.

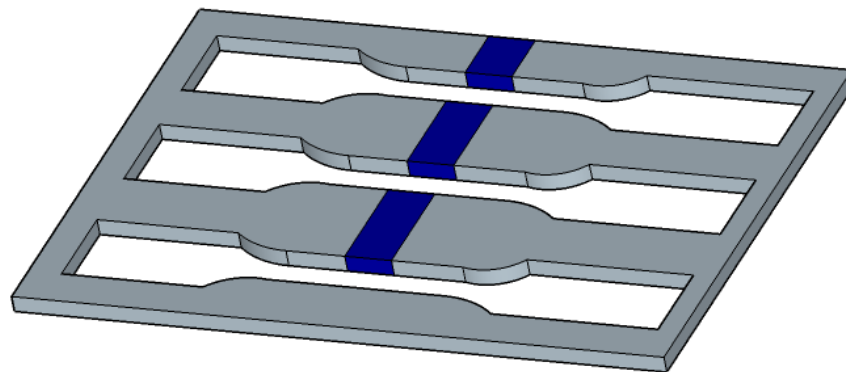


Figure 16. Cutting diagram of the hardness test specimens for each series.

The cut specimens were ground using SiC (Silicon Carbide) grinding paper with grit 150 to 500 then 1000 to ensure there is no deformation on the test surface. The specimens were polished with diamond suspension liquid 3 micron to a smooth surface. The polishing process can be seen in Figure 17 below.



Figure 17. Polishing process with diamond suspension liquid of a hardness specimen.

Subsequently, the polished samples were etched with Nital solution 2% to reveal the microstructure of the different material at the weld. The hardness tests were conducted with the test force of 30kgf. A diamond indenter was forced into the test surface in 15 seconds. Figure 18 below shows that the indentation lengths were measured using microscope.

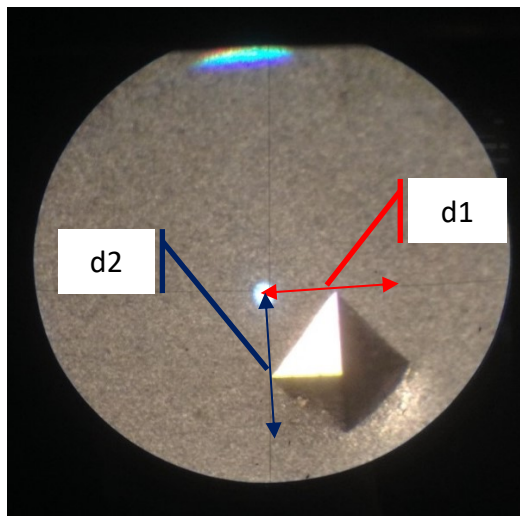


Figure 18. The diagonal lengths of the indentation measured using microscopic device.

The indentation took place in each area of base metal, HAZ and filler material. Below in Figure 19 is the diagram of the indentation plan for each sample.

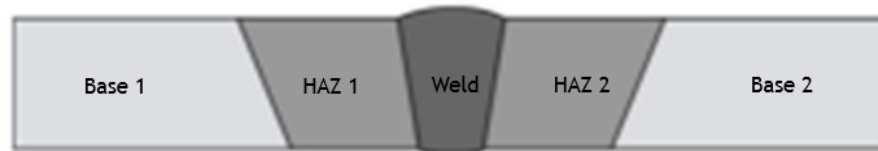


Figure 19. Indentation plan for each sample.

After all the diagonal lengths were measured, the Vickers hardness values were calculated using the formula:

$$HV=0.1891*\frac{F}{d^2} \quad (8)$$

Where:

HV is the hardness of the specimen. F is the test force in N and d is the mean of the two diagonal lengths d1 and d2.

## 4 RESULTS AND ANALYSIS

In order to have a comparison in the tensile strength between the HAZ, welded joint and the base metal, the hardness value of the base metal in each test sample was converted to tensile strength following the formula  $HV = 3 \cdot \alpha \cdot \sigma_{UTS}$  (Zhang, Li & Zhang. 2011, 62-73.)

Where  $\alpha$  is parameter,  $\sigma_{UTS}$  is the ultimate strength of the material and HV is the Vickers hardness value. In table 10 below is the hardness – tensile strength conversion table of all base metal used for the test.

Table 10. Hardness to tensile strength conversion table

	Base metal hardness(HV)	Base metal tensile strength(MPa)
S700-1R	275.74	870.00
S700-2R	275.63	870.00
S700-3R	275.05	870.00
<b>Average</b>	<b>275.47</b>	<b>870.00</b>
S960-1R	305.00	957.50
S960-2R	306.95	965.00
S960-3R	307.09	965.00
<b>Average</b>	<b>306.35</b>	<b>962.33</b>
S500-1R	219.78	693.00
S500-2R	216.25	684.00
S500-3R	214.68	678.00
<b>Average</b>	<b>216.90</b>	<b>685.00</b>
S420-1R	184.33	550.00
S420-2R	186.54	595.00
S420-3R	180.43	580.00
<b>Average</b>	<b>183.77</b>	<b>575.00</b>

## 4.1 S420 series analysis

### 4.1.1 S420 specimens tensile test results

Tensile results of S420 series are shown in Table 11 below.

Table 11. Tensile test results of S420 series

Sample <sup>1)</sup>	Heat input	Average calculated $t_{8/5}$ <sup>2)</sup>	Average measured $t_{8/5}$ <sup>3)</sup>	Ultimate tensile strength of welded samples $f_{uw}$ <sup>4)</sup>	Ultimate tensile strength of material $f_{ub}$ <sup>5)</sup>	Strength capacity <sup>6)</sup>
	(kJ/mm)	(s)	(s)	(N/mm <sup>2</sup> )	(N/mm <sup>2</sup> )	(%)
S420-1R -1	1,48	35,19	36,12	555,93	575,00	96,68
S420-1R -2				509,42		88,60
<b>Average</b>				<b>532,68</b>		<b>92,64</b>
<b>Standard deviation</b>				32,89		5,72
S420-2R -1	0,68	7,66	7,31	524,33	575,00	91,19
S420-2R -2				547,35		95,19
<b>Average</b>				<b>535,84</b>		<b>93,19</b>
<b>Standard deviation</b>				16,28		2,83
S420-3R -1	0,48	3,71	5,73	574,61	575,00	99,93
S420-3R -2				574,44		99,90
<b>Average</b>				<b>574,53</b>		<b>99,92</b>
<b>Standard deviation</b>				0,12		0,02

1) Sample name: [Steel grade]-[Number of weld run(R)]-[Specimen number]

2) Average calculated  $t_{8/5}$  obtained by using formula (2) and (3) (see page 3)

3) Average measured  $t_{8/5}$  attained after analysing the data from infrared camera temperatures

4) Ultimate tensile strength of welded sample  $f_{uw}$  taken after tensile testing the welded samples

5) Ultimate tensile strength of base material  $f_{ub}$  achieved by converting the hardness value of the base metal

6) The strength capacity of the joints when compared to the base metal strength

It can be seen in table 11 that the higher the heat input and cooling time, the lower the tensile strength of the specimen. Three-weld-run series have the highest tensile strength, two-weld-runs have less strength. One-weld-run series has the lowest ultimate strength. It is also noted that the specimens failed at the HAZ. The type of failure is ductile, indicated by the necking at the loaded area. The filler material is ESAB x69, which has a higher yield strength and tensile strength than the base metal of S420 (805 MPa vs 575 MPa). The high strength of the filler material means the HAZ

would fail before the filler material did when loaded in the tensile tests. This means the results of S420 and S500 series are reliable. Figure 20 shows the necking failure at the HAZ of S420-3R-1 series.



Figure 20. S420 series failed at the HAZ

The graph in Figure 21 below shows the comparison of the cooling time  $t_{8/5}$  and the ultimate strength of the welded sample.

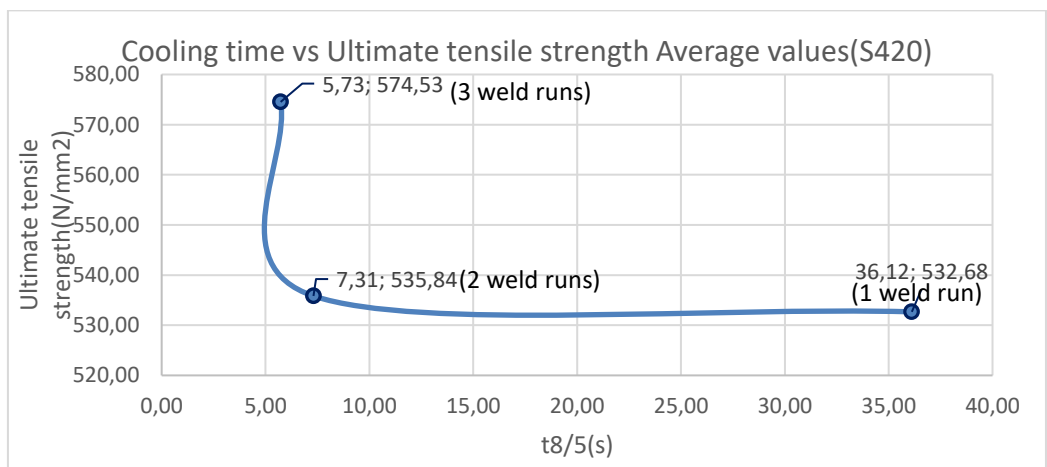


Figure 21. Cooling time  $t_{8/5}$  vs ultimate tensile strength values of the S420 series

Figure 22 demonstrates the comparison of the cooling time  $t_{8/5}$  vs ultimate tensile strength of the welded samples relative to base metal.

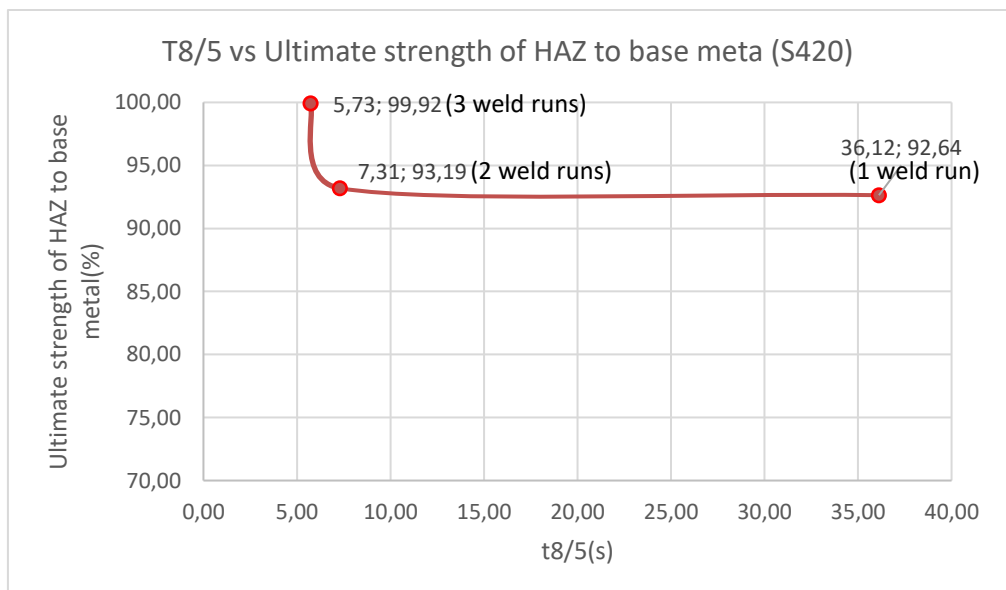




Figure 22. Cooling time  $t_{8/5}$  vs ratio of the strength of the welded samples relative to base metal in S420

Figure 22 indicates that for a very short cooling time, the microstructure changes that occurs when steel is subjected to heat are moderate. S420-3R series have a very high strength capacity (99.9 %). The deterioration of the HAZ in the two-run and one-run series is more apparent. It is notable that the strength capacities of the two-run and one-run series are very close. The phenomenon is further investigated by hardness tests and microscopic analysis.

#### 4.1.2 S420 specimens hardness test results

Figure 23 demonstrates the position of the indentation on the surface of the welded joint in microscopic examination.

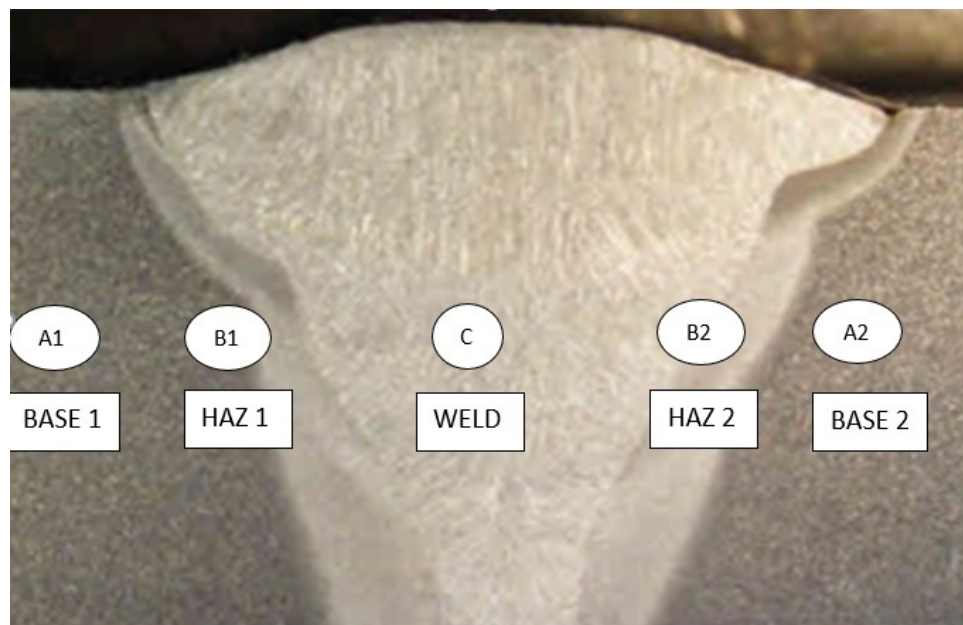


Figure 23. Location and name of indentation point in each hardness specimen.

Table 12 shows the results of the hardness test for S420

Table 12. Hardness test results of S420 series

Series <sup>1)</sup>	Name <sup>2)</sup>	Base 1(A1)	HAZ 1 (B1)	Weld (C)	HAZ 2 (B2)	Base 2 (A2)
S420-1R	S420-1R-1	192	168	242	176	189
	S420-1R-2	179	162	225	164	165
	S420-1R-3	194	174	237	179	188
<b>Average</b>		<b>188</b>	<b>168</b>	<b>235</b>	<b>173</b>	<b>180</b>
S420-2R	S420-2R-1	183	177	242	179	187
	S420-2R-2	191	167	249	174	187
	S420-2R-3	189	174	250	183	183
<b>Average</b>		<b>188</b>	<b>173</b>	<b>247</b>	<b>179</b>	<b>185</b>
S420-3R	S420-3R-1	181	180	253	178	189
	S420-3R-2	184	189	241	179	158
	S420-3R-3	185	181	268	173	185
<b>Average</b>		<b>183</b>	<b>183</b>	<b>254</b>	<b>177</b>	<b>178</b>

<sup>1)</sup> Sample name: [Steel grade]-[Number of weld run(R)]

<sup>2)</sup> Sample name: [Steel grade]-[Number of weld run(R)]-[Specimen number]

Table 13 shows the averaged hardness value of base metal and HAZ and the conversion of the hardness value to tensile strength for each series

Table 13. Averaged hardness value and converted tensile strength of S500 series

Series <sup>1)</sup>	Base		HAZ		Weld	
	Hardness Value (HV)	Strength (MPa)	Hardness Value (HV)	Strength (MPa)	Hardness Value (HV)	Strength (MPa)
S420-1R	184,33	613,00	170,51	576,60	235,06	780,50
Strength capacity <sup>2)</sup> (%)	100,00	100,00	92,50	94,06	127,52	127,32
S420-2R	186,54	626,00	175,94	806,00	246,95	590,00
Strength capacity (%)	100,00	100,00	94,32	128,75	132,38	94,25
S420-3R	180,43	615,00	179,84	810,00	253,98	605,00
Strength capacity (%)	100,00	100,00	99,67	131,71	140,76	98,37

<sup>1)</sup> Sample name: [Steel grade]-[Number of weld run(R)]

<sup>2)</sup> The strength capacity of the joints when compared to the base metal strength

When examining the HAZ results, three-weld-runs have the highest hardness values. The two-run series has less hardness. One-weld-run specimens have the lowest hardness. It is notable that the hardness of the weld is the highest due to the filler material having a much higher strength than the base metal. Figure 24 demonstrates the difference of hardness value between HAZ, filler material and the base metal. Figure 25 shows the hardness values of HAZ relative to the hardness values of base metal of S420 series.

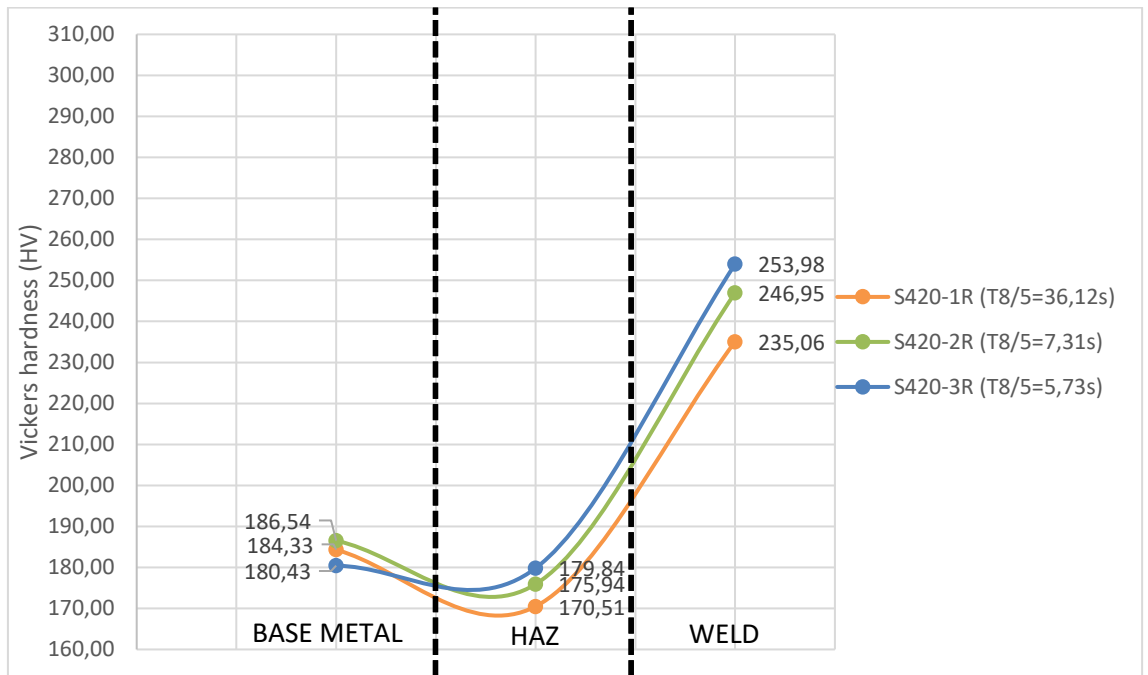


Figure 24. Effect of cooling time on hardness in different regions of S420 series

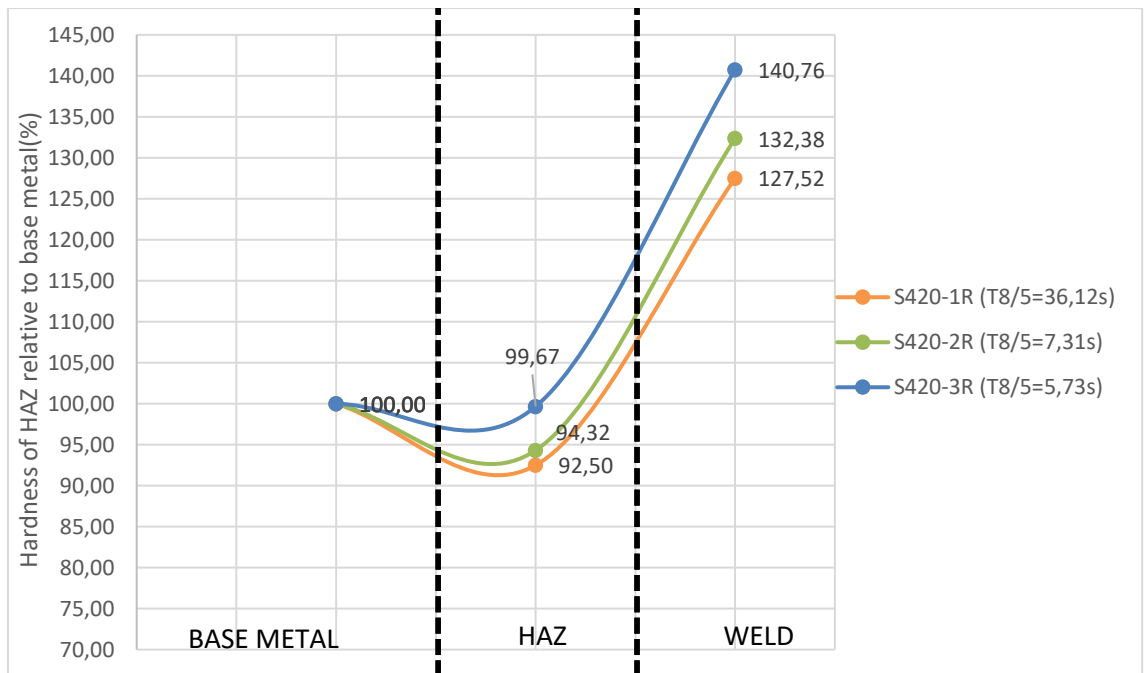


Figure 25. Hardness values relative to base metal hardness of S420 series

When comparing the hardness of HAZ relative to base metal, it can be seen that S420-3R series retains the highest capacity. S420-2R has less strength followed by S420-1R. It is notable that the results of S420 hardness tests are similar to the tensile tests that the three-weld-run has very high

strength capacity. The strength capacities of the two and one weld runs are close to each other and much less than that of the three-weld-runs. The hardness of the HAZ in the S420 series is converted to ultimate tensile strength and compared with the  $T_{8/5}$  in Figure 26 below.

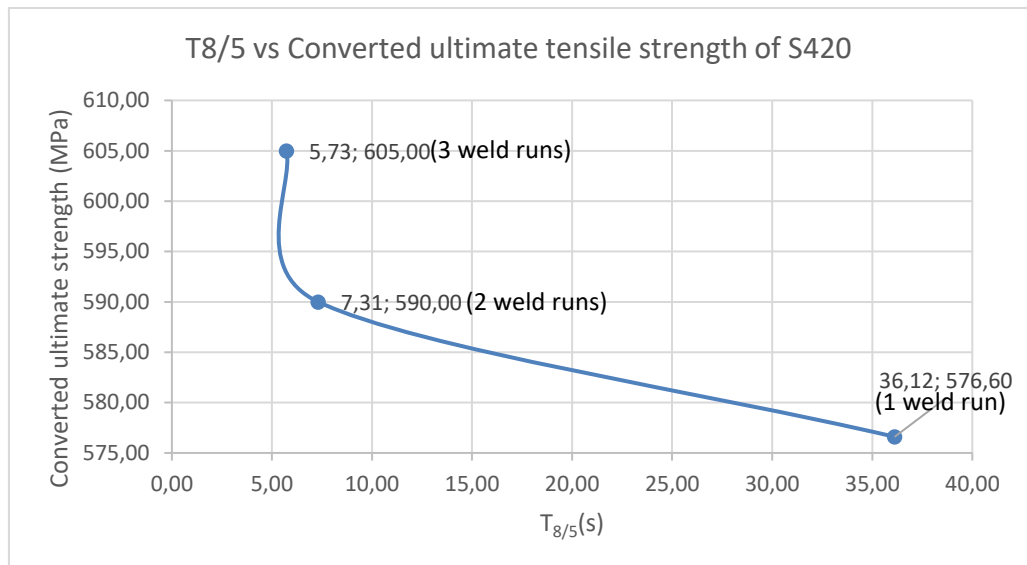


Figure 26.  $T_{8/5}$  vs Converted tensile strength of S420 series

The converted ultimate strength are then compared to the base metal, as shown in Figure 27 below.

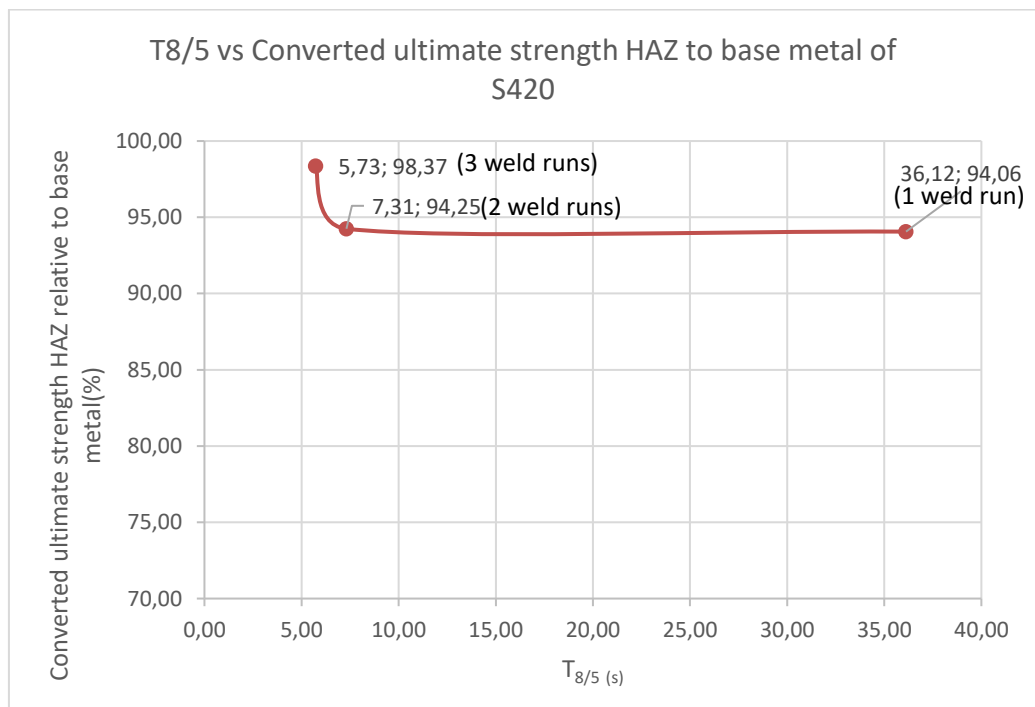


Figure 27.  $T_{8/5}$  vs Converted ultimate strength HAZ to base metal (%) of S420 series

A microscope was used to examine the quality of the weld. Cracks were present inside the weld structure. However, the S420 specimens did not fail at the weld during tensile tests. Alternatively, the HAZ in these specimens failed, characterized by the necking and the uneven length of the broken parts of the tested samples. It can be assumed that the HAZ reached the critical stress and failed before the joints did. Although the cracks produce a stress concentration at the joint and reduce its efficiency, the filler's strength was too high in comparison with the HAZ. Figure 28 shows microscopic images of the cracks in the weld of S420-2R and S420-1R.

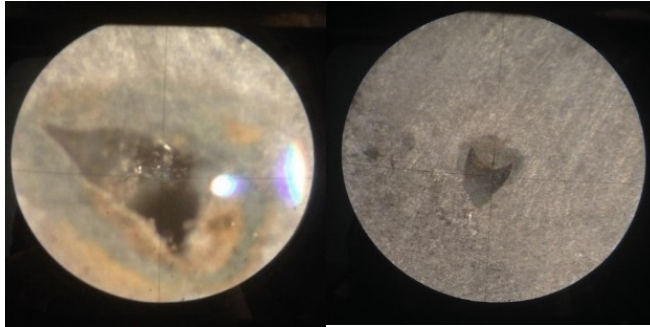


Figure 28. Microscopic image of the cracks in the welds of S420-1R and S420-2R (not in scale)

## 4.2 S500 series analysis

### 4.2.1 S500 specimens tensile test results

The result of S500 tensile tests is shown in table 14 below

Table 14. Tensile test results of S500 series

Sample <sup>1)</sup>	Heat input	Average calculated $t_{8/5}$ <sup>2)</sup>	Average measured $t_{8/5}$ <sup>3)</sup>	Ultimate tensile strength of welded samples $f_{uw}$ <sup>4)</sup>	Ultimate tensile strength of material $f_{ub}$ <sup>5)</sup>	Strength capacity <sup>6)</sup>
	(kJ/mm)	(s)	(s)	(N/mm <sup>2</sup> )	(N/mm <sup>2</sup> )	(%)
S500-1R -1	1,47	34,72	32,60	620,32	685,00	90,56
S500-1R -2				607,95		97,27
<b>Average</b>				<b>614,14</b>		<b>89,65</b>
<b>Standard deviation</b>				8,75		4,75
S500-2R -1	0,72	9,59	7,99	641,51	685,00	93,65
S500-2R -2				653,21		104,51
<b>Average</b>				<b>647,36</b>		<b>94,50</b>
<b>Standard deviation</b>				8,27		7,68
S500-3R -1	0,48	3,72	5,55	662,38	685,00	96,70
S500-3R -2				656,01		95,77
<b>Average</b>				<b>659,20</b>		<b>96,23</b>
<b>Standard deviation</b>				4,50		0,66

1) Sample name: [Steel grade]-[Number of weld run(R)]-[Specimen number]

2) Average calculated  $t_{8/5}$  obtained by using formula (2) and (3) (see page 3)

3) Average measured  $t_{8/5}$  attained after analysing the data from infrared camera temperatures

4) Ultimate tensile strength of welded sample  $f_{uw}$  taken after tensile testing the welded samples

5) Ultimate tensile strength of base material  $f_{ub}$  achieved by converting the hardness value of the base metal

6) The strength capacity of the joints when compared to the base metal strength

The tensile test results of S500 series are similar to that of S420. Three-weld-run samples have the highest strength, followed by two-run series. The one-weld-run series has the longest cooling time and lowest tensile strength. The filler material is ESAB x69, stronger than the base material (805MPa vs 685MPa). The tested specimens all failed at the HAZ, with the characteristic necking. When comparing the ultimate strength of HAZ to base metal, the three-run series have the highest percentage at 96%. The two-weld-run has slightly less relative strength capacity at 94%. One-weld-

run has the lowest capacity at 89.9%. The graph below in Figure 29 shows the comparison of the cooling time  $t_{8/5}$  and the ultimate strength of S500:

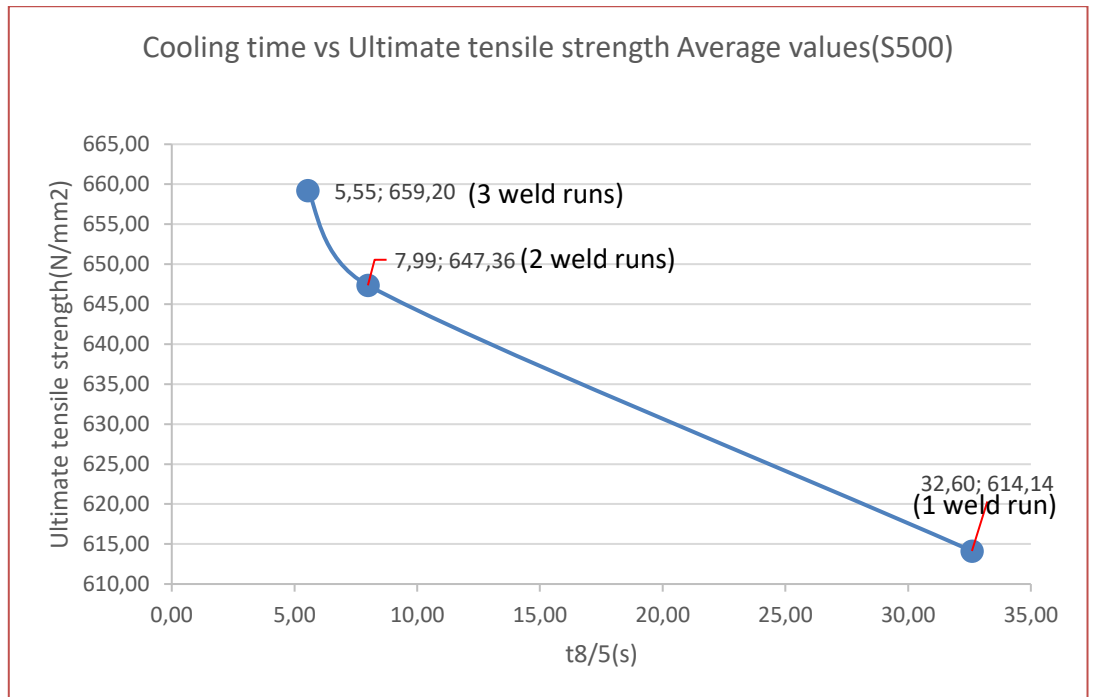


Figure 29. Cooling time  $t_{8/5}$  vs ultimate tensile strength values of the S500 series

Figure 30 shows the ratio of the strength of the HAZ in S500 series relative to base metal.

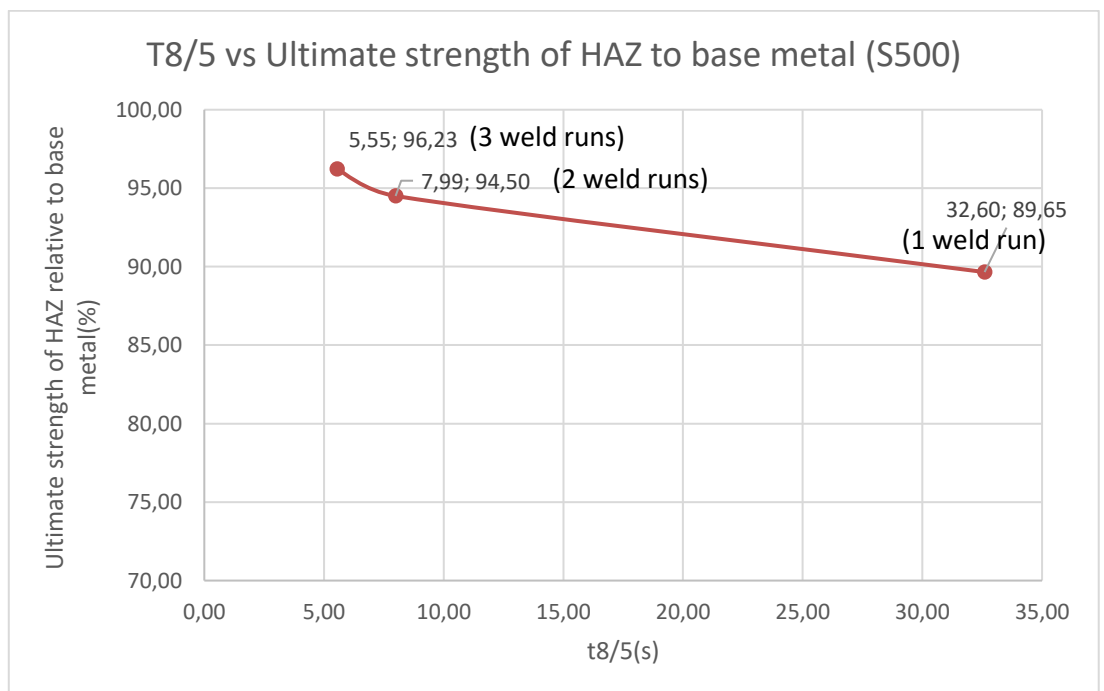


Figure 30. Cooling time  $t_{8/5}$  vs ratio of the strength of the welded samples relative to base metal in S500

#### 4.2.2 S500 specimens hardness test results

Table 15 shows the results of S500 hardness tests.

Table 15. Hardness test results of S500 series

Series <sup>1)</sup>	Name <sup>2)</sup>	Base 1(A1)	HAZ 1 (B1)	Weld (C)	HAZ 2 (B2)	Base 2 (A2)
S500-1R	S500-1R-1	223	190	238	194	223
	S500-1R-2	213	195	241	187	218
	S500-1R-3	220	191	249	197	223
<b>Average</b>		<b>218</b>	<b>192</b>	<b>243</b>	<b>193</b>	<b>221</b>
S500-2R	S500-2R-1	216	201	248	194	220
	S500-2R-2	206	213	249	200	213
	S500-2R-3	221	191	254	200	222
<b>Average</b>		<b>214</b>	<b>202</b>	<b>250</b>	<b>198</b>	<b>218</b>
S500-3R	S500-3R-1	221	192	232	202	200
	S500-3R-2	216	271	276	216	200
	S500-3R-3	203	198	248	187	248
<b>Average</b>		<b>214</b>	<b>220</b>	<b>252</b>	<b>202</b>	<b>216</b>

<sup>1)</sup> Sample name: [Steel grade]-[Number of weld run(R)]

<sup>2)</sup> Sample name: [Steel grade]-[Number of weld run(R)]-[Specimen number]

Table 16 shows the averaged hardness value of base metal and HAZ and the conversion of the hardness value to tensile strength for S500

Table 16. Averaged hardness value and converted tensile strength of S500 series

Series <sup>1)</sup>	Base		Weld		HAZ	
	Hardness Value	Strength	Hardness Value	Strength	Hardness Value	Strength
	(HV)	(MPa)	(HV)	(MPa)	(HV)	(MPa)
S500-1R	220	712	243	770	192	626
Strength capacity <sup>2)</sup> (%)	100,00	100,00	110,50	108,21	87,53	87,97
S500-2R	216	705	250	797	200	650
Strength capacity (%)	100,00	100,00	115,65	113,00	92,48	92,20
S500-3R	215	708	252	803	211	693
Strength capacity (%)	100,00	100,00	117,27	113,42	98,31	97,81

<sup>1)</sup> Sample name: [Steel grade]-[Number of weld run(R)]

<sup>2)</sup> The strength capacity of the joints when compared to the base metal strength

It can be seen that S500 hardness tests follows the same trend as S420 series in the research, with the higher the cooling time, the lower the hardness values. S500-3R has the highest hardness value. S500-2R has lower average hardness value and S500-1R has the lowest hardness in all three weld types. The hardness of HAZ relative to base metal also follows



the trend with three-run series having the highest percentage, followed by two-run then one-run. Figure 31 and 32 compares hardness values and hardness of HAZ relative to base metal of different regions of 3 weld types.

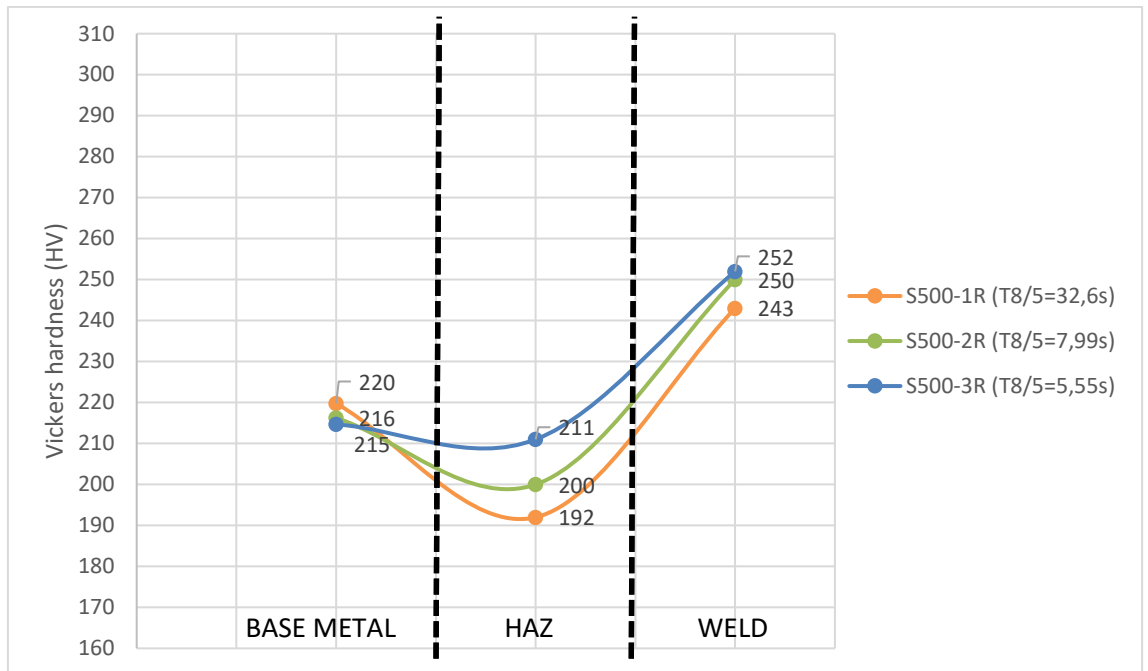


Figure 31. Effect of cooling time on hardness in different regions of S500

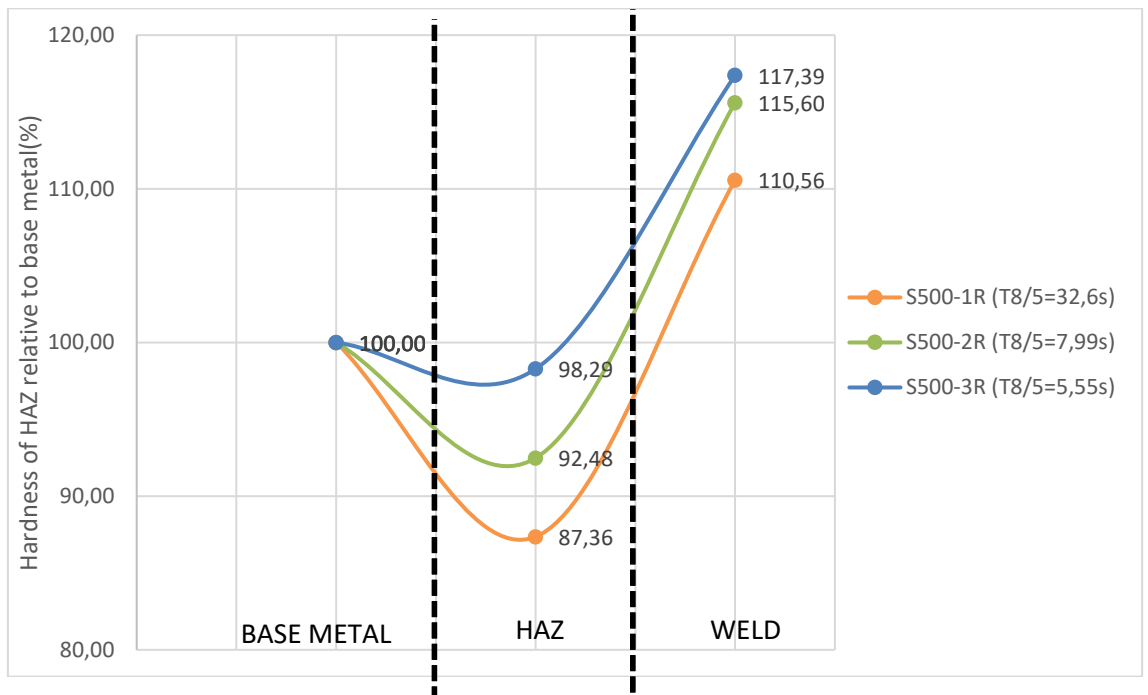


Figure 32. Hardness values relative to base metal hardness of S500 series

When comparing the cooling time with the tensile strength converted from hardness values, the results of S500 is similar to the rest of steel grade in the research. The higher the cooling time, the higher the strength and

strength capacity of the specimens. The hardness of S500 is also converted to ultimate strength and compared to the cooling time and to the ultimate strength of base metal. This can be seen in Figure 33 and Figure 34 below.

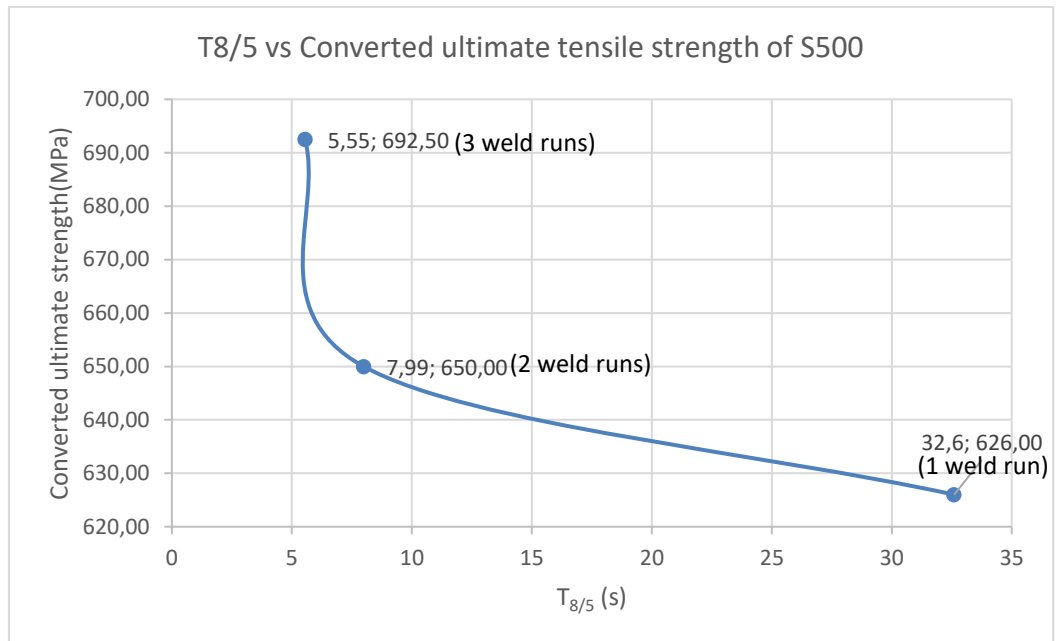


Figure 33.  $T_{8/5}$  vs Converted tensile strength of S420 series

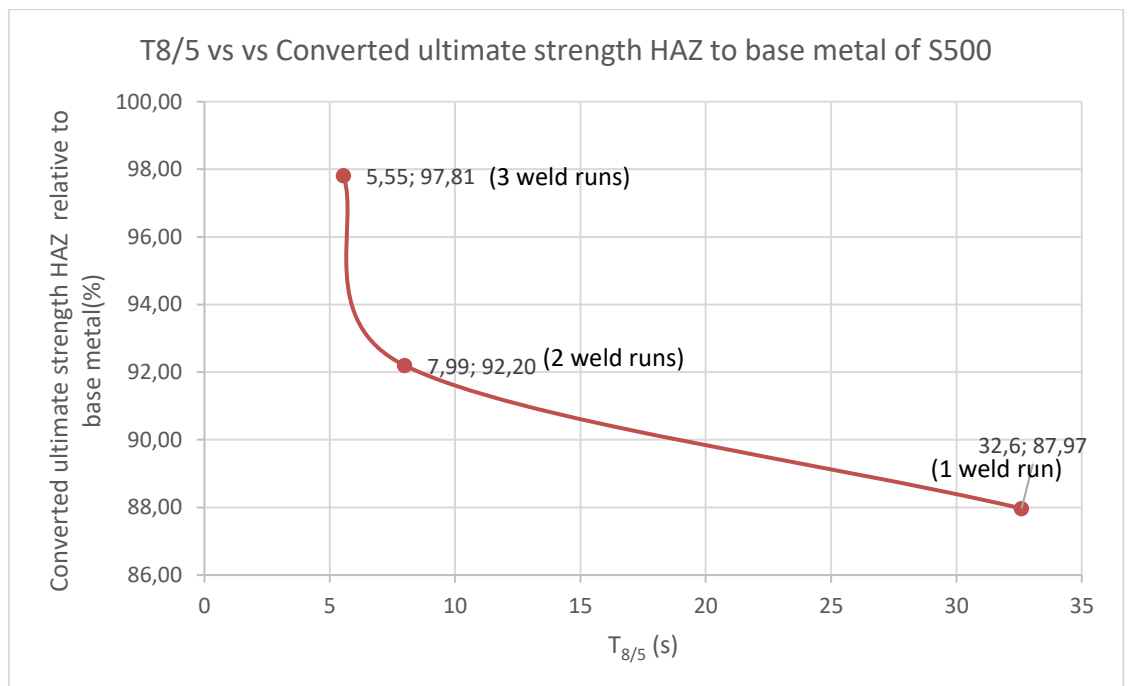


Figure 34.  $T_{8/5}$  vs Converted ultimate strength HAZ to base metal of S500 series

A microscope was also used to examine the cracks in the specimens. Similarly to S420, even though there were cracks at the joints, the specimens failed at the HAZ. This confirms that if the strength of the material is much higher than the base metal, the cracks do not affect the

results of the tensile test because the HAZ will fail before the cohesive strength of the filler material is reached. Figure 35 shows microscopic image of the cracks in the welds of S500-2R and S500-3R

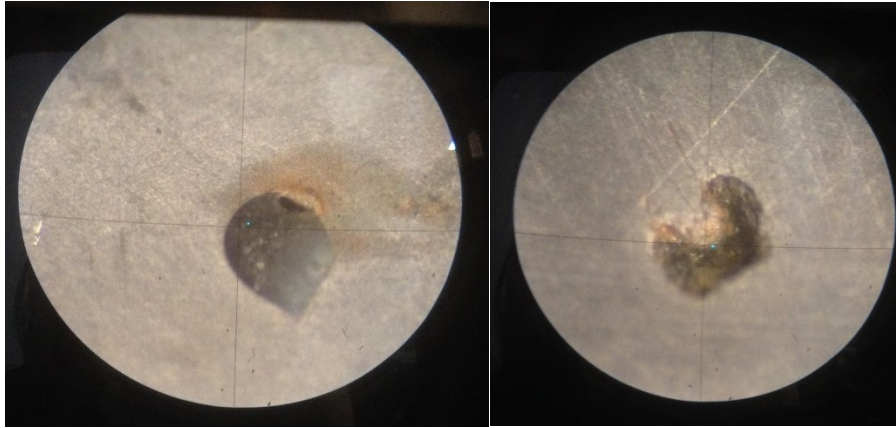


Figure 35. Microscopic image of the cracks in the welds of S500-2R and S500-3R (not in scale)

### 4.3 S700 series analysis

#### 4.3.1 S700 specimens tensile test results

The tensile test results of S700 series are shown in Table 17.

Table 17. Tensile test results of S700 series

Sample <sup>1)</sup>	Heat input	Average calculated $t_{8/5}$ <sup>2)</sup>	Average measured $t_{8/5}$ <sup>3)</sup>	Ultimate tensile strength of welded samples $f_{uw}$ <sup>4)</sup>	Ultimate tensile strength of material $f_{ub}$ <sup>5)</sup>	Strength capacity <sup>6)</sup>
	(kJ/mm)	(s)	(s)	(N/mm <sup>2</sup> )	(N/mm <sup>2</sup> )	(%)
700-1R -1	1,37	30,15	20,70	674,08	870,00	77,48
700-1R -2				630,31		72,45
<b>Average</b>				<b>652,19</b>		<b>74,96</b>
<b>Standard deviation</b>				30,95		3,56
700-2R -1	0,79	10,13	8,46	686,52	870,00	78,91
700-2R -2				710,63		81,68
<b>Average</b>				<b>698,57</b>		<b>80,30</b>
<b>Standard deviation</b>				17,05		1,96
700-3R -1	0,61	6,28	6,12	709,80	870,00	81,59
700-3R -2				531,97		61,15
<b>Average</b>				<b>620,88</b>		<b>71,37</b>
<b>Standard deviation</b>				125,7454344		14,45

1) Sample name: [Steel grade]-[Number of weld run(R)]-[Specimen number]

2) Average calculated  $t_{8/5}$  obtained by using formula (2) and (3) (see page 3)

3) Average measured  $t_{8/5}$  attained after analysing the data from infrared camera temperatures

4) Ultimate tensile strength of welded sample  $f_{uw}$  taken after tensile testing the welded samples

5) Ultimate tensile strength of base material  $f_{ub}$  achieved by converting the hardness value of the base metal

6) The strength capacity of the joints when compared to the base metal strength

The results did not follow the trend of S420 and S500 that the longer the cooling time, the lower the strength capacity will be. The actual tests show that the two-weld-run samples have the highest strength capacity, followed by one-weld-run. The three-weld run samples have the lowest strength capacity out of all the three weld types in this case. However, the high standard deviation in the three-weld-run type (125.75) suggests unreliability in the test results. It can be observed that the S700-1R series have a ductile failure characterized by significant plastic deformation and a reduction of cross section in the loaded area (necking). This can be seen in figure 36 below.



Figure 36. S700-1R-1 tensile specimen after tensile test and magnified pictures of the failure area.

In contrast to S700-1R; the S700-2R and S700-3R series does not have necking deformation at the joint. The 45° diagonal crack is a sign of shear failure. This suggests a low level of material penetration between the filler material and the base metal, or there were deformations at the weld that produces stress concentrations. They disturb the normal stress distribution and produce local co-generations of stress (Maleque & Salit 2013, 19-21.)

The phenomenon is investigated further by hardness tests and microscopic examination on the leftover pieces of the series. Hardness values can be converted to tensile strength and then compared with the real tensile test value. This will clarify whether the low strength of the two-run and three-run series came from the heat input or the weld quality. The failure mode of S700-2R-2 is shown in Figure 37 below.



Figure 37. S700-2R-2 tensile specimen after tensile test and magnified pictures of the failure area.

The graph in Figure 38 shows the comparison of the cooling time  $t_{8/5}$  and the ultimate strength of the welded samples.

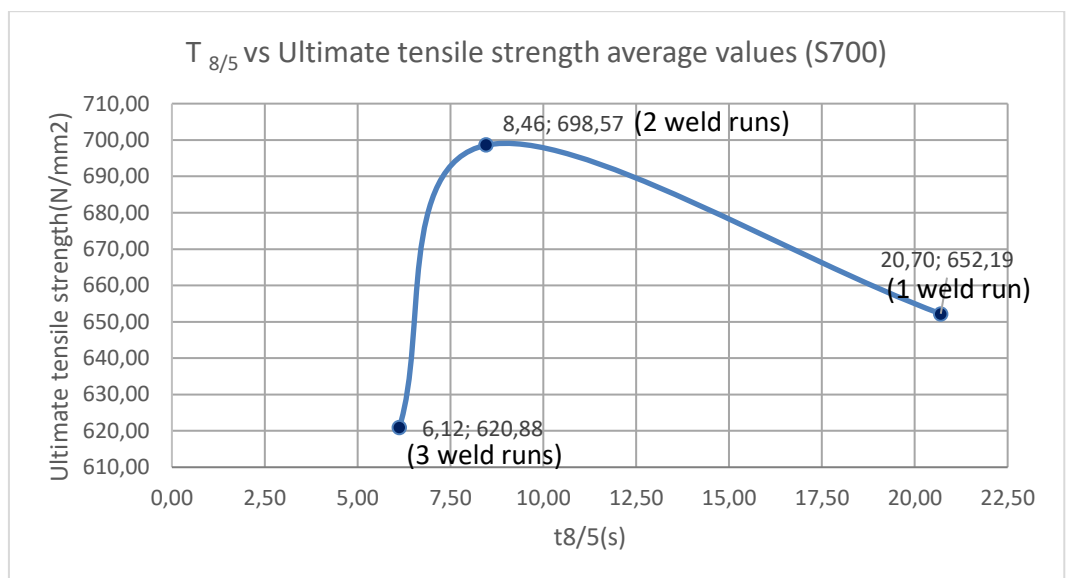


Figure 38. Cooling time  $t_{8/5}$  vs ultimate tensile strength values of the S700 series

Figure 39 shows the ultimate tensile strength of the welded samples relative to base metal samples and the cooling time.

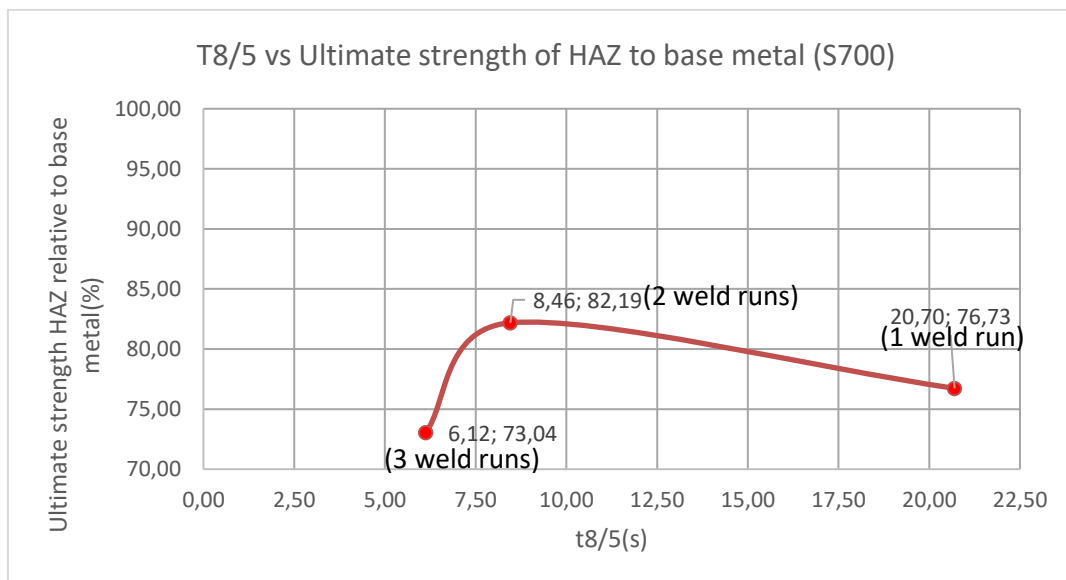


Figure 39. Cooling time  $t_{8/5}$  vs ratio of the strength of the welded samples relative to base metal in S700

#### 4.3.2 S700 specimens hardness test results

Table 18 below shows the hardness results of S700 series

Table 18. Hardness test result of S700 series

Series <sup>1)</sup>	Name <sup>2)</sup>	Base 1 (A1)	HAZ 1 (B1)	Weld (C)	HAZ 2 (B2)	Base 2 (A2)
S700-1R	S700-1R-1	271	214	246	215	281
	S700-1R-2	281	202	247	214	268
	S700-1R-3	265	212	256	213	289
<b>Average</b>		<b>272</b>	<b>209</b>	<b>249</b>	<b>214</b>	<b>279</b>
S700-2R	S700-2R-1	278	220	243	237	277
	S700-2R-2	264	223	265	207	280
	S700-2R-3	276	217	249	209	278
<b>Average</b>		<b>273</b>	<b>220</b>	<b>252</b>	<b>217</b>	<b>278</b>
S700-3R	S700-3R-1	272	234	243	220	285
	S700-3R-2	283	207	232	226	268
	S700-3R-3	270	223	258	227	272
<b>Average</b>		<b>275</b>	<b>221</b>	<b>245</b>	<b>224</b>	<b>275</b>

1) Sample name: [Steel grade]-[Number of weld run(R)]

2) Sample name: [Steel grade]-[Number of weld run(R)]-[Specimen number]

Table 19 below shows the averaged hardness value of base metal and HAZ and the conversion of the hardness value to tensile strength for each series.

Table 19. Averaged hardness value and converted tensile strength of S700 series

Series <sup>1)</sup>	Base		HAZ		Weld	
	Hardness Value	Strength	Hardness Value	Strength	Hardness Value	Strength
	(HV)	(MPa)	(HV)	(MPa)	(HV)	(MPa)
S700-1R	275	870	212	695	249	793
Strength capacity <sup>2)</sup> (%)	100	100	77	80	91	91
S700-2R	275	870	219	710	252	803
Strength capacity (%)	100	100	80	82	92	92
S700-3R	275	870	223	720	245	778
Strength capacity (%)	100	100	81	83	89	89

1) Sample name: [Steel grade]-[Number of weld run(R)]

2) The strength capacity of the joints when compared to the base metal strength

It can be seen that the HAZ has the lowest hardness value when compared to base metal and the weld. The weld has less strength than base metal and more strength than HAZ. The base metal hardness is the same in all series and has the highest value. Figure 40 shows the hardness values of the HAZ, the filler material and the base metal. Figure 41 compares the hardness value of the different areas to the hardness value of the base metal.

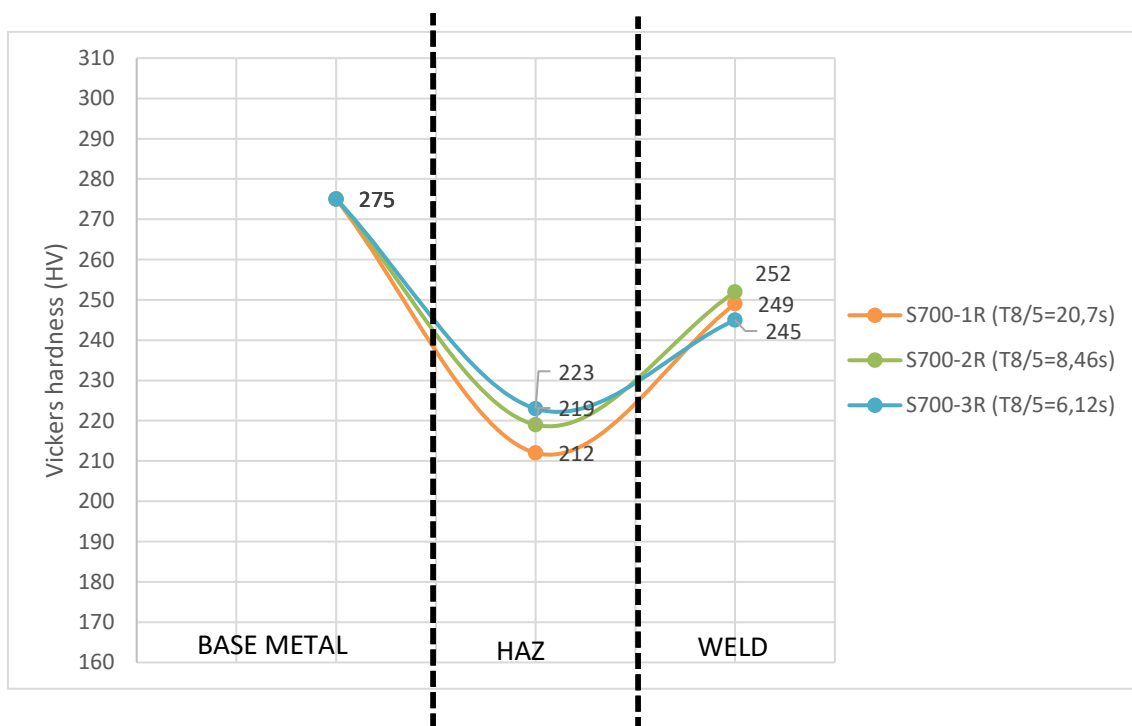


Figure 40. Effect of cooling time on hardness in different regions of S700



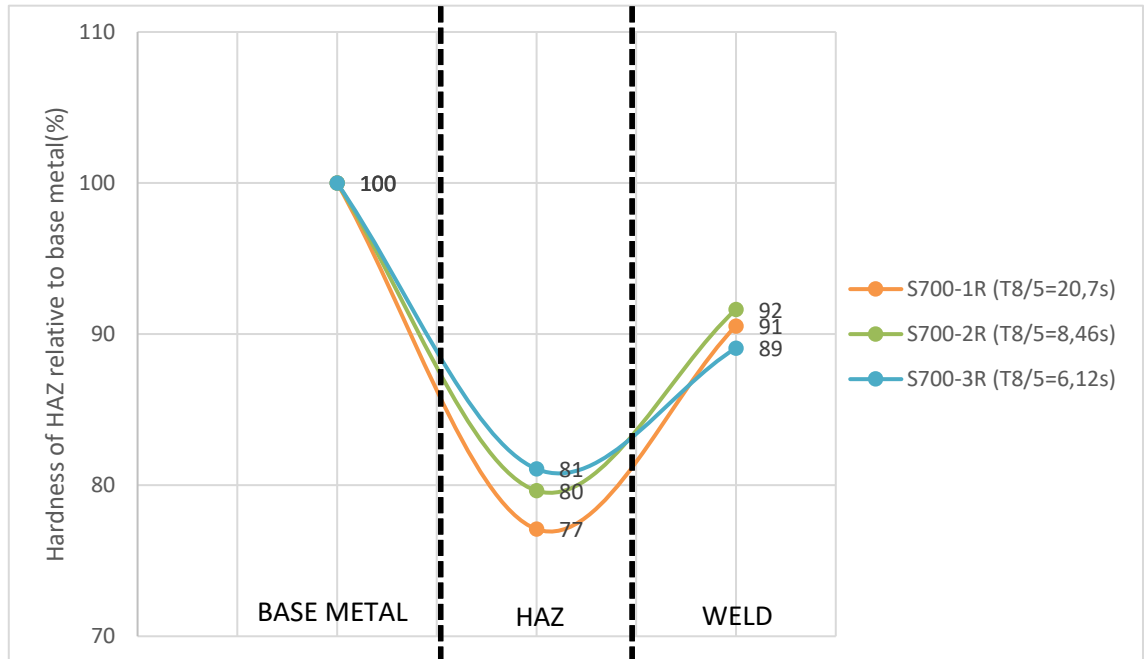


Figure 41. Hardness values relative to base metal hardness of S700 series

When converting the hardness to ultimate tensile strength, the one-weld-run series have the lowest ultimate tensile strength because they have the highest cooling time. The two-weld-run series has higher ultimate tensile strength and the three-weld-run series have the highest ultimate tensile strength. This contradicts with the result of the S700 series tensile test where the two-weld-run series have the highest ultimate tensile strength, the one-weld-run specimens have less strength and the three-weld-run series have the lowest tensile strength out of all three weld types. When comparing the cooling time with the tensile strength converted from hardness values, the results are similar to those of S420 and S500, showing that the higher the cooling time, the lower the tensile strength. Figure 42 further demonstrates this phenomenon.

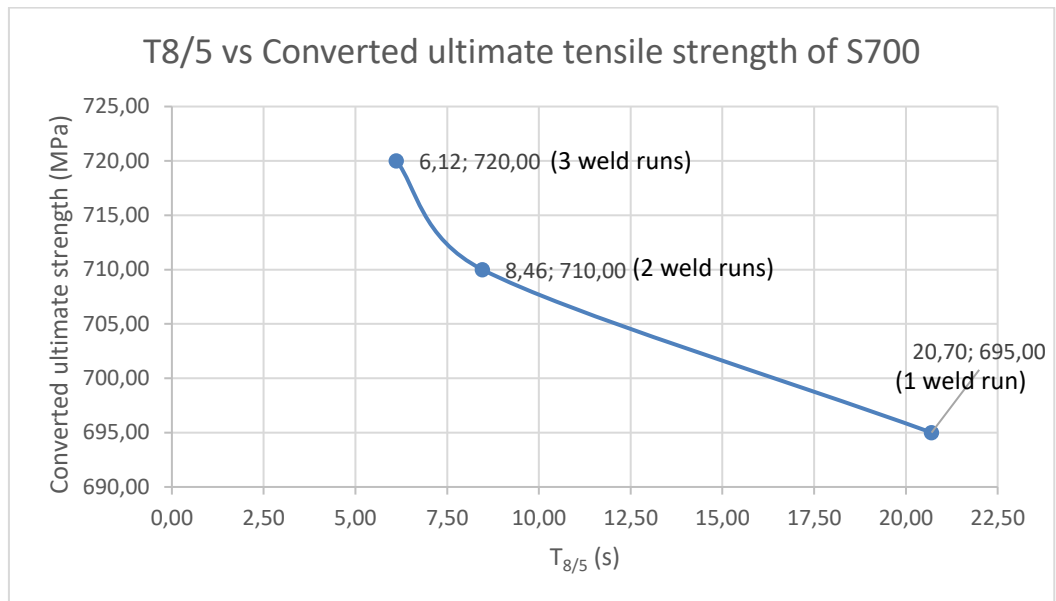


Figure 42.  $T_{8/5}$  vs Converted tensile strength of S700 series

Figure 43 shows the converted ultimate strength of HAZ compared to the ultimate strength of base metal in S700 series.

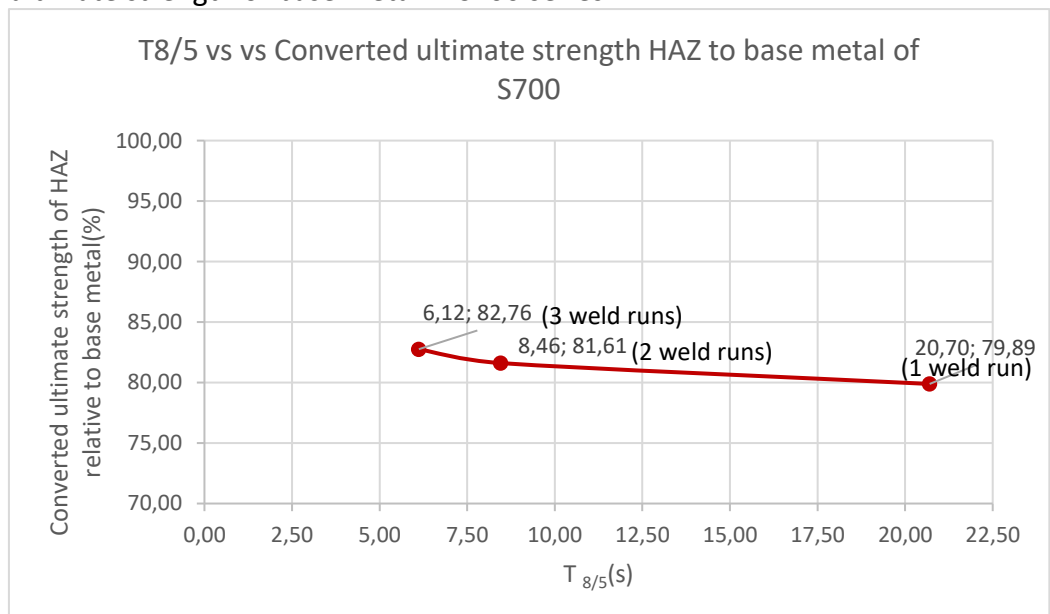


Figure 43.  $T_{8/5}$  vs vs Converted ultimate strength HAZ to base metal of S700 series

The results of the hardness test show that the heat input did affected the material as predicted (the longer the cooling time, the lower the strength). All of the S700 specimens failed at the weld instead of the HAZ. This means that the weld failed before the HAZ did although the HAZ has a lower hardness and tensile strength. The difference between the tests and theory results suggests there were deformations in the joints before the tensile testing.

Microscopic examination displays the cracks within the filler materials of S700-2R-1 and S700-3R-2 in Figure 44.

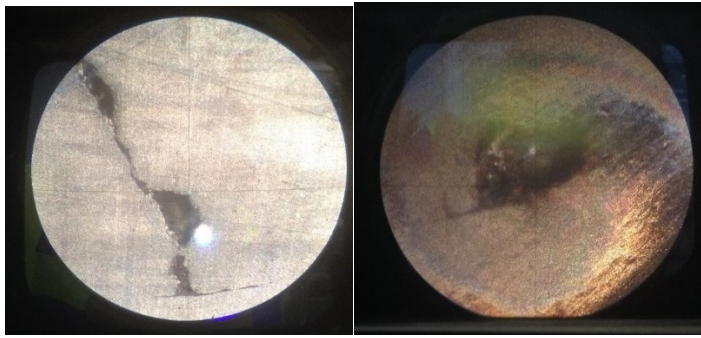


Figure 44. Microscopic examination of cracks in S700-2R-1 and S700-3R-2 series (not in scale)

The results of the tensile tests show that the S700-3R-2 sample has a much lower tensile value compared to the rest of the specimens. The cracks in the weld could have affected the test results.

Table 20. S700 series tensile strengths, S700-3R-2 has a noticeably lower strength compared to other specimens

Sample <sup>1)</sup>	Ultimate tensile strength of welded samples $f_{uw}$ <sup>2)</sup>
	(N/mm <sup>2</sup> )
700-1R -1	674
700-1R -2	630
700-2R -1	687
700-2R -2	711
700-3R -1	710
<b>700-3R -2</b>	<b>532</b>

Anomalies (dust, sand, small particles...) can come in the joint surface after the first weld run. The second and third weld have a high risk of forming porosity from the anomalies. The reduction in cross section areas by these cracks could cause the localization increase of stress. The stress can exceed the material's theoretical cohesive strength and cause a failure at the joint. This explains why the tensile strength values of the two-weld-run and three-weld-run series in real tests are smaller than the theoretical strength converted from hardness values. The filler material ESAB x69 has a lower yield strength and tensile strength than the base metal (805 MPa vs 870 MPa). This could also contribute to the premature failure of the joint.

#### 4.4 S960 series analysis

##### 4.4.1 S960 specimens tensile test results

The tensile test results of S960 series are shown in Table 21.

Table 21. Tensile test results of S960 series

Sample <sup>1)</sup>	Heat input	Average calculated $t_{8/5}$ <sup>2)</sup>	Average measured $t_{8/5}$ <sup>3)</sup>	Ultimate tensile strength of welded samples $f_{uw}$ <sup>4)</sup>	Ultimate tensile strength of material $f_{ub}$ <sup>5)</sup>	Strength capacity <sup>6)</sup>
	(kJ/mm)	(s)	(s)	(N/mm <sup>2</sup> )	(N/mm <sup>2</sup> )	(%)
S960-1R -1	1,48	35,19	33,47	779,93	962,33	81,05
S900-1R -2				773,35		80,36
<b>Average</b>				<b>776,64</b>		80,70
<b>Standard deviation</b>				4,65		0,48
S960-2R -1	0,71	8,46	9,94	601,69	962,33	62,52
S960-2R -2				767,72		79,78
<b>Average</b>				<b>684,70</b>		71,15
<b>Standard deviation</b>				117,40		12,20
S960-3R -1	0,49	3,92	7,17	829,85	962,33	86,23
S960-3R -2				812,21		84,40
<b>Average</b>				<b>821,03</b>		85,32
<b>Standard deviation</b>				12,47		1,30

1) Sample name: [Steel grade]-[Number of weld run(R)]-[Specimen number]

2) Average calculated  $t_{8/5}$  obtained by using formula (2) and (3) (see page 3)

3) Average measured  $t_{8/5}$  attained after analysing the data from infrared camera temperatures

4) Ultimate tensile strength of welded sample  $f_{uw}$  taken after tensile testing the welded samples

5) Ultimate tensile strength of base material  $f_{ub}$  achieved by converting the hardness value of the base metal

6) The strength capacity of the joints when compared to the base metal strength

It can be seen that the three-weld-run samples have the highest strength, followed by one-weld-run sample. The two-run specimens have the lowest tensile strength in all weld types of S960. When comparing the steel samples, S960-2R-1 has a significantly lower strength comparing to the rest of the specimens. This can be seen in table 22 below.

Table 22. S960-2R-1 ultimate tensile strength compared to other specimens of S960

Sample <sup>1)</sup>	Ultimate tensile strength of welded samples $f_{uw}$ <sup>4)</sup>
	(N/mm <sup>2</sup> )
S960-1R -1	780
S960-1R -2	773
<b>S960-2R -1</b>	<b>602</b>
S960-2R -2	768
S960-3R -1	830
S960-3R -2	812

The results of S960 series, like the S700 series, could be compromised by two factors: the use of filler material ESAB x69 which has much lower tensile values than the base metal and the cracks propagated by improper cleaning between the weld runs. The graph below in Figure 45 shows the comparison of the cooling time  $t_{8/5}$  and the ultimate strength of the S960 series:

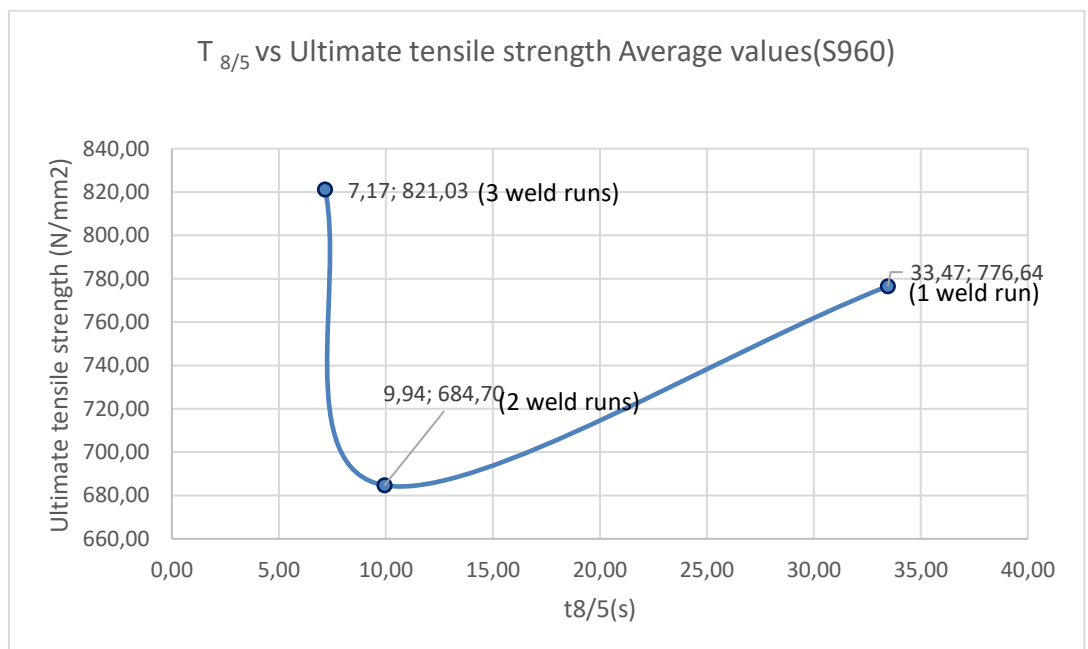


Figure 45. Cooling time  $t_{8/5}$  vs ultimate tensile strength values of the S960 series

Figure 46 shows the ultimate strength of the HAZ in comparison with the ultimate strength of the base metal of S960.

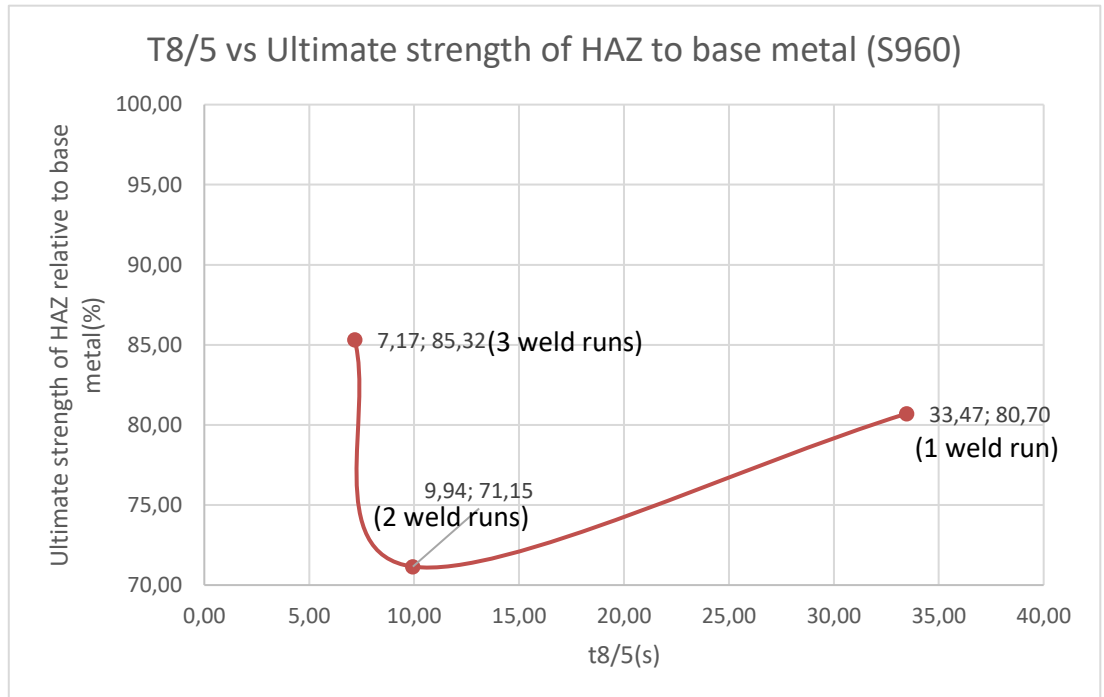


Figure 46. Cooling time  $t_{8/5}$  vs ratio of the strength of the welded samples relative to base metal in S960

#### 4.4.2 S960 specimens hardness test results

Here are the results of the hardness test for S960

Table 23. Hardness test result of S960 series

Series <sup>1)</sup>	Name <sup>2)</sup>	Base 1(A1)	HAZ 1 (B1)	Weld (C)	HAZ 2 (B2)	Base 2 (A2)
S960-1R	S960-1R-1	333	247	254	243	272
	S960-1R-2	291	253	261	248	291
	S960-1R-3	336	264	250	232	305
<b>Average</b>		<b>320</b>	<b>255</b>	<b>255</b>	<b>241</b>	<b>290</b>
S960-2R	S960-2R-1	326	294	256	263	270
	S960-2R-2	315	251	253	287	314
	S960-2R-3	317	276	254	283	299
<b>Average</b>		<b>319</b>	<b>274</b>	<b>254</b>	<b>278</b>	<b>294</b>
S960-3R	S960-3R-1	305	305	251	298	314
	S960-3R-2	308	248	262	293	315
	S960-3R-3	315	250	243	280	285
<b>Average</b>		<b>310</b>	<b>267</b>	<b>252</b>	<b>290</b>	<b>305</b>

<sup>1)</sup> Sample name: [Steel grade]-[Number of weld run(R)]

<sup>2)</sup> Sample name: [Steel grade]-[Number of weld run(R)]-[Specimen number]

Table 24 below shows the averaged hardness value of base metal and HAZ and the conversion of the hardness value to tensile strength for each series.

Table 24. Averaged hardness value and converted tensile strength of S960 series

Series <sup>1)</sup>	Base		HAZ		Weld	
	Hardness Value	Strength	Hardness Value	Strength	Hardness Value	Strength
	(HV)	(MPa)	(HV)	(MPa)	(HV)	(MPa)
S960-1R	305	957	248	790	255	813
Strength capacity <sup>2)</sup> (%)	100	100	81	83	84	85
S960-2R	307	965	276	873	254	810
Strength capacity (%)	100	100	90	90	83	84
S960-3R	307	965	279	880	252	778
Strength capacity (%)	100	100	91	91	82	81

1) Sample name: [Steel grade]-[Number of weld run(R)]

2) The strength capacity of the joints when compared to the base metal strength

The results of the hardness tests show that the longer the cooling time, the higher the hardness value in the HAZ. Three-weld-run samples have the highest hardness value. Two-weld-run samples have lower values and one-weld-run samples have the lowest values. This can be seen in figure 47.

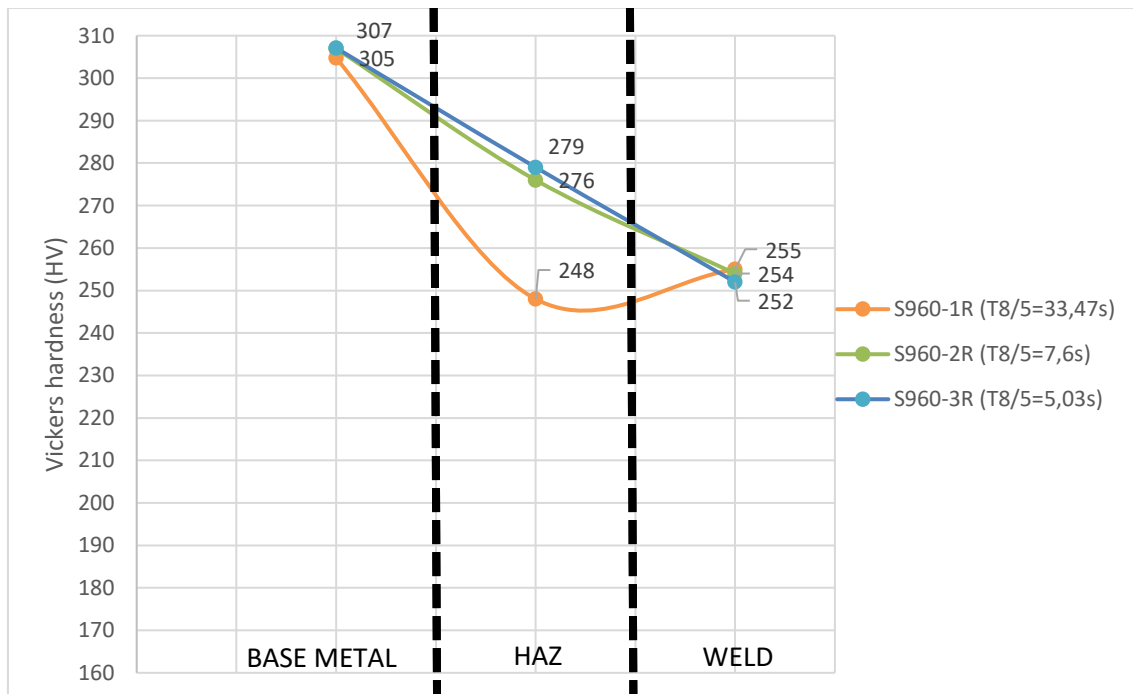


Figure 47. Effect of cooling time on hardness in different regions of S960

The hardness values relative to the base metal ratio also follows this trend; with S960-3R have the highest ratio of hardness of HAZ to base metal,

followed by S960-2R and then S960-1R. Table 48 demonstrates this phenomenon.

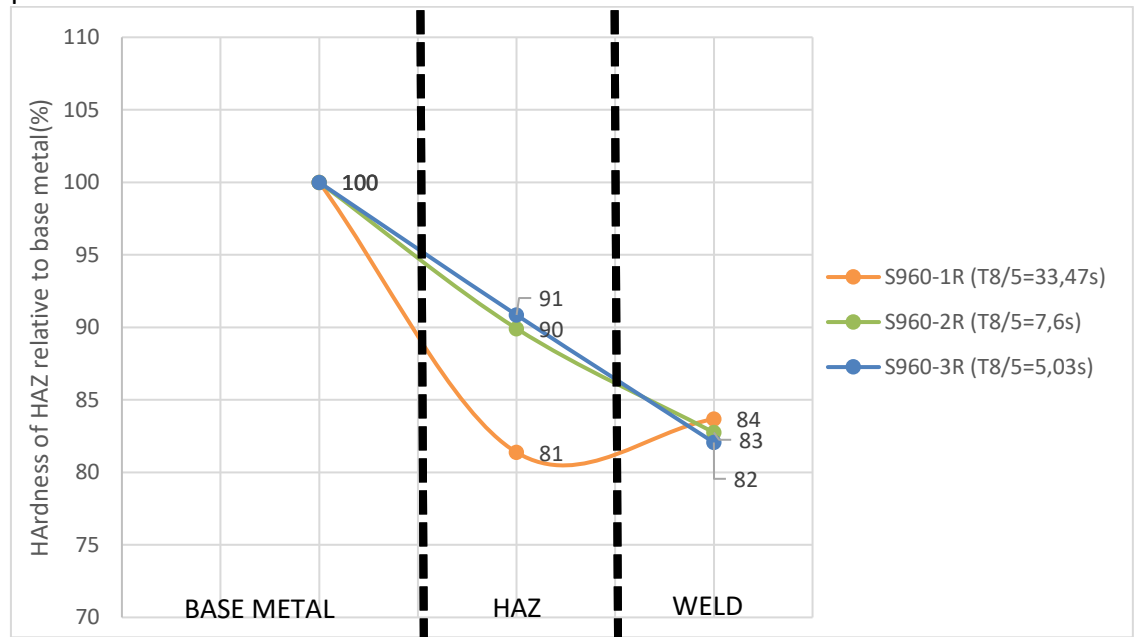


Figure 48. Hardness values relative to base metal of S960 series

The cooling time when comparing with the tensile strength converted from hardness values of S960 also demonstrates a similar tendency to S700. Three-weld-run series have the lowest heat input and cooling time, and the highest tensile strength. The two-weld-run series have a longer cooling time and weaker strength. The one-weld-run series have the highest heat input and cooling time and have the lowest tensile strength. It can be seen that the two-weld-run and three-weld-run series have very similar hardness relative to base metal, thus there might be no need for the third weld run in S960 series to retain most of the hardness of the HAZ. Figure 49 shows the ultimate converted tensile strength of the three weld runs of S960 comparing to the different cooling time.

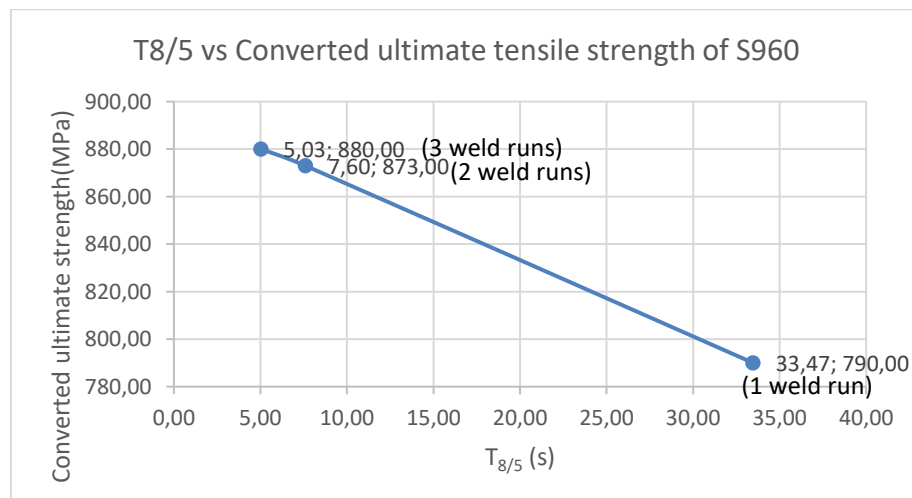




Figure 49 shows the converted ultimate tensile strength of the HAZ when compared with that of the base metal.

Figure 49.  $T_{8/5}$  vs Converted ultimate tensile strength relative to base metal of S960 series

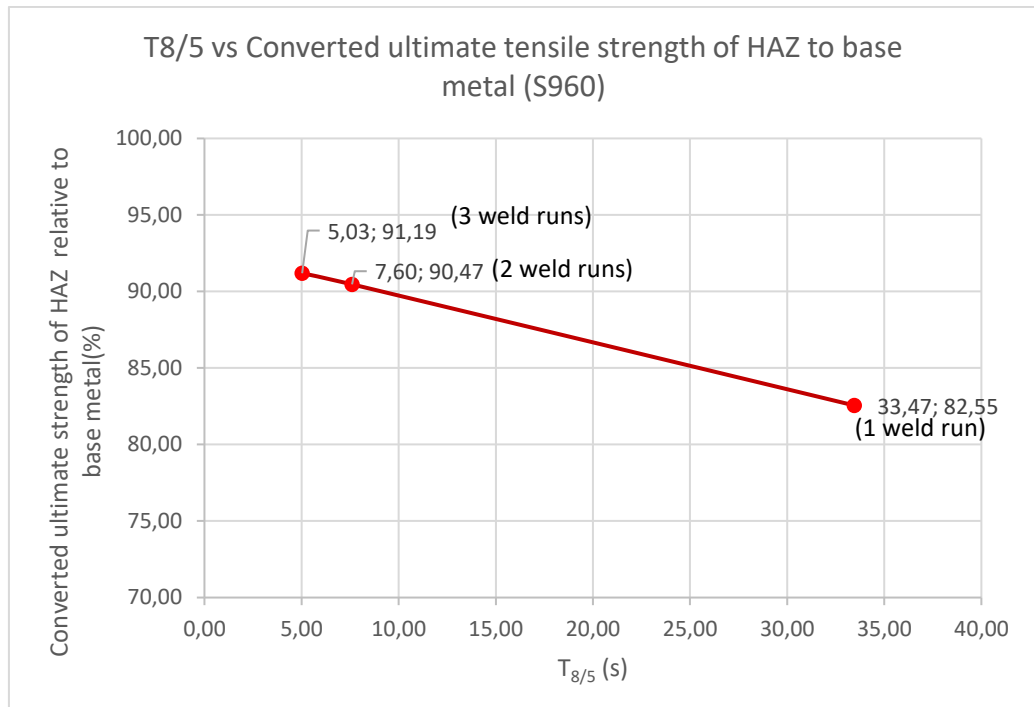


Figure 50.  $T_{8/5}$  vs Converted ultimate tensile strength relative of S960 series

It was noted in S700 hardness test that the higher the cooling time, the lower the tensile strength value of HAZ/base metal ratio.

The difference between the real tests and theory results of the S960 series, similar to S700 series, suggests there were deformations in the joints before the tensile testing. Microscopic examination confirms that S960-2R series have cracks in the joint, thus explaining the irregularly low strength of S960-2R -1. Figure 51 shows the crack in S960-2R series.

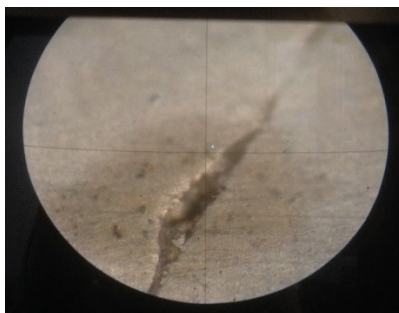


Figure 51. The crack in S960-2R hardness sample shown in microscopic imaging

#### 4.5 Comparing all steel types and analysis

Table 24 shows the summary of the tensile and hardness tests for all steel grades of the research

Steel grades	Name <sup>1)</sup>	Heat input <sup>2)</sup>	Average calculated $t_{8/5}$ <sup>3)</sup>	Average measured $t_{8/5}$ <sup>4)</sup>	Ultimate tensile strength of welded samples $f_{uw}$ <sup>5)</sup>	Strength capacity <sup>6)</sup>	Hardness <sup>7)</sup>	Hardness to base metal <sup>8)</sup>
		(kJ/mm)	(s)	(s)	(N/mm <sup>2</sup> )	(%)	(HV)	(%)
S420	S420-1R	1,48	35,19	36,12	532,68	92,64	171,00	92,50
	S420-2R	0,68	7,66	7,31	535,84	93,19	176,00	94,32
	S420-3R	0,48	3,71	5,73	574,53	99,92	180,00	99,67
S500	S500-1R	1,47	30,15	32,60	614,14	89,65	192,00	87,53
	S500-2R	0,72	10,13	7,99	647,36	94,50	200,00	92,48
	S500-3R	0,48	6,28	5,55	659,20	96,23	211,00	98,37
S700	S700-1R	1,37	30,15	20,70	652,19	74,96	212,00	77,00
	S700-2R	0,79	10,13	8,46	698,57	80,30	219,00	80,00
	S700-3R	0,61	6,28	6,12	620,88	71,37	223,00	81,00
S960	S960-1R	1,48	35,19	33,47	776,64	80,70	248,00	81,00
	S960-2R	0,71	8,46	9,94	684,70	71,15	276,00	90,00
	S960-3R	0,49	3,92	7,17	821,03	85,32	279,00	91,00

1) Sample name: [Steel grade]-[Number of weld run(R)]

2) Average heat input taken from the weld sessions

3) Average calculated  $t_{8/5}$  obtained by using formula (2) and (3)

4) Average measured  $t_{8/5}$  attained after analysing the data from infrared camera temperatures

5) Ultimate tensile strength of welded sample  $f_{uw}$  taken after tensile testing the welded samples

6) The strength capacity of the joints when compared to the base metal strength

7) Average hardness values of the HAZ of each steel sample

8) Hardness of HAZ in relative with hardness of base metal

When analysing S420 and S500, it can be seen that the higher the cooling time, the lower the strength and strength capacity of the joint. The results of S420 and S500 show a relation between the cooling times and tensile strength of the samples. Higher heat inputs lead to longer cooling times, and longer cooling times lead to weaker weld joints. A low heat in-put could be used during three run welding and the samples made using this technique gave the highest tensile strength results (the strength capacity of the specimens of the S420-3R and S500-3R series were more than 96%). The hardness results of S420 and S500 also follow the trend of the tensile test as three-run series have the highest hardness and HAZ's hardness to the hardness of base metal ratio. The two-weld-run sample have less hardness and hardness capacity and one-run samples have the least hardness and hardness capacity of three weld run types. Figures 52 and 53 show the tensile and hardness value of S420 and S500 in relation to their base metal.

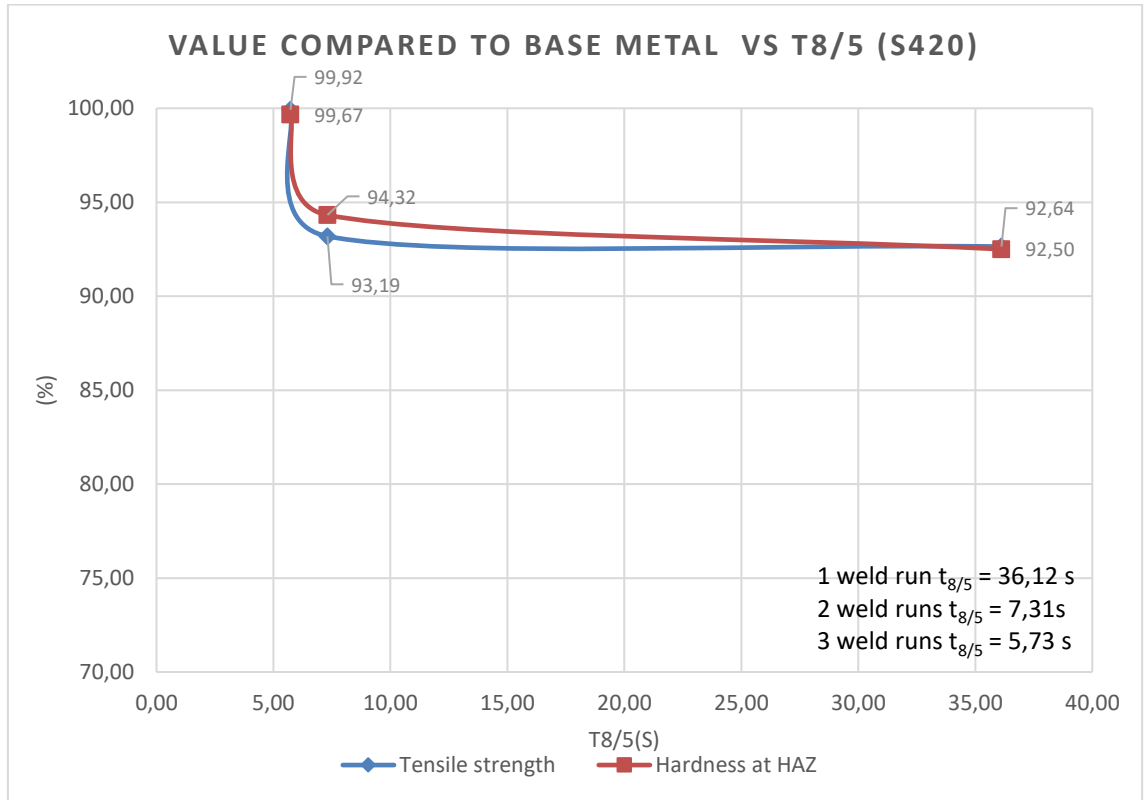


Figure 52. Value compared to base metal vs T8/5 (S420)

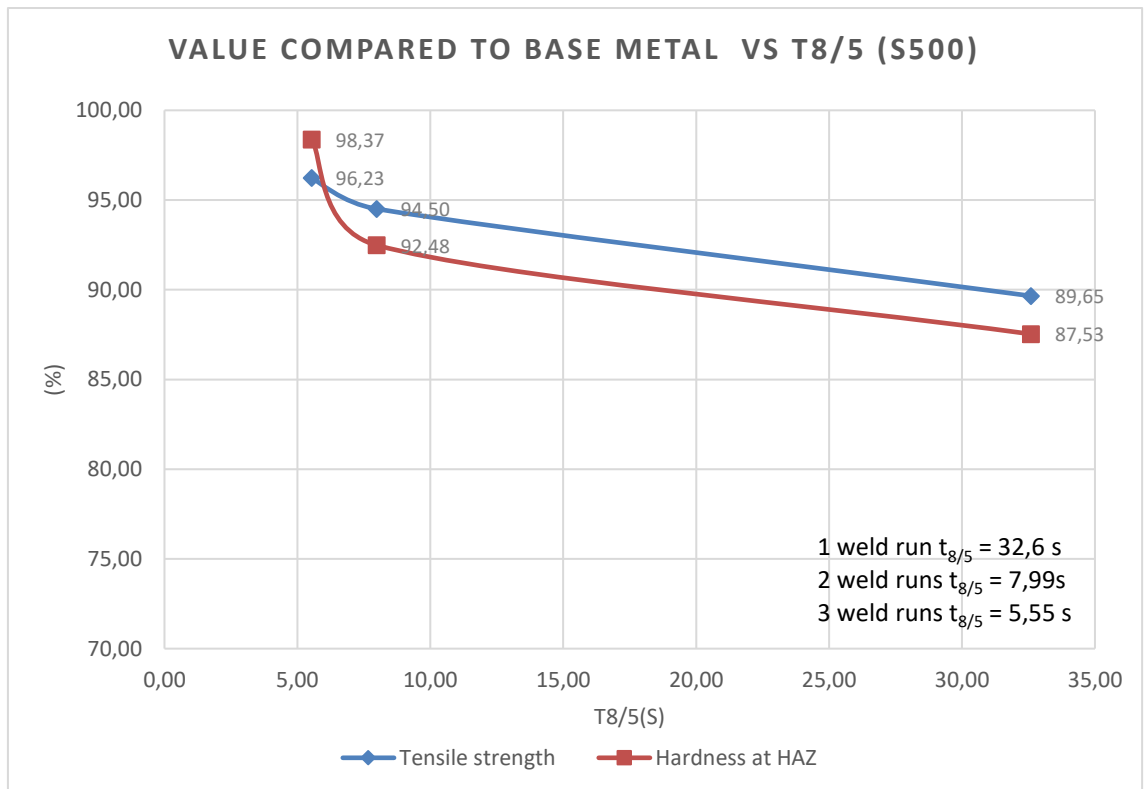


Figure 53. Value compared to base metal vs T8/5 (S500)

Based on the two graphs in figure 52 and 53, it can be seen that the tensile values have a direct relation with the hardness values. The increase in the

hardness value also contributes to the increase in the tensile values. It can also be seen that if the cooling time is less than 6 seconds, the deterioration of the quality of the joint is less significant. With 6 seconds or less cooling time, the strength of HAZ equals to 96 to 99 per cent of the base metal. This can be expressed by the equation:

$$F_{uw} = F_{ub} * \alpha \quad (9)$$

Where  $F_{uw}$  is the ultimate strength of the HAZ (MPa),  $F_{ub}$  is the ultimate strength of the base metal (MPa) and  $\alpha$  is the coefficient ( $0,96 \leq \alpha \leq 0,99$ ) The hardness of the HAZ remains almost 99% if the cooling time is less than 6 seconds.

$$HV(\text{HAZ}) = HV(\text{B}) * 0,99 \quad (10)$$

Where  $HV(\text{HAZ})$  is the Vickers hardness of the HAZ (HV) and  $HV(\text{B})$  is the Vickers hardness of the base metal (HV)

However, too low a cooling time can lead to inadequate weld fusion or brittle joint. It is recommended in future testing that the heat input and welding be monitored carefully, preferably with a robot so that all the parameters are controlled and reliable.

As mentioned in the previous chapters, the tensile results of S700 and S960 series were unpredictable and did not follow any trend. Both series failed at the weld during tensile tests. The high standard deviation values of some samples suggest that there were some abnormalities in the joint quality. When analysing hardness test results, it can be seen that the higher the cooling time of S700 and S960, the lower the hardness values become. The HAZ hardness to base metal hardness ratio also follows this tendency; with the three-weld-run having the highest percentage. The two-run series have less HAZ to base metal percentage and the one-run series has the least HAZ to base metal percentage. It can be assumed that the low strength of the filler material and bad welding practice affected the quality of the joint. The cracks inside the joints of some specimens could have caused the premature failure of the weld instead of the HAZ. The two graphs in Figure 54 and Figure 55 show the tensile and hardness value of S700 and S960 in relation to their base metal.

When examining the hardness of HAZ relative to base metal of these 4 series, it is notable that the three-weld-run and two-weld-run of S700 and S960 have very close percentage (81% to 80% in S700 case and 91% to 90% in S960). On the other hand, the difference of HAZ to base metal ratio in S420 and S500 is more remarkable (99% to 94% in S420 case and 98% to 92% in S500 case). It can be assumed that in the case of high strength steel like S700 and S960, the difference in hardness of three and two-weld-run is not significant. In lower strength steel, the differences in hardness between three and two-weld-run is more distinguished.

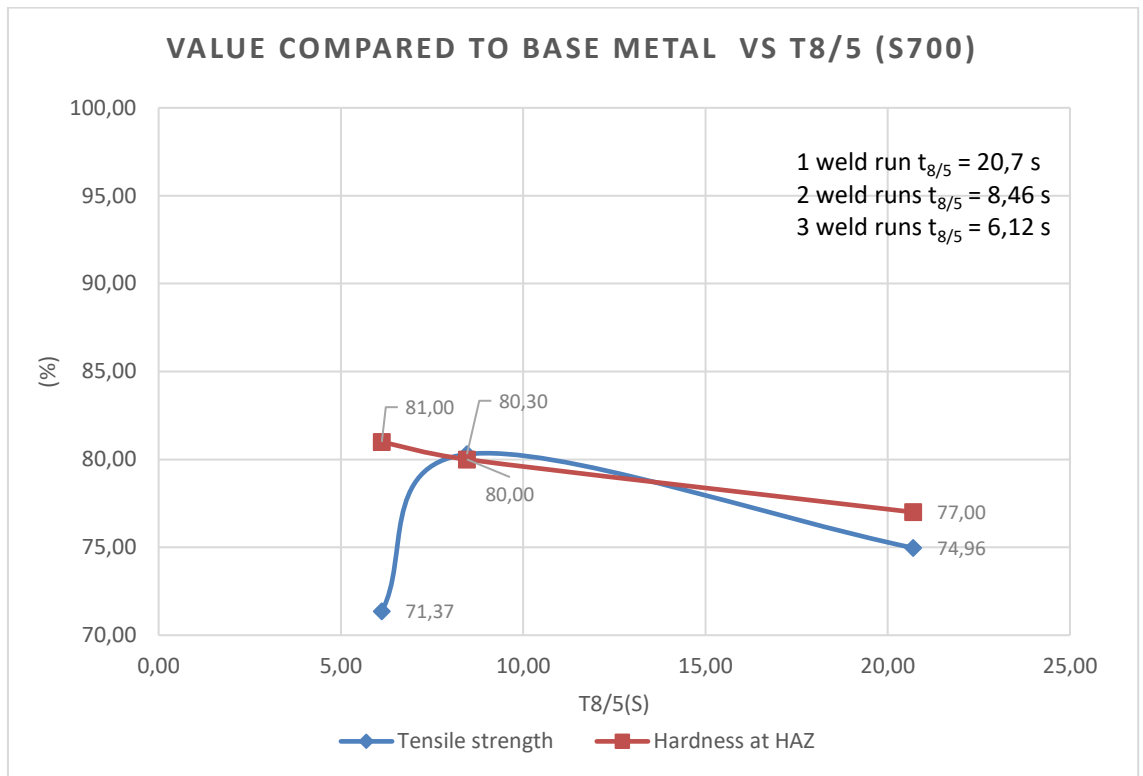


Figure 54. Value compared to base metal vs T8/5 (S700)

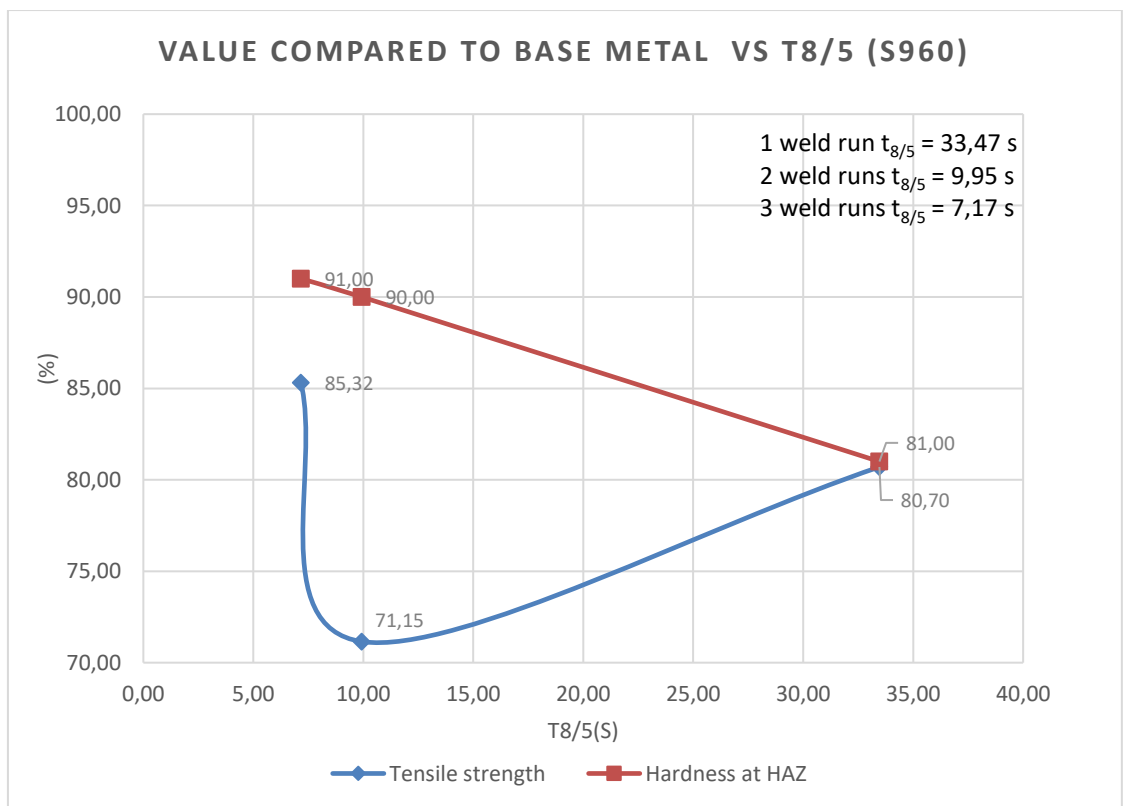
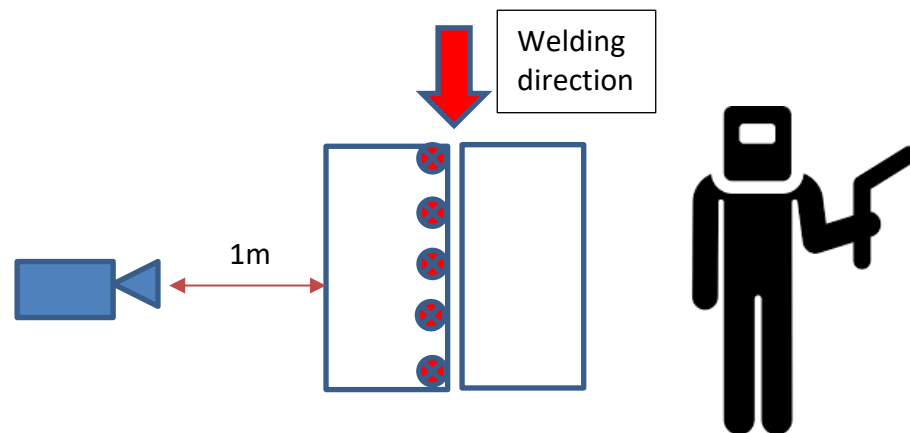


Figure 55. Value compared to base metal vs T8/5 (S960)

It is recommended in future researches that a filler material with stronger tensile strength than base metal should be used. The type of filler material

should be chosen according to EN ISO 16834-A. The reliability of the tests depends on the quality of the weld. Proper care should be taken during and after the weld runs such as cleaning of the weld after each run to remove dusts and anomalies that can appear inside the weld. The ultimate strength of the HAZ cannot be tested if the weld fails like in the case of S700 and S960.

It is also recommended that in future tests, thermocouples and infrared camera technique should be used and further developed to confirm the accuracy. The reference model should have more thermocouples because the welding speed is not stable during welding so the cooling time of each point along the weld is different. The position of infrared camera is also important so that the vision of the thermocouple spots is not blocked by the welder during the welding sessions. Using robot welding is advised because the welding speed remains constant and the blocking of the view is less likely to happen. Figure 56 demonstrates the recommended set up for the future test with a human welder (diagram not in scale).



Infrared camera	Welded plates	Welder
Recommended distance 1 m from the welded plates	Having at least 5 thermocouples along the weld for more accuracy	Stay in the opposite side of the infrared camera to not block the view of the camera

Figure 56. Recommendation for setting up the welding session in the future

## 5 CONCLUSION

The research confirms that the parameters such as heat input, cooling time and the types of filler materials are crucial when doing butt-welded joints.

Insufficient strength of the filler materials and inadequate welding technique can lead to instability of the joint. Cracks inside the weld can become stress concentration points and likely fail before the HAZ does. Therefore, it is important to ensure that the strength of the filler material to be equal or higher than the base metal so this type of tensile failure will not occur.

It is recommended that thermocouples and infrared camera are used in future tests to examine the accuracy of the technique. The method should be more developed because it proved to reduce the time to set up the tests significantly.

The research shows that HAZ is the critical part of the welded joint because it usually has the lowest tensile strength in the joint and prone to fail during tension. Based on all the test results, the welded samples show a low decrease in quality when the cooling time is below 10 seconds. The lower the cooling time, the better the strength and hardness of the specimens can be. This is achieved easiest with multiple weld runs, with each weld run having a low heat input. However, too low a cooling time can lead to inadequate weld fusion or brittle joint. Proper establishment of the test parameter and careful monitoring is of utmost importance for a good weld quality.

Four steel types, which are S420, S500, S700 and S960, were investigated during the research. However, the results of S700 and S960 series are not reliable due to the faulty welding techniques and insufficient strength of the filler material. Further research maybe carried out for S960 with the appropriate filler strength and S700 with better welding techniques to investigate the behaviour of the joint before comparison can be made between the four mentioned steel types.

When analysing the reliable specimens of S420 and S500, it can be seen that the heat input has direct relations with the tensile strength of the specimens. Samples welded with the highest heat input had less than 93% strength of the base metal. Samples with a lower heat input amounted to around 93 to 94% of the base metal while samples welded with the lowest heat input had more than 96% strength of the base metal. It can be seen from the hardness test results that the heat input affects the hardness the same way as it does tensile strength. Samples welded with the highest heat input have less than 92% the hardness of the base metal. Specimens with a lower heat input reached around 92 to 94% and specimens with the lowest heat input achieved more than 98 % the hardness of the base metal.

## REFERENCES

Ashby, M.F & Hunkin-Jone, D.R (2005). *Engineering Materials 2: An Introduction to Microstructures, Processing, and Design*. Butterworth-Heinemann

Croft, D. (1996). *Heat treatment of welded steel structures*. Cambridge. Abington Publishing.

EN 1011-2 D4. Welding. Recommendations for welding of metallic materials. Part 2: Arc welding of ferritic steels. SFS Online. Retrieved 15 April 2018 from <https://online.sfs.fi>

EN ISO 16834-A (2012). Welding consumables. Wire electrodes, wires, rods and deposits for gas shielded arc welding of high strength steels. SFS Online. Retrieved 18 May 2018 from <https://online.sfs.fi>

EN ISO 15609-1(2004). Specification and qualification of welding procedures for metallic materials. Welding procedure specification. Part 1: Arc welding. SFS Online. Retrieved 25 May 2018 from <https://online.sfs.fi>

EN ISO 6892-1(2016). Metallic materials – Tensile testing - Part 1: Method of test at room temperature. SFS Online. Retrieved 17 June from <https://online.sfs.fi>

EN ISO 5178 (2001). Destructive tests on welds in metallic materials. Longitudinal tensile test on weld metal in fusion welded joints. Retrieved 17 June from <https://online.sfs.fi>

EN ISO 6507-1(2005). Metallic materials – Vickers hardness test – Part 1: Test Method. Retrieved 8 July from <https://online.sfs.fi>

EN ISO 15612 (2004). Specification and qualification of welding procedures for metallic materials. Qualification by adoption of a standard welding procedure. SFS Online. Retrieved 2 June from <https://online.sfs.fi>

Greiçevci, B. (2016). *Effect of heat input on the mechanical properties of high strength steel butt-welded joints*. Bachelor's thesis. Degree Programme in Construction Engineering. HAMK University of Applied Science

Maleque, M.A ; Salit, M.S. (2013). *Material selection and design*. Springer Science and Business Media

Raabe, D.; Choi, P. P.; Li, Y. J.; Kostka, A.; Sauvage, X.; Lecouturier, F.; Hono, K.; Kirchheim, R.; Pippan, R.; Embury, D. (2010). *Metallic composites*



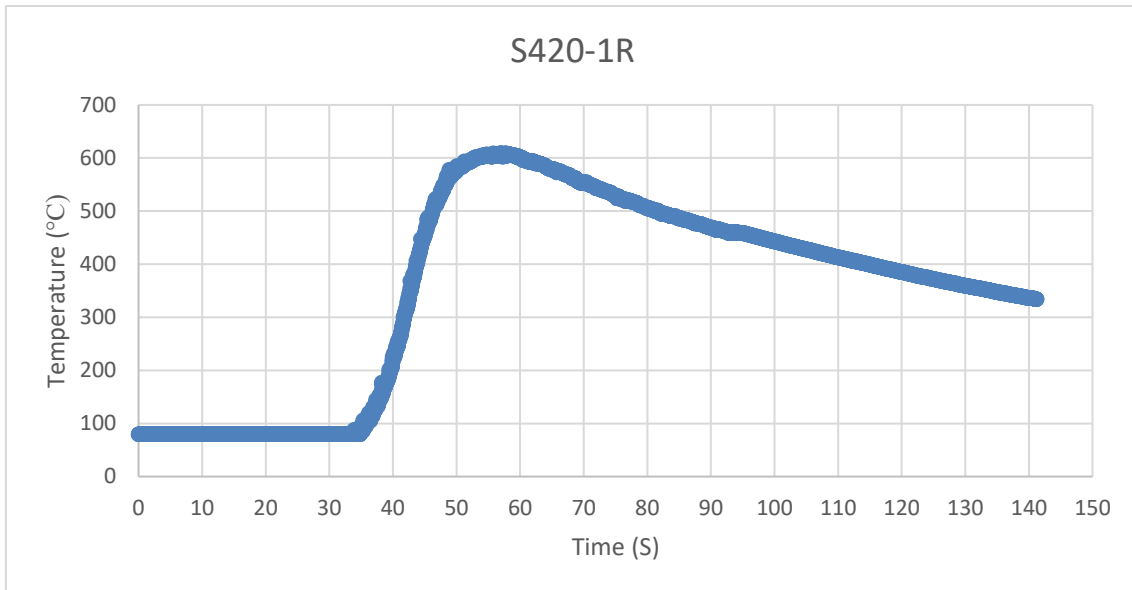
*processed via extreme deformation - Toward the limits of strength in bulk materials*. Cambridge. MRS Bulletin.

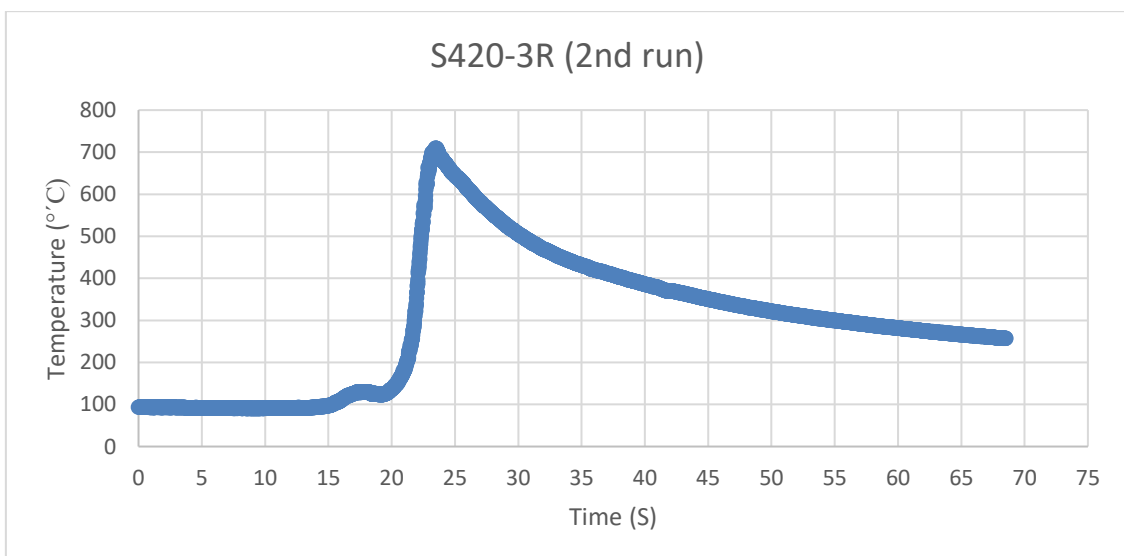
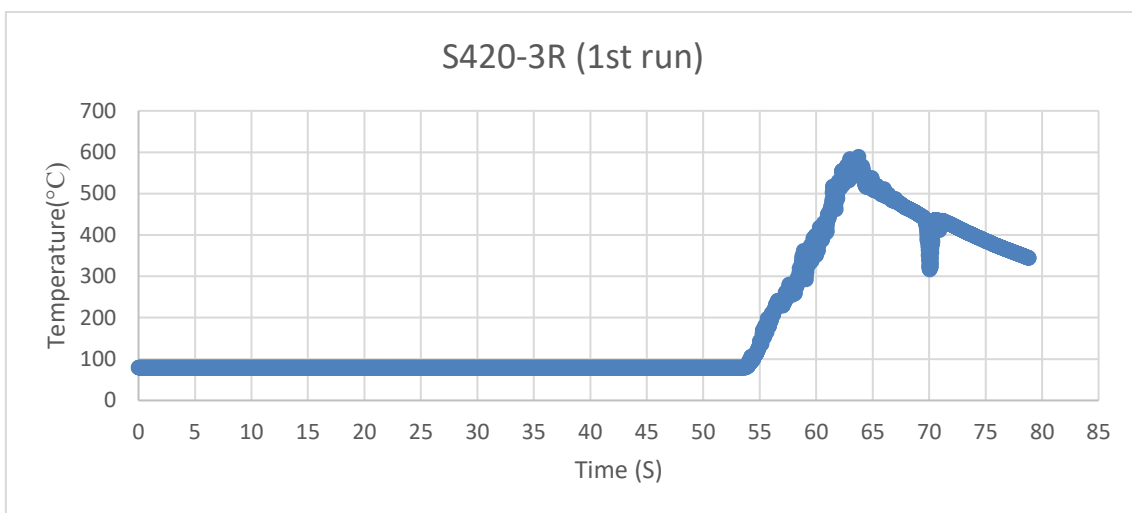
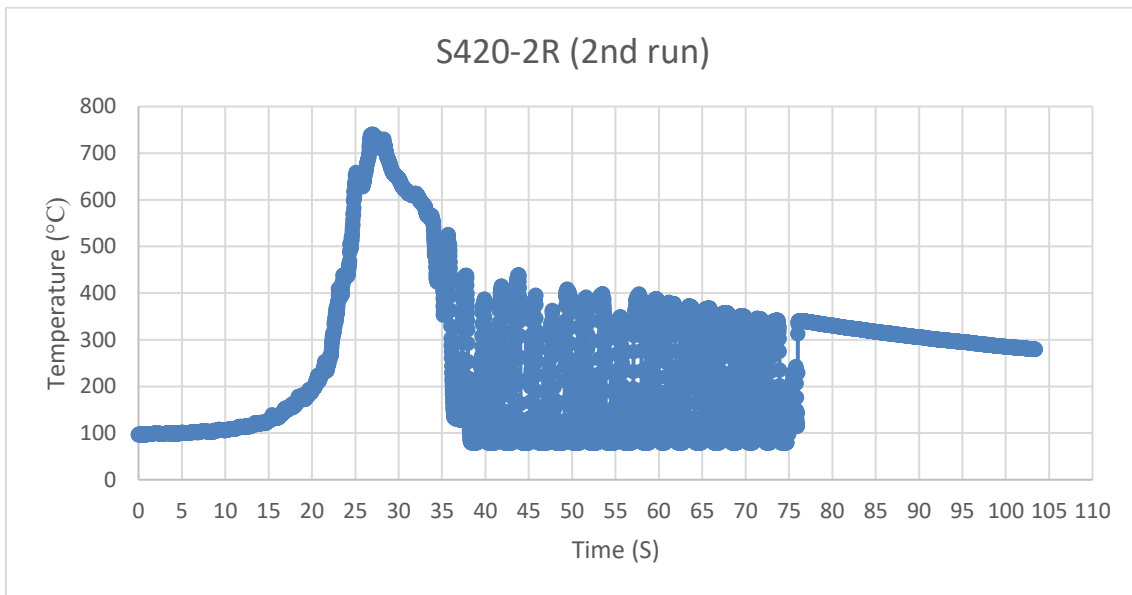
SFS-EN ISO 4136 (2012). Destructive tests on welds in metallic materials. Transverse tensile tests. SFS Online. Retrieved 2 June from <https://online.sfs.fi>

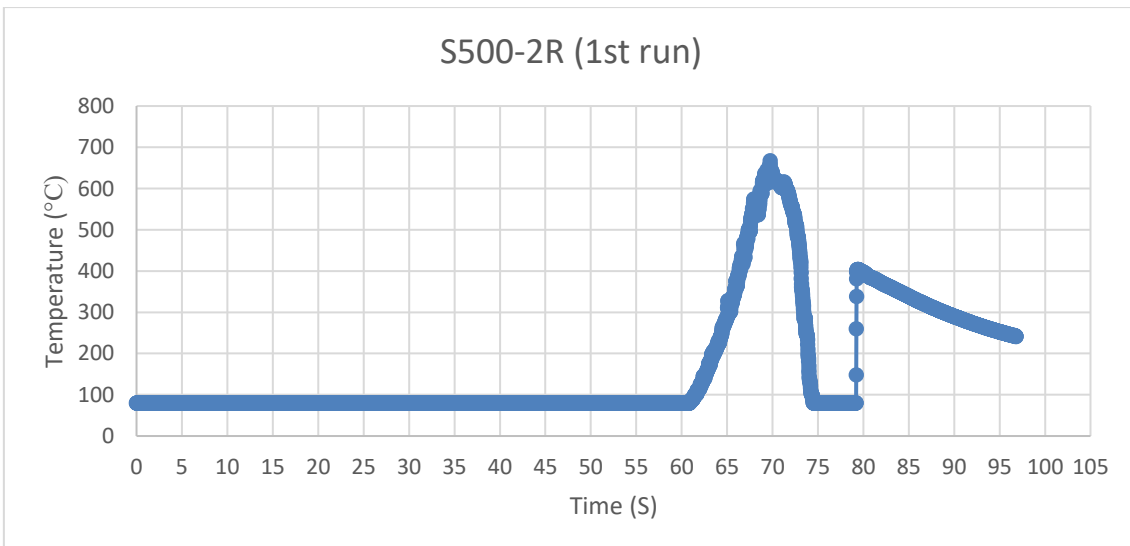
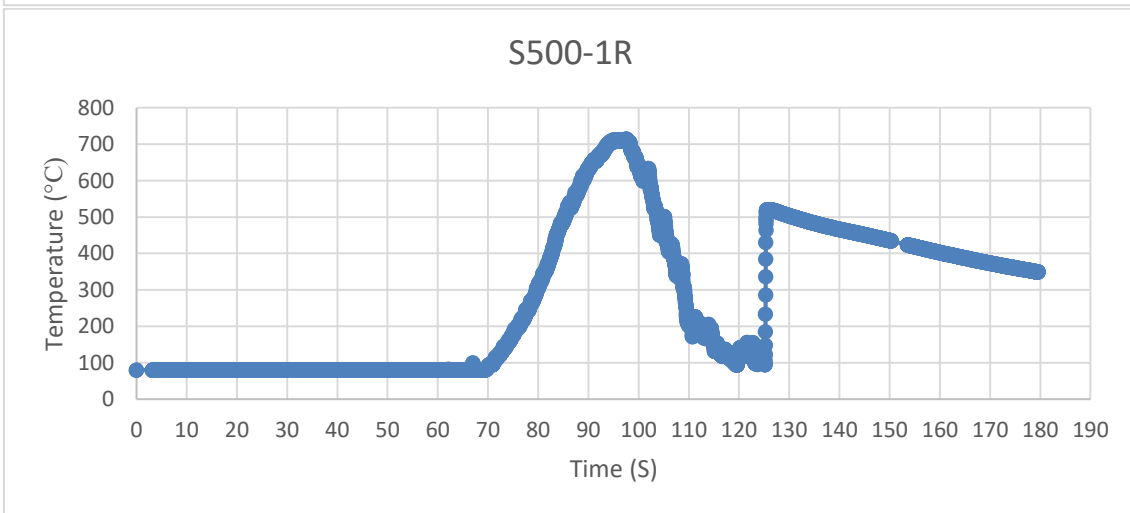
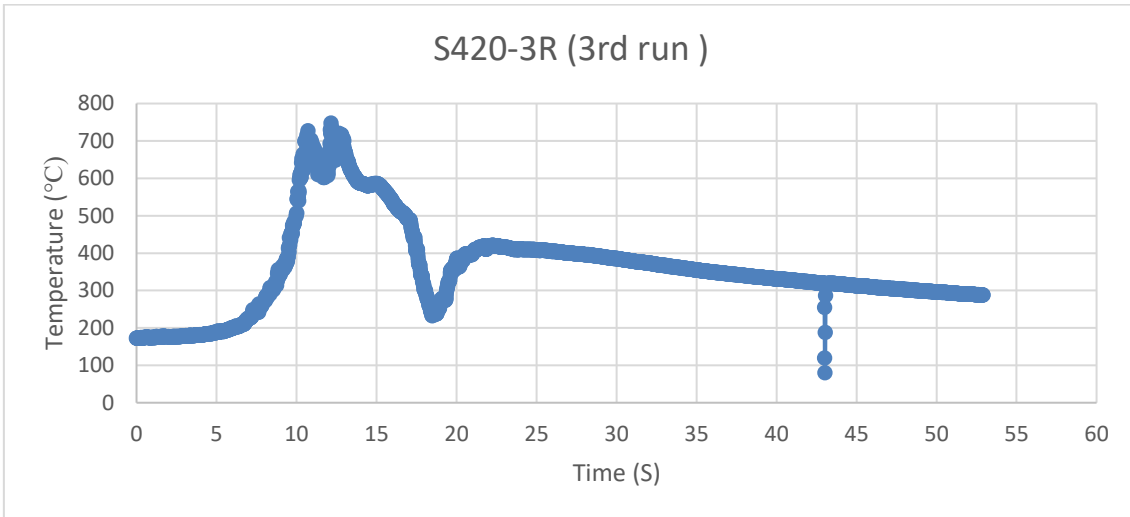
Zhang, P., Li, S. and Zhang, Z. (2011). *General relationship between strength and hardness*. *Materials Science and Engineering*. Chinese Academy of Sciences, Shenyang 110016, PR China

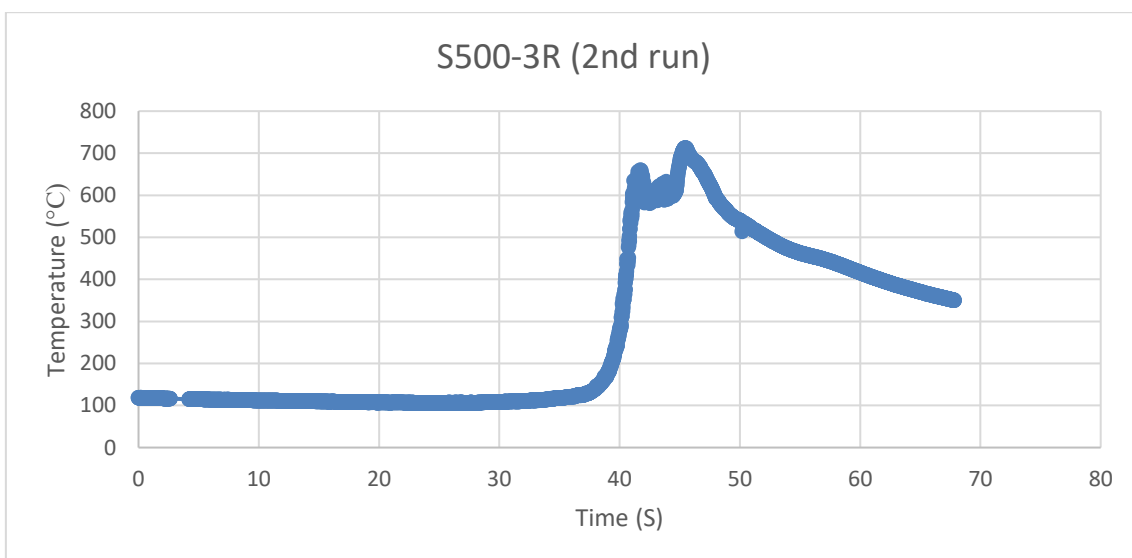
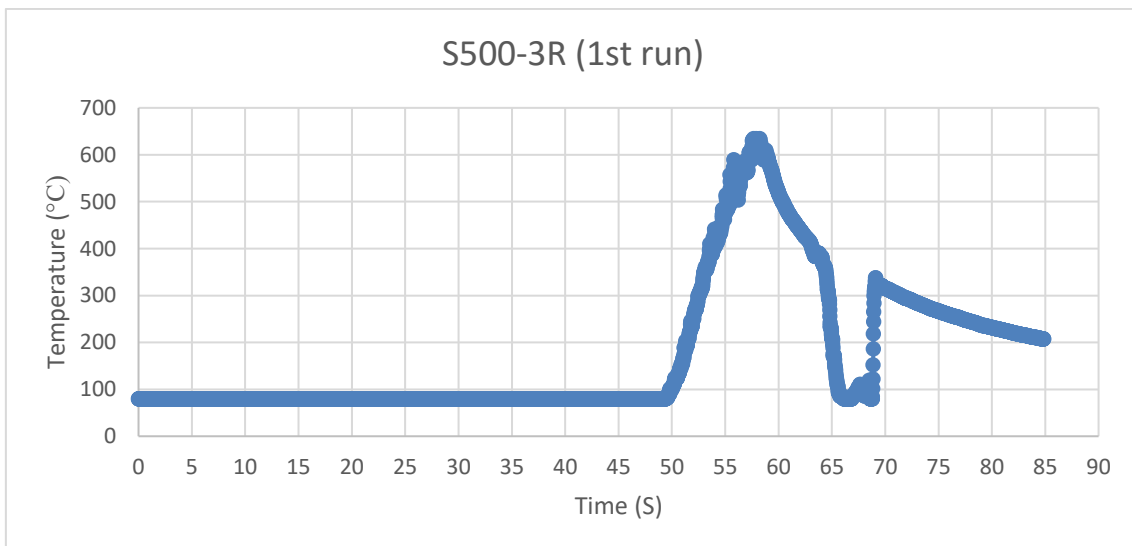
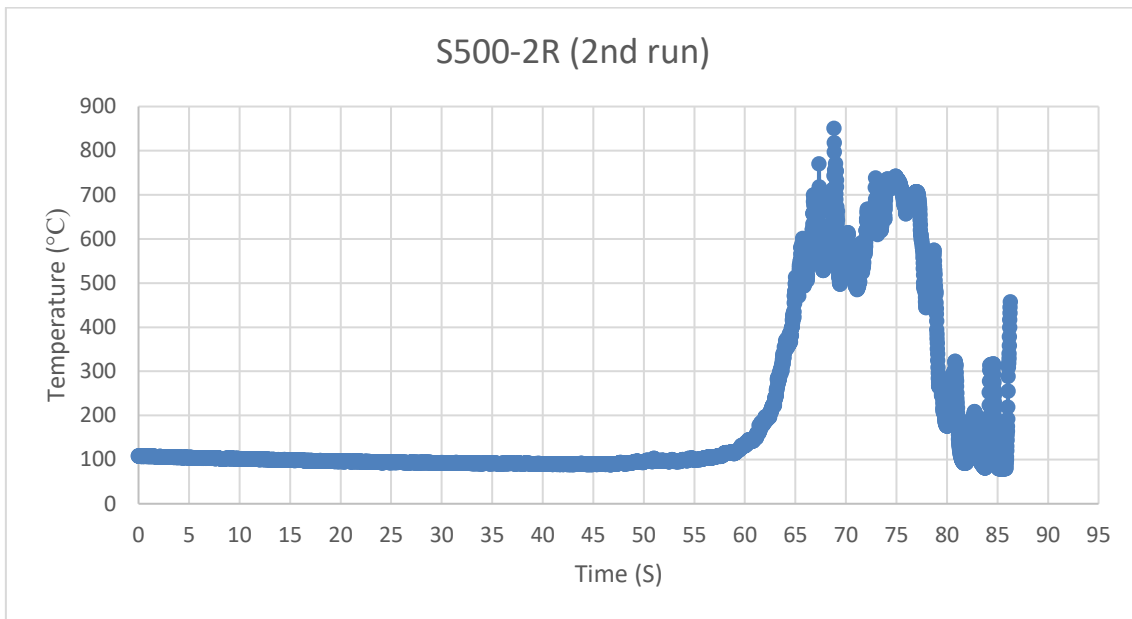
## APPENDIX 1

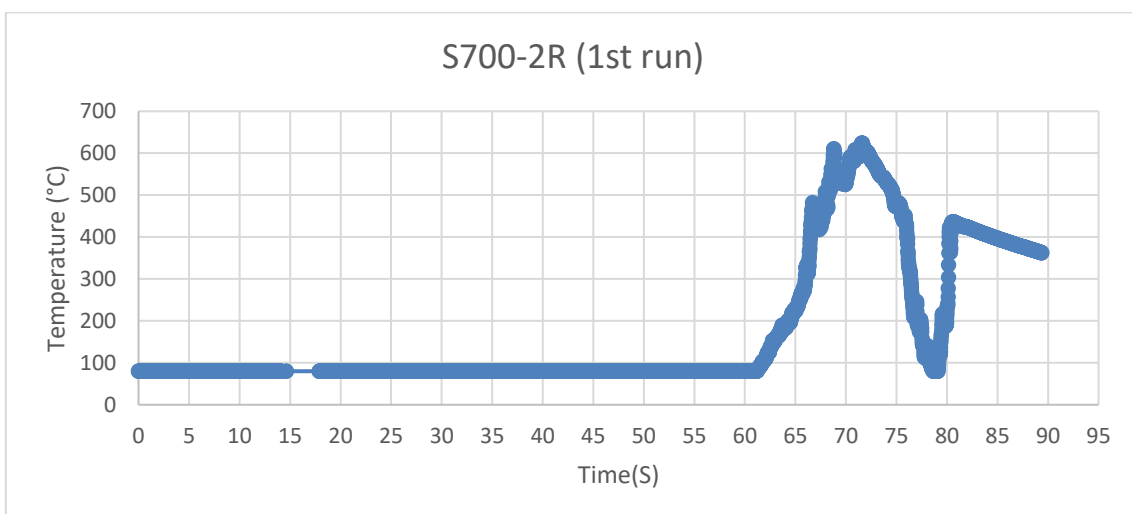
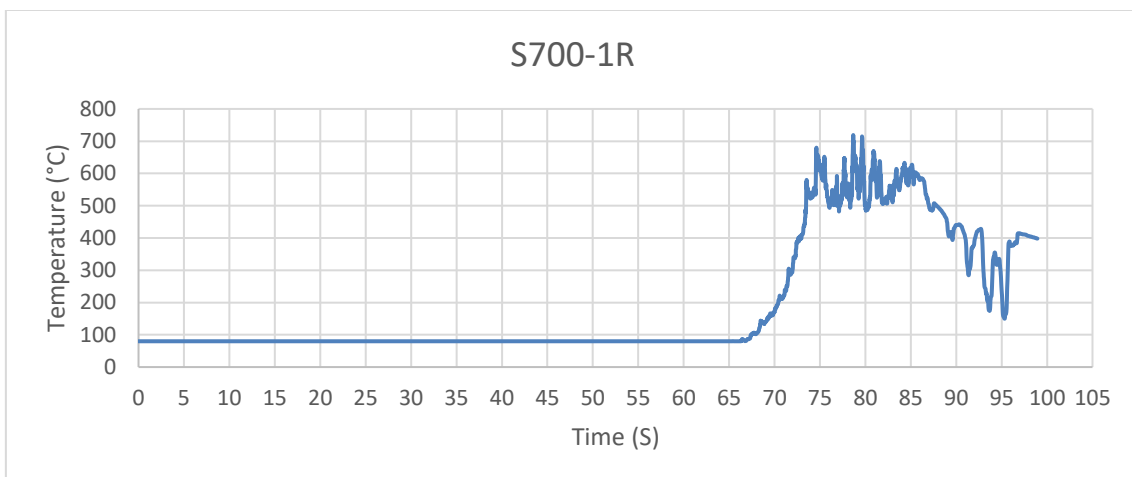
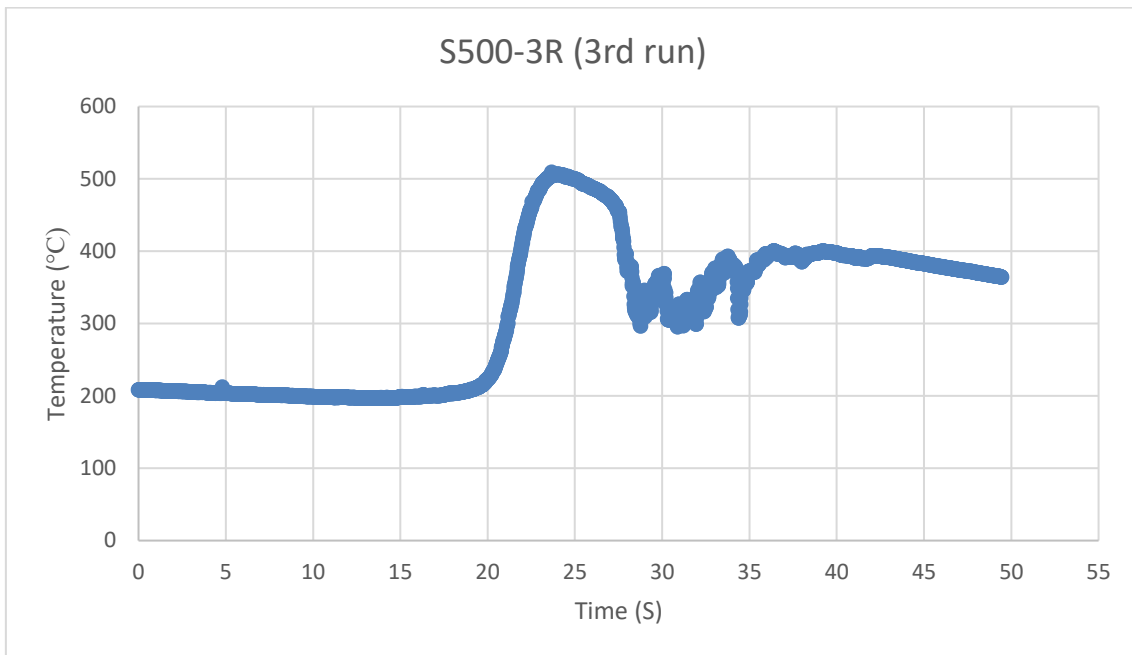
## COOLING TIME GRAPHS FROM INFRARED CAMERA

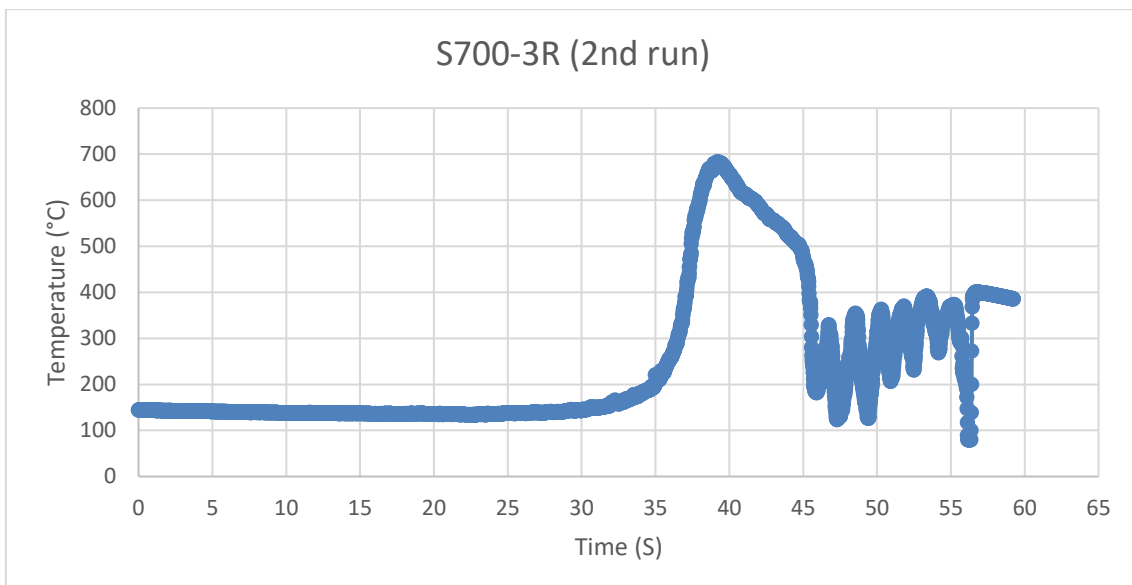
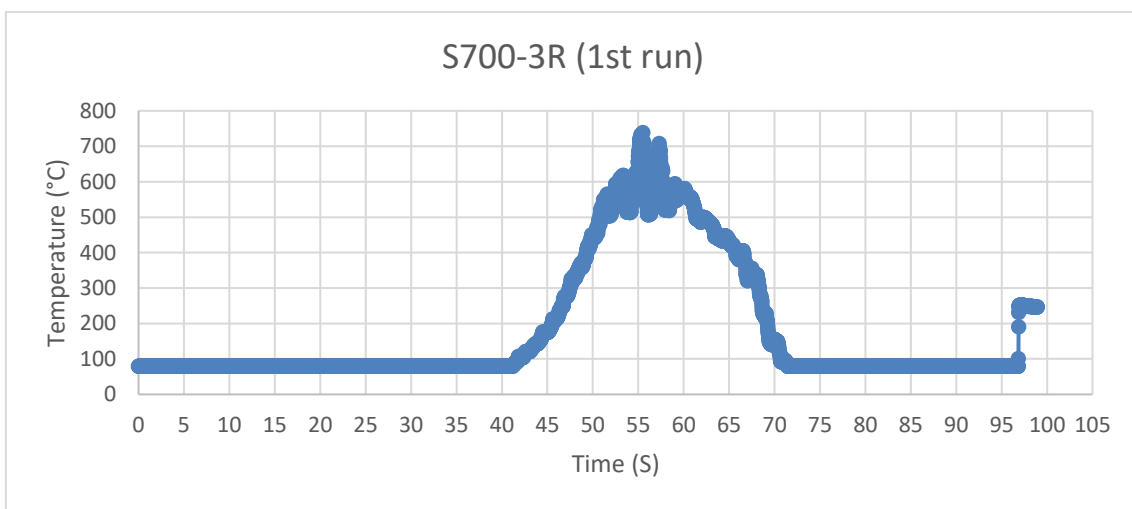
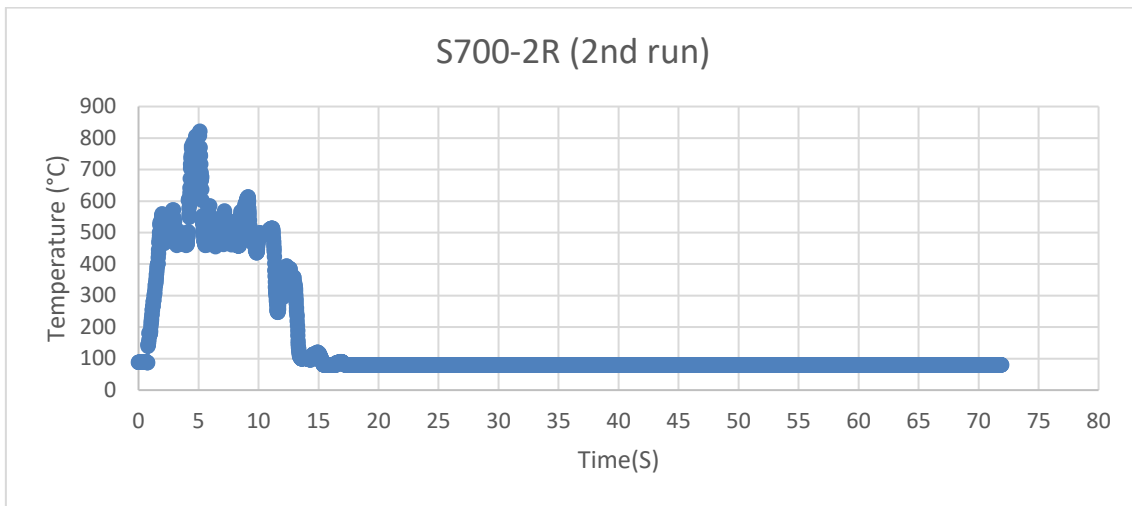


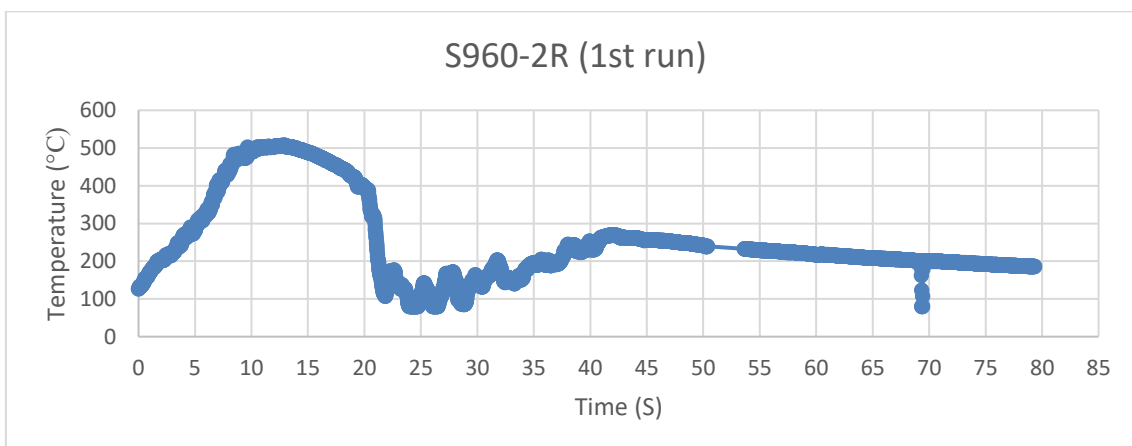
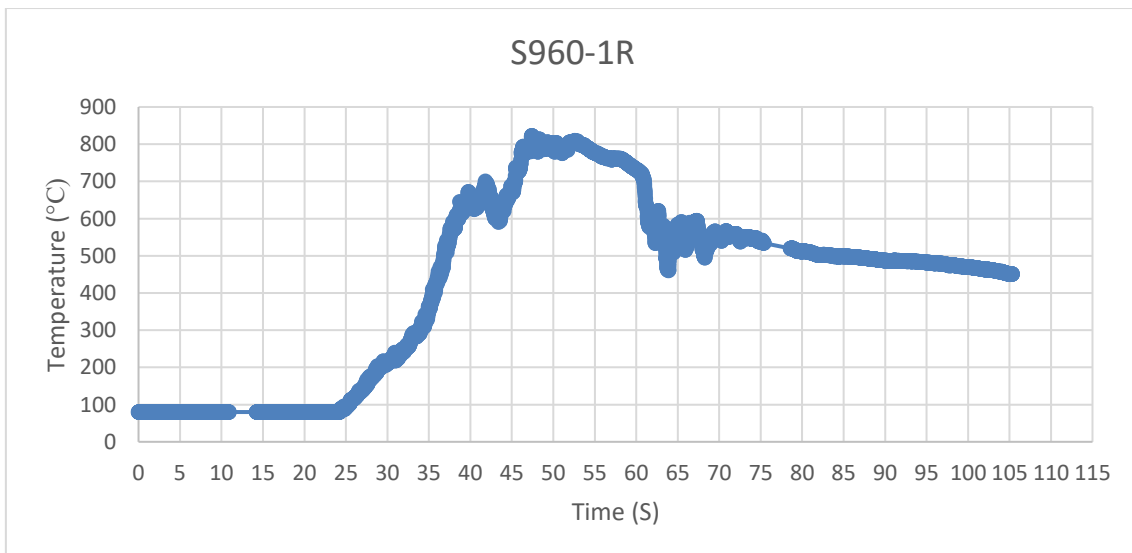
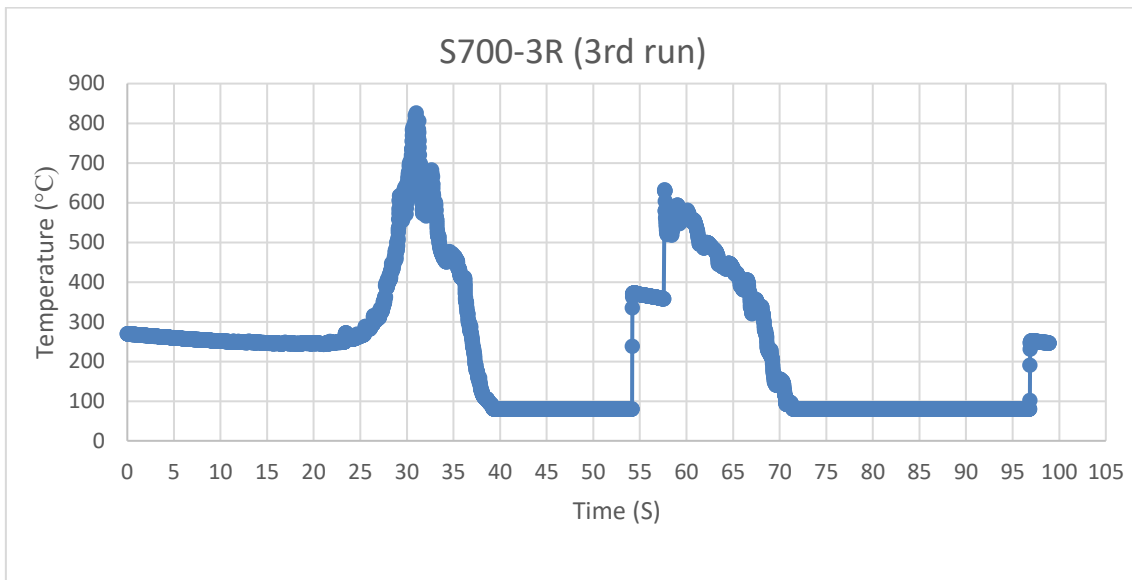




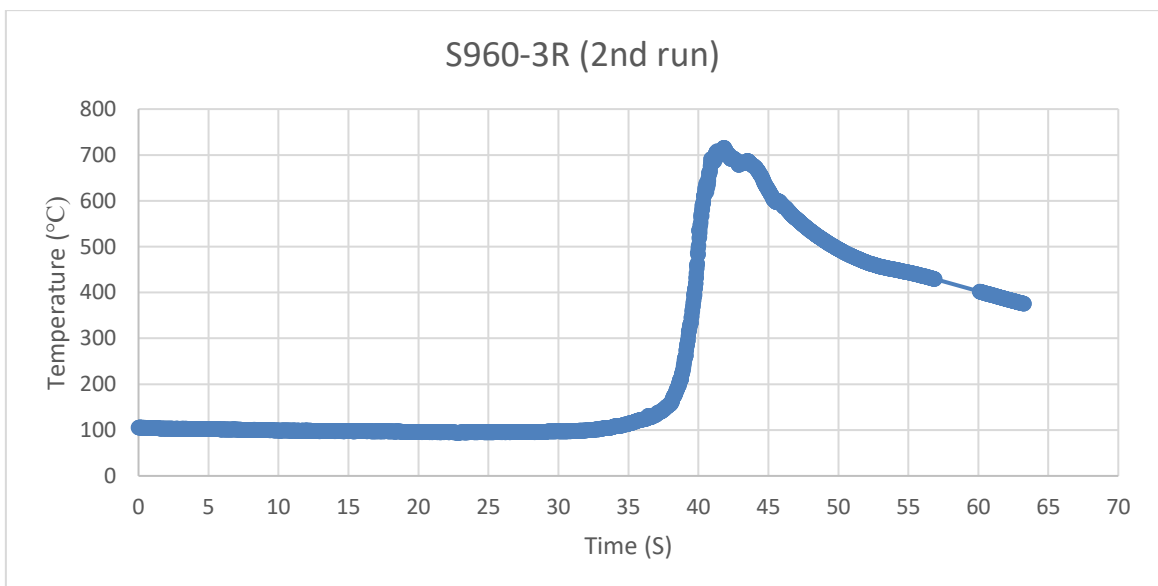
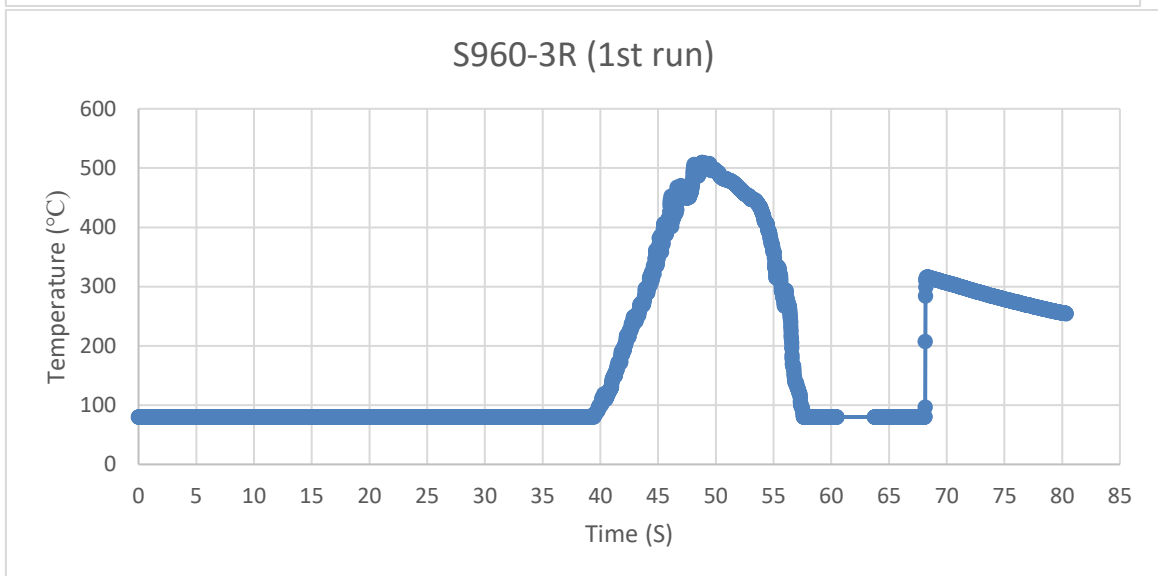
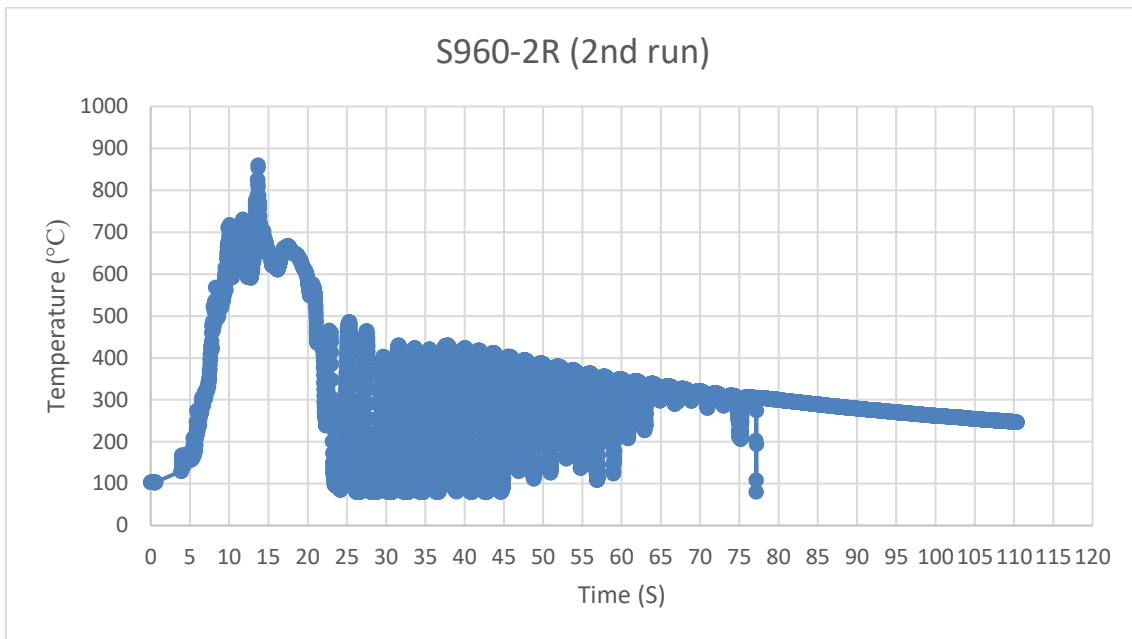


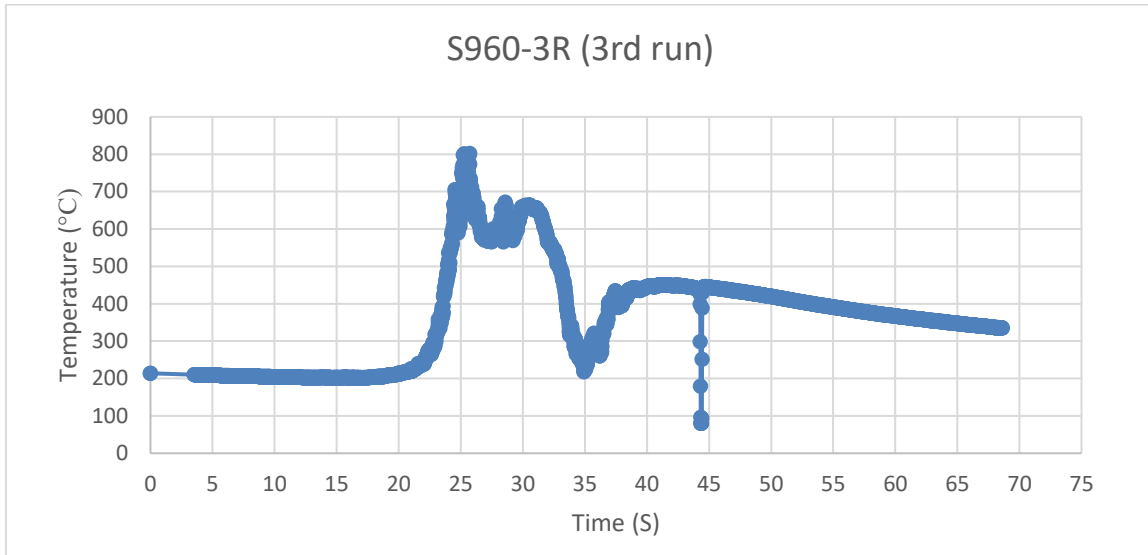




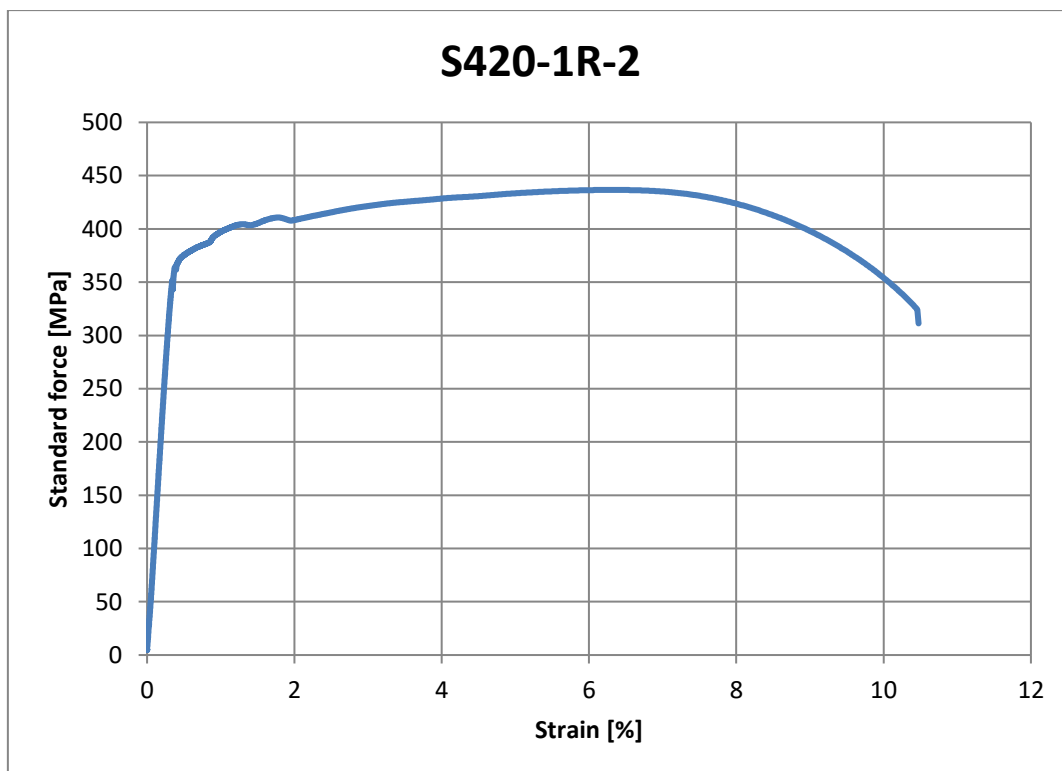
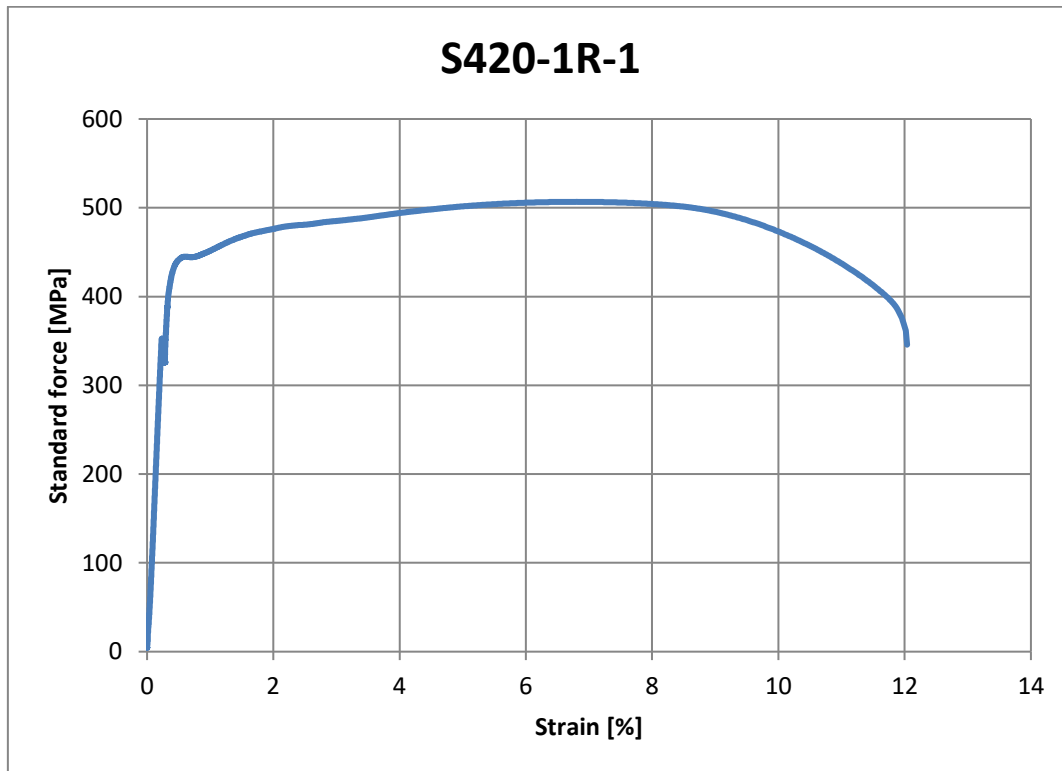


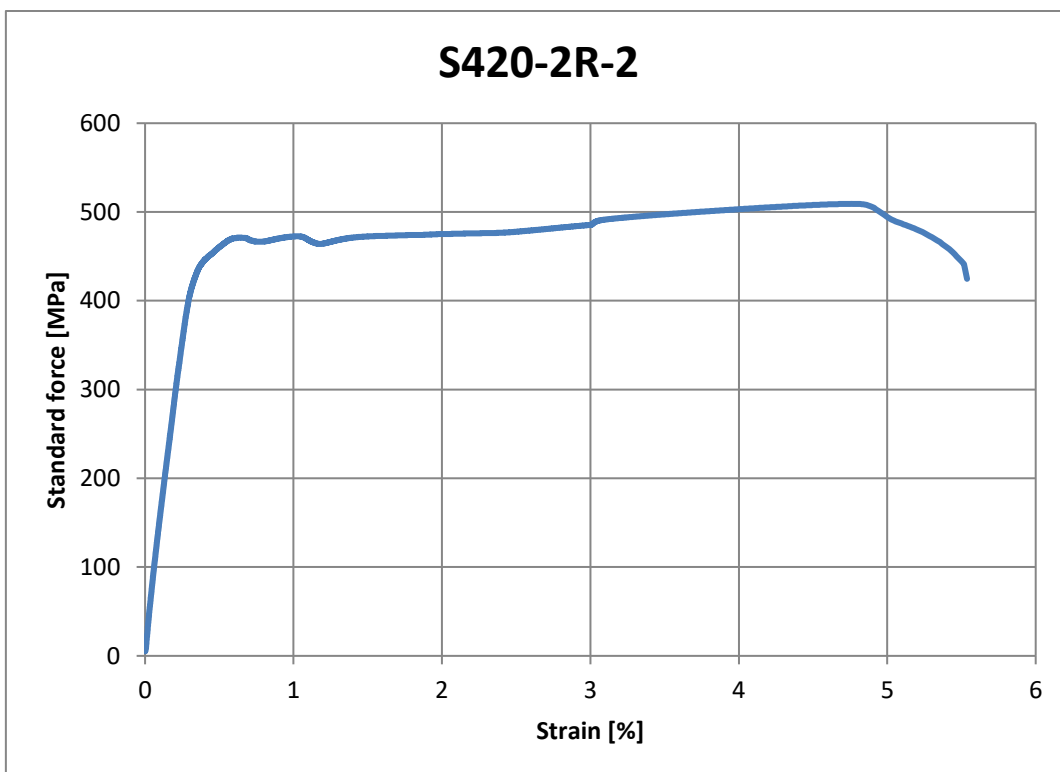
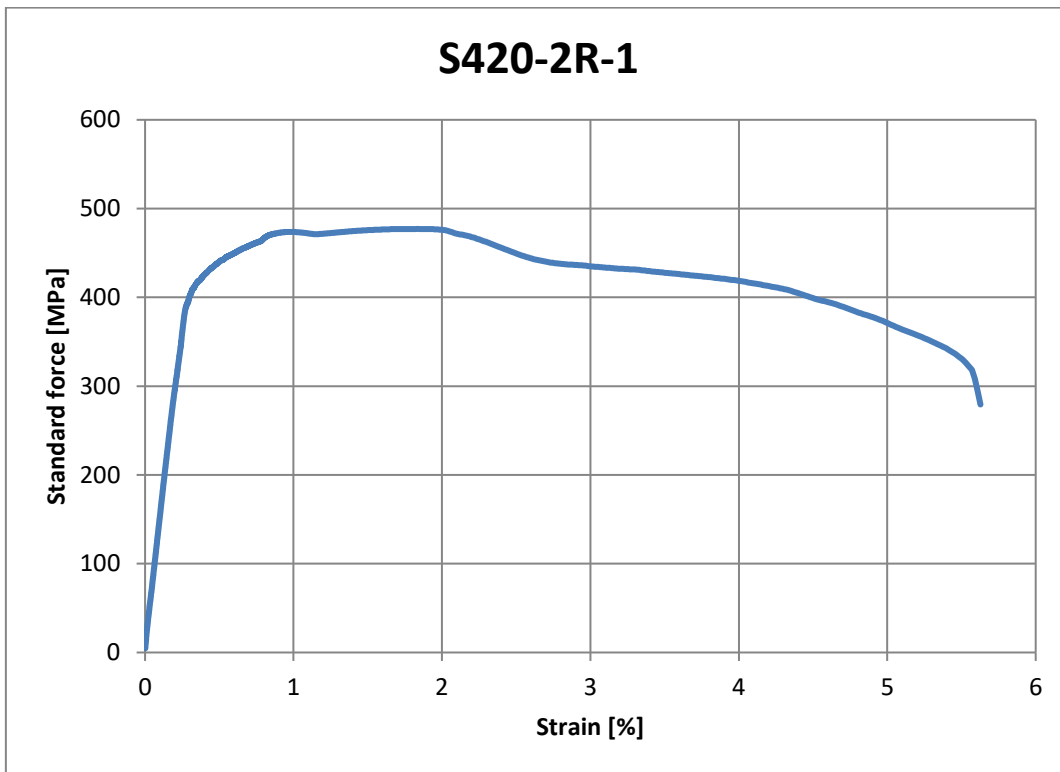


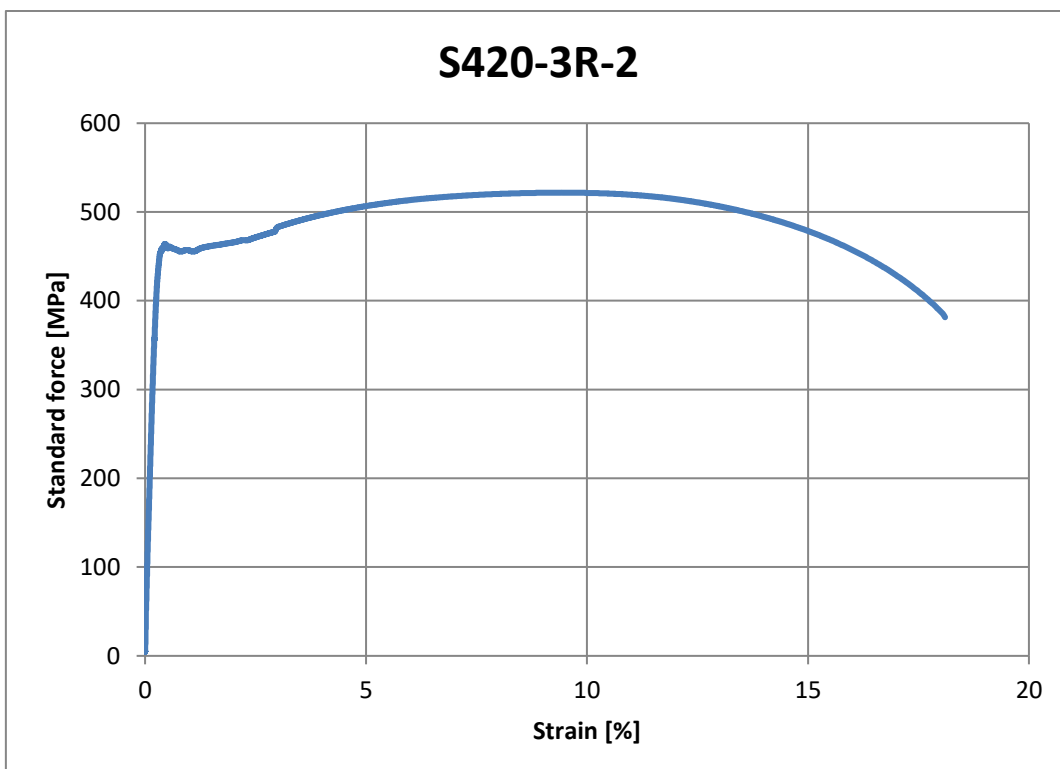
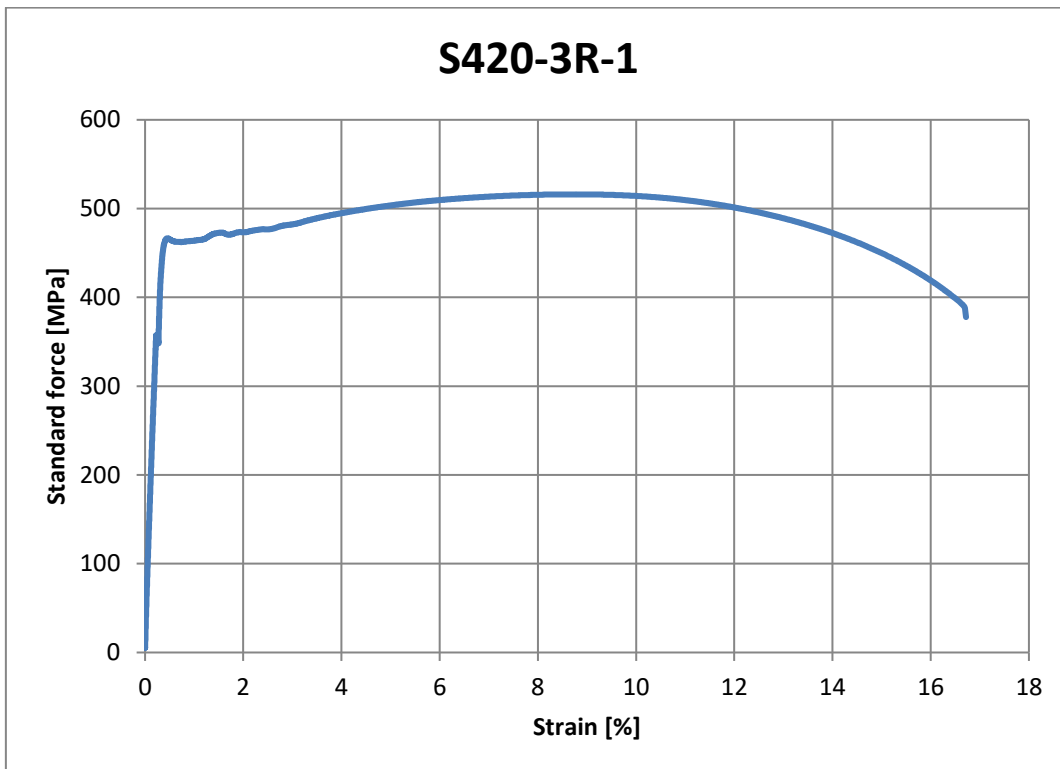


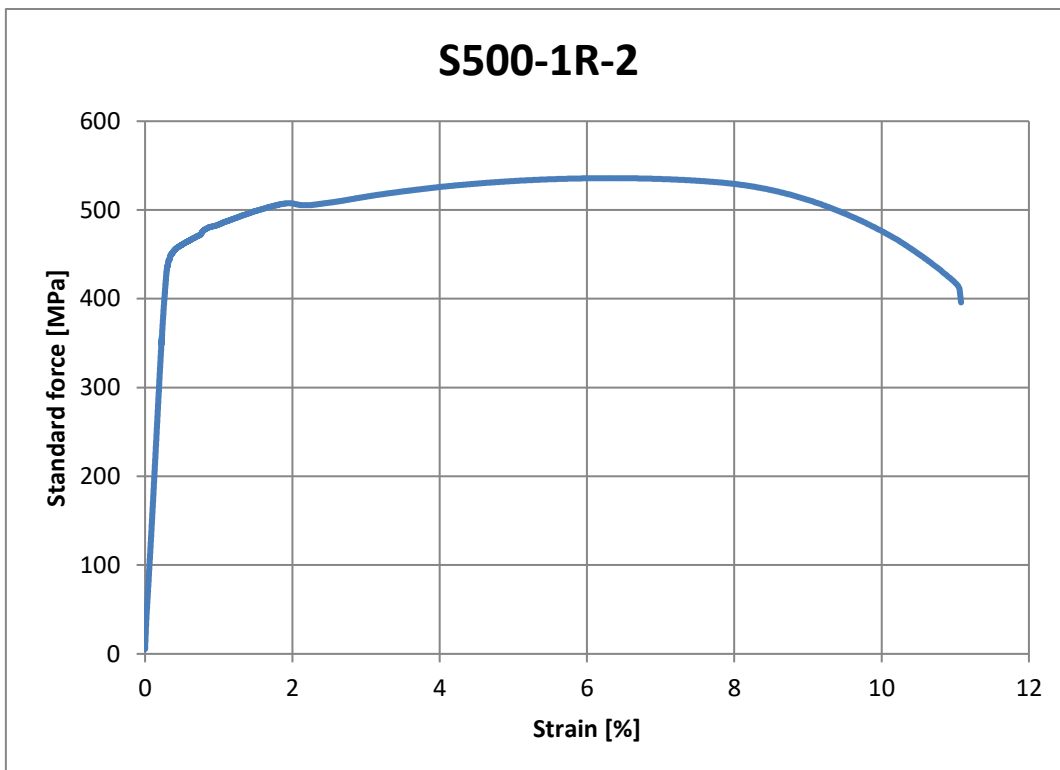
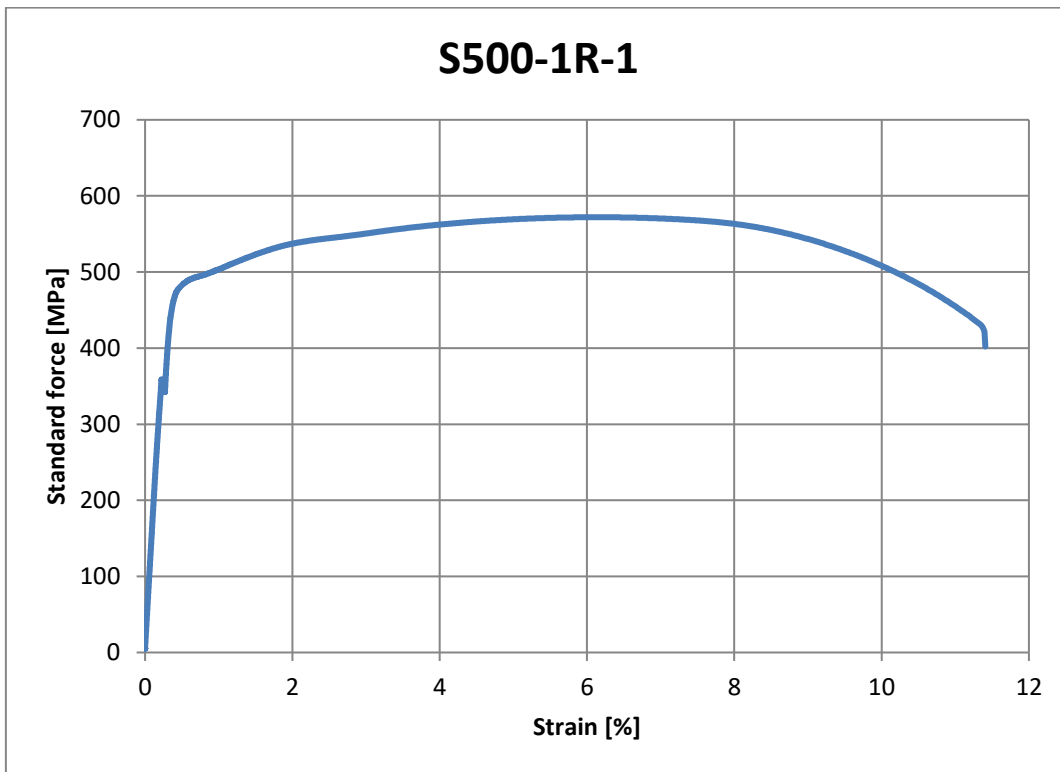


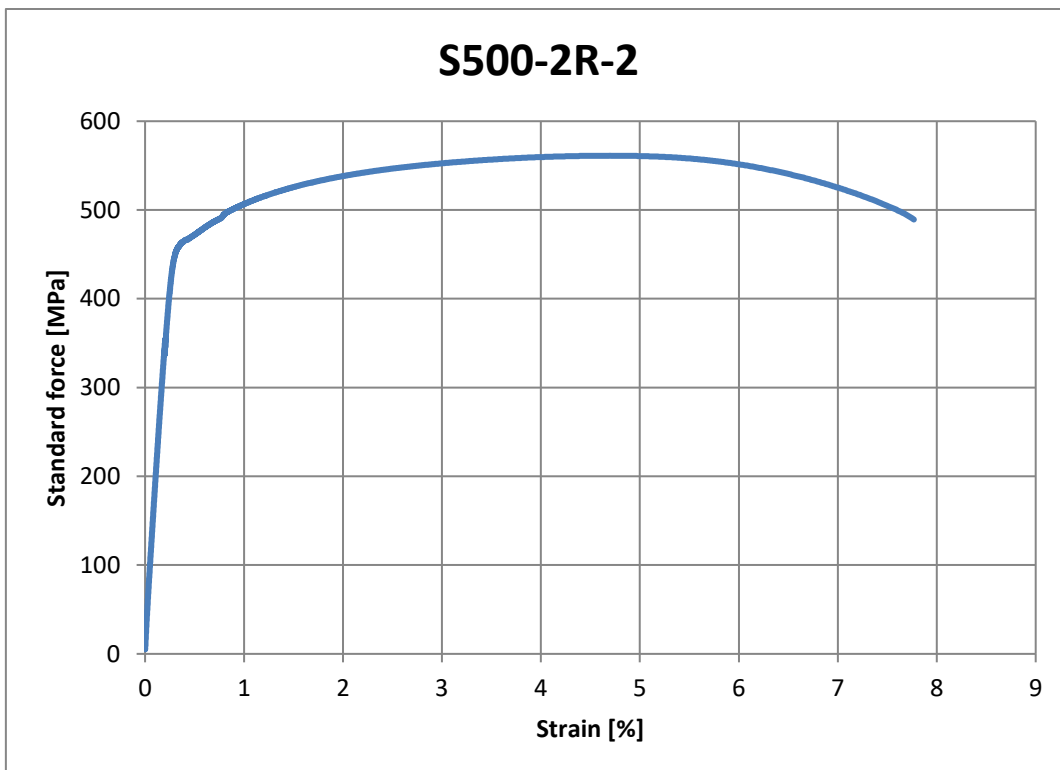
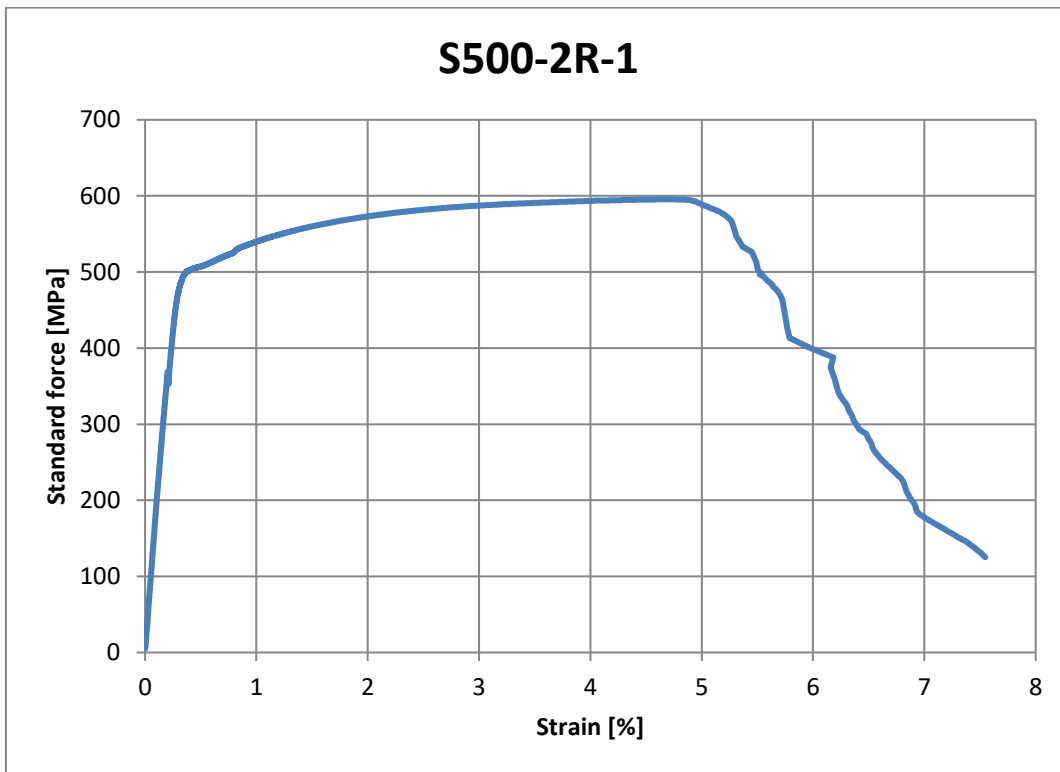
## TENSILE TEST GRAPHS

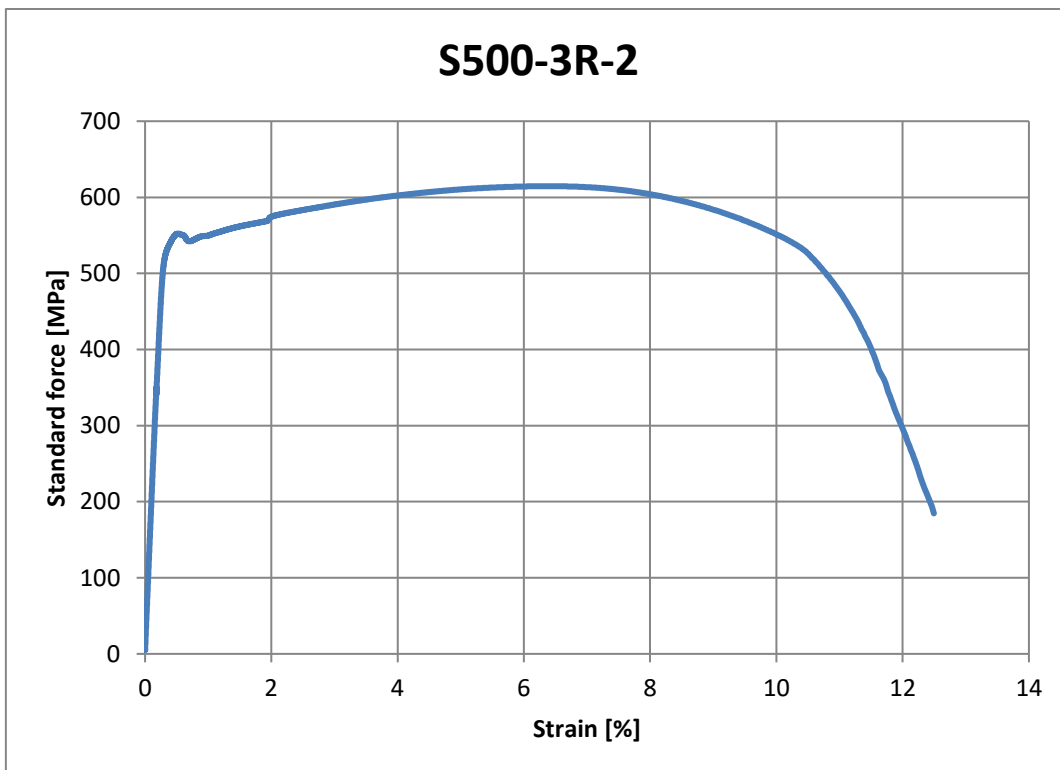
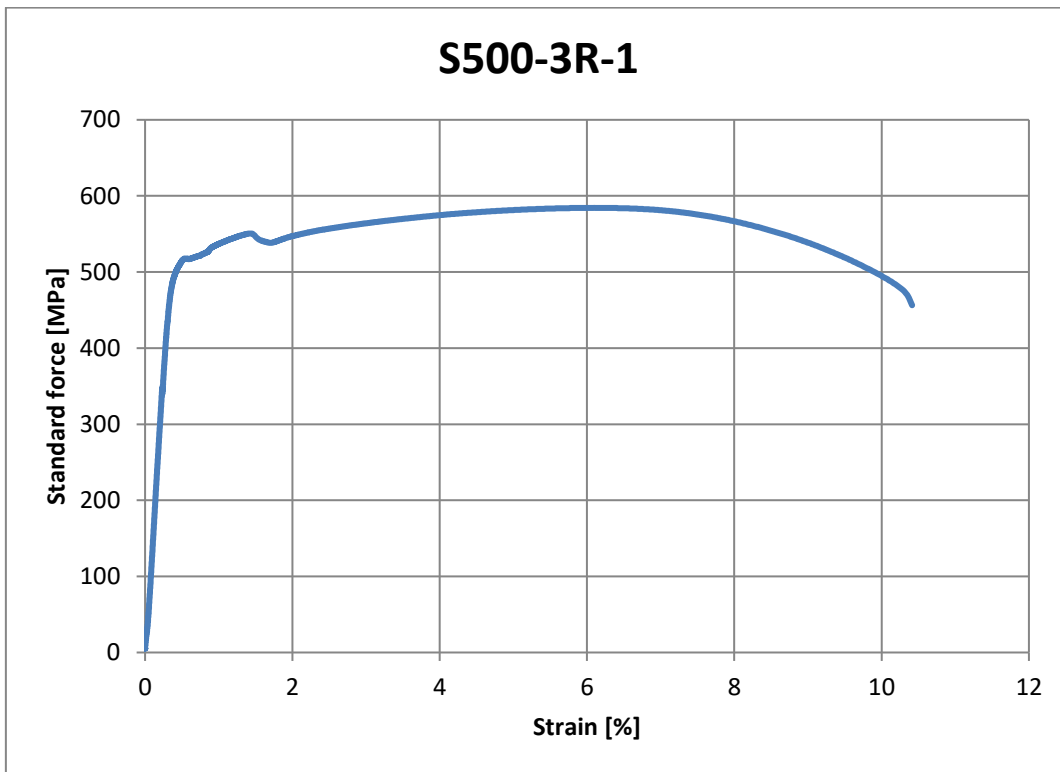




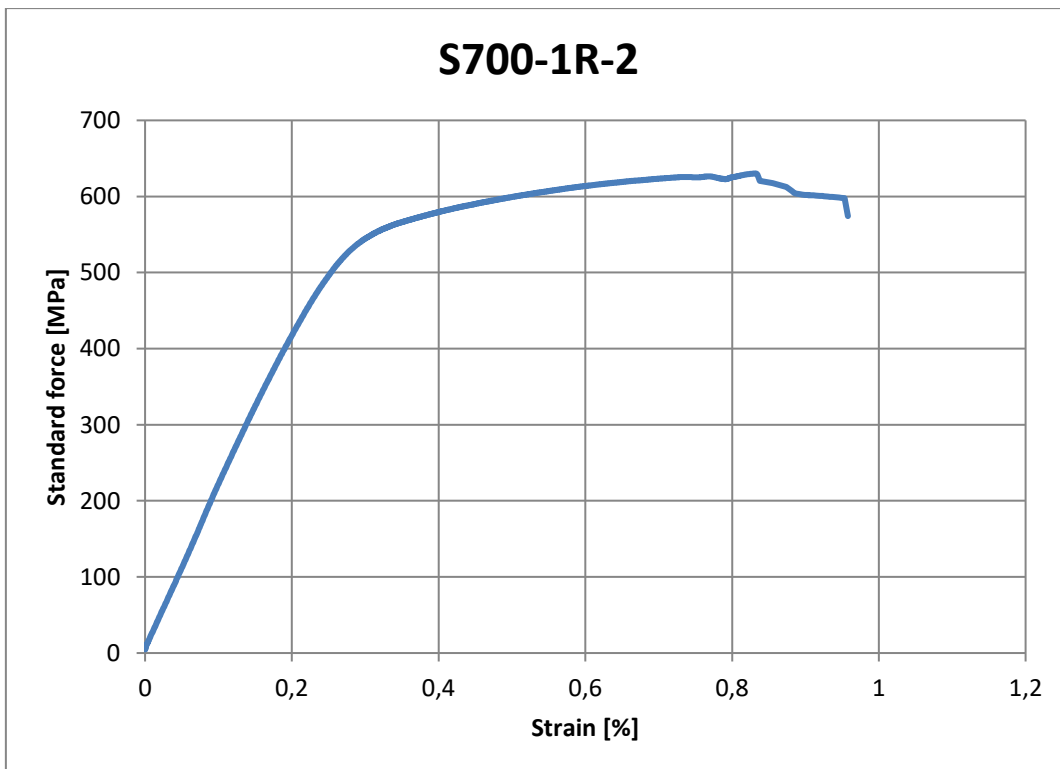
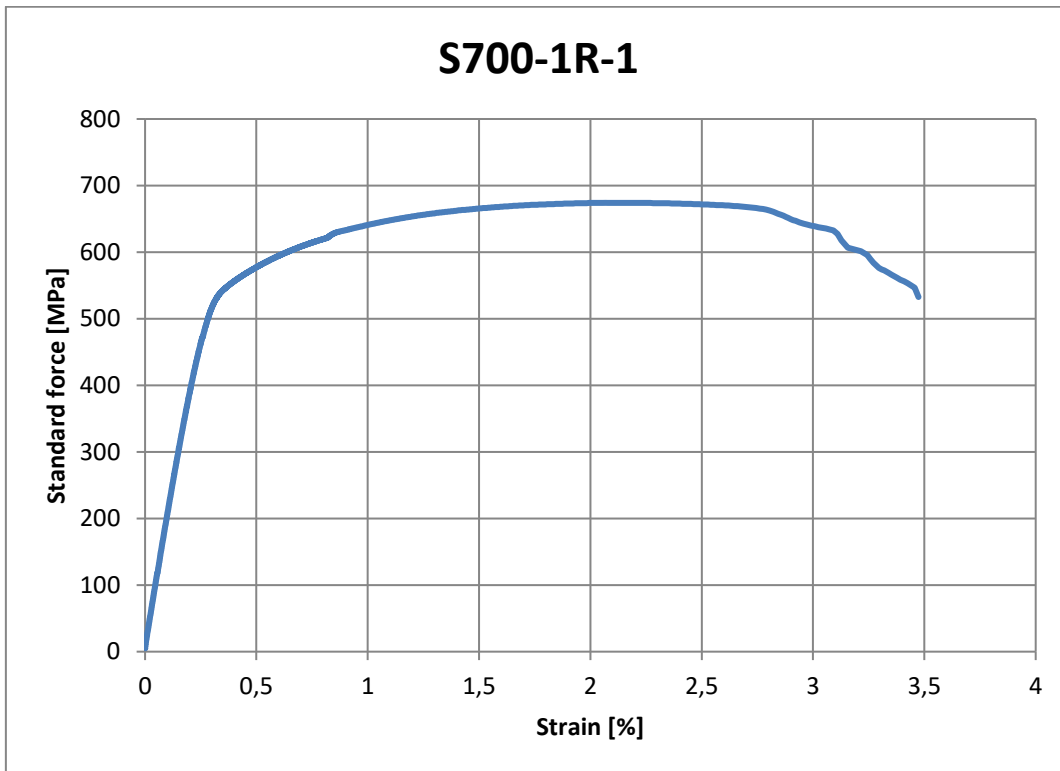


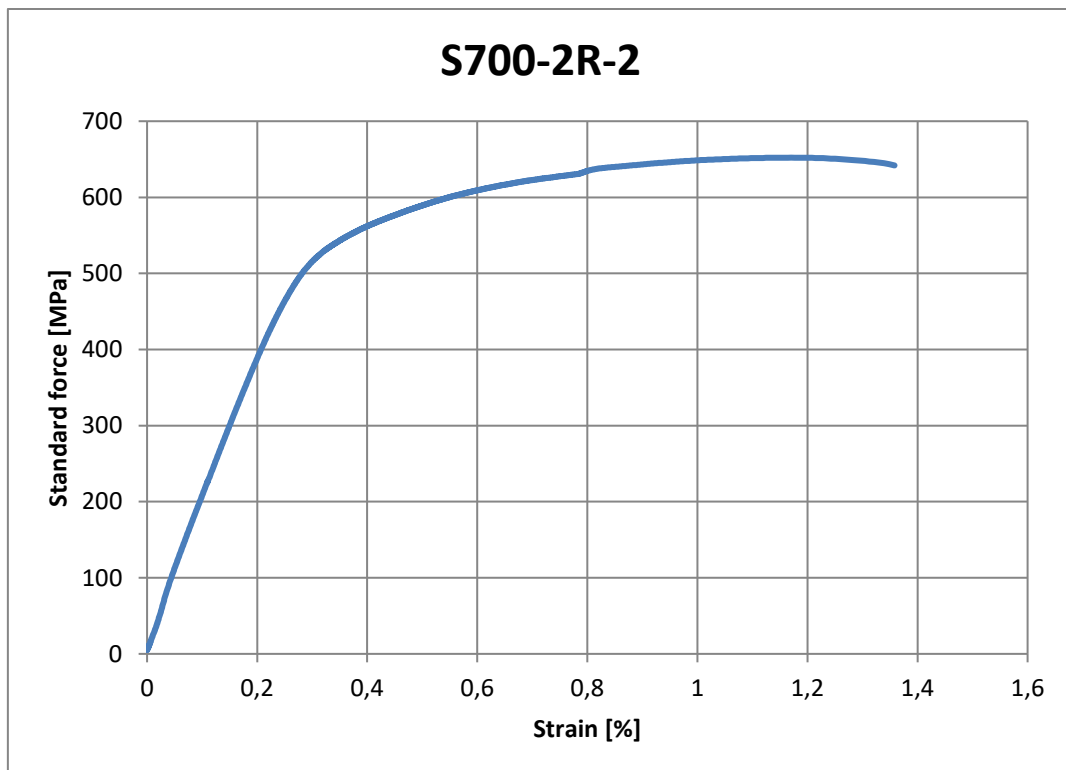
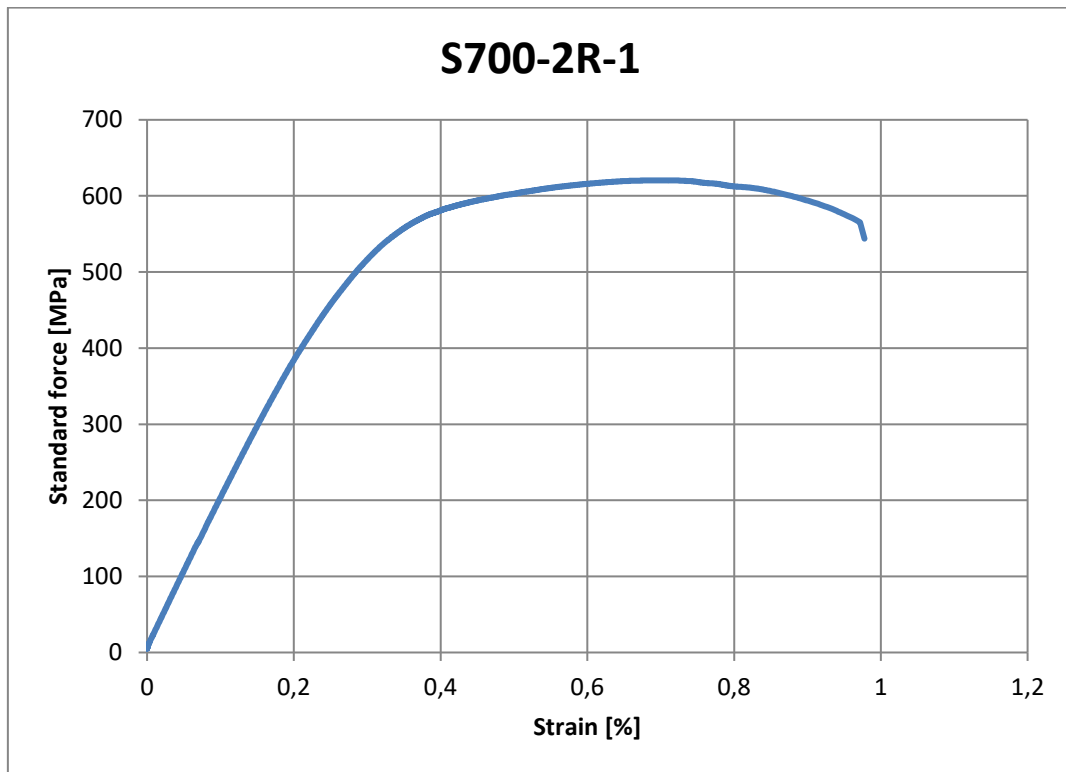


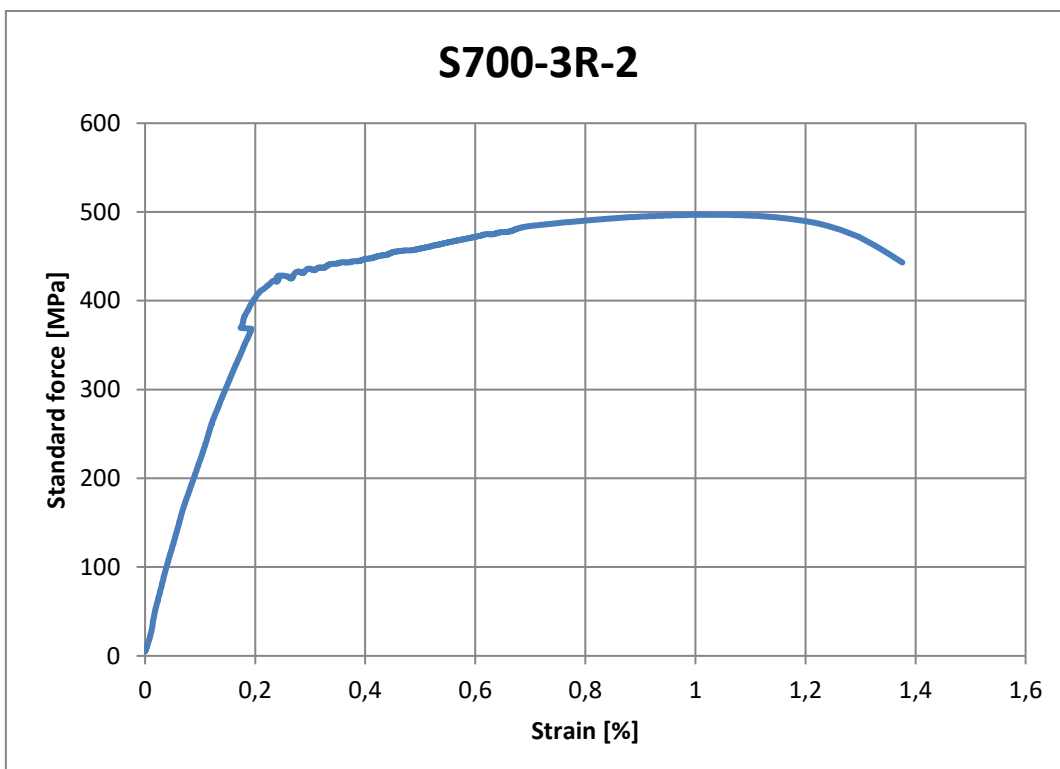
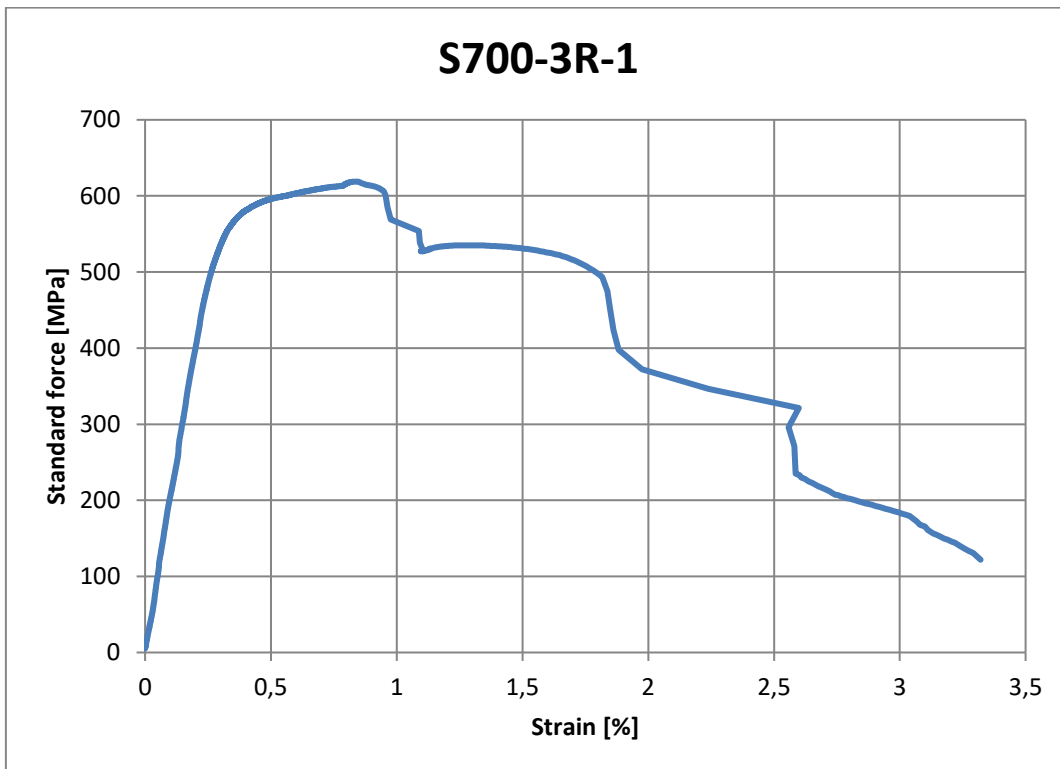


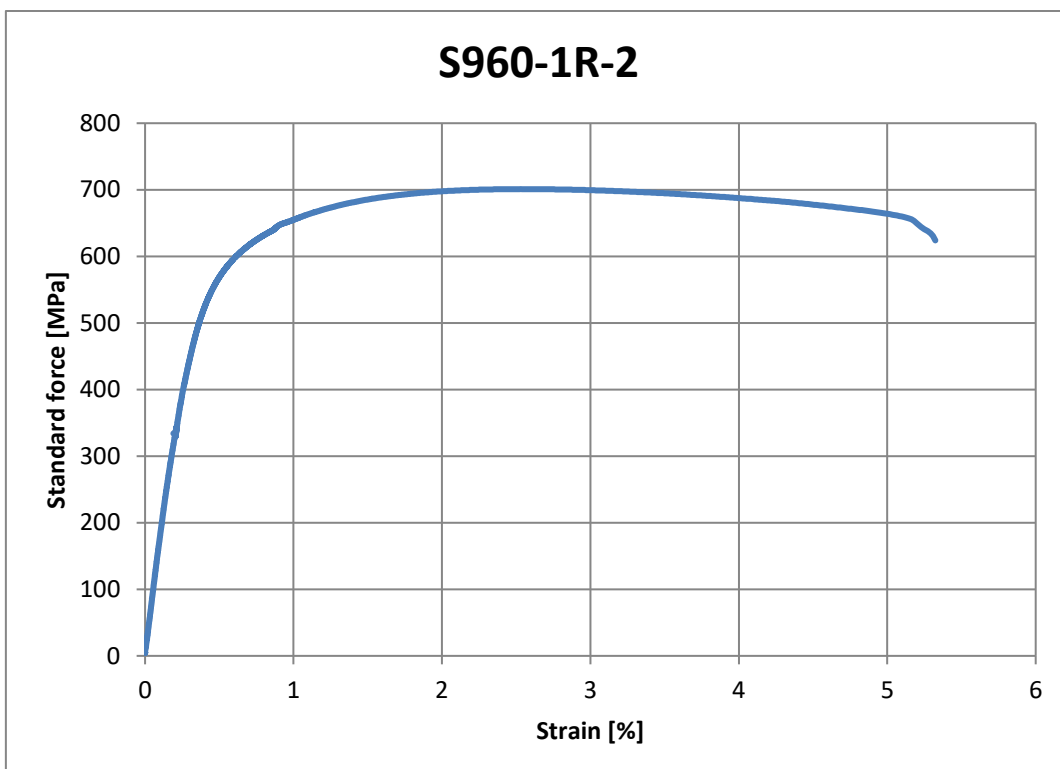
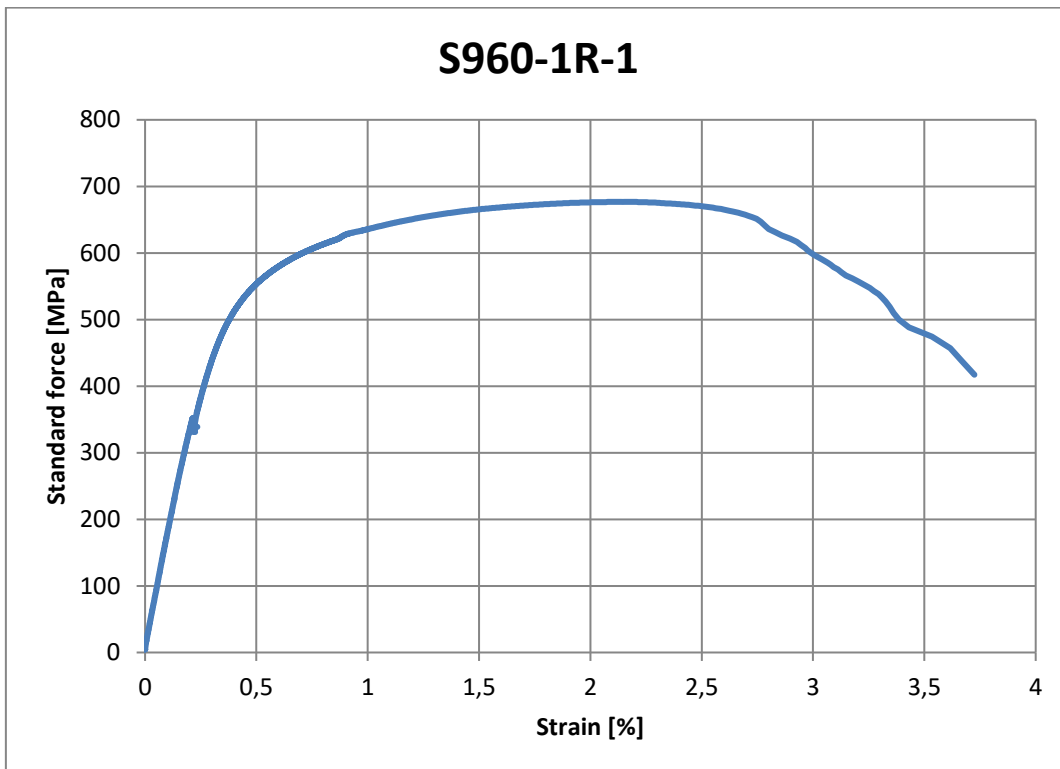


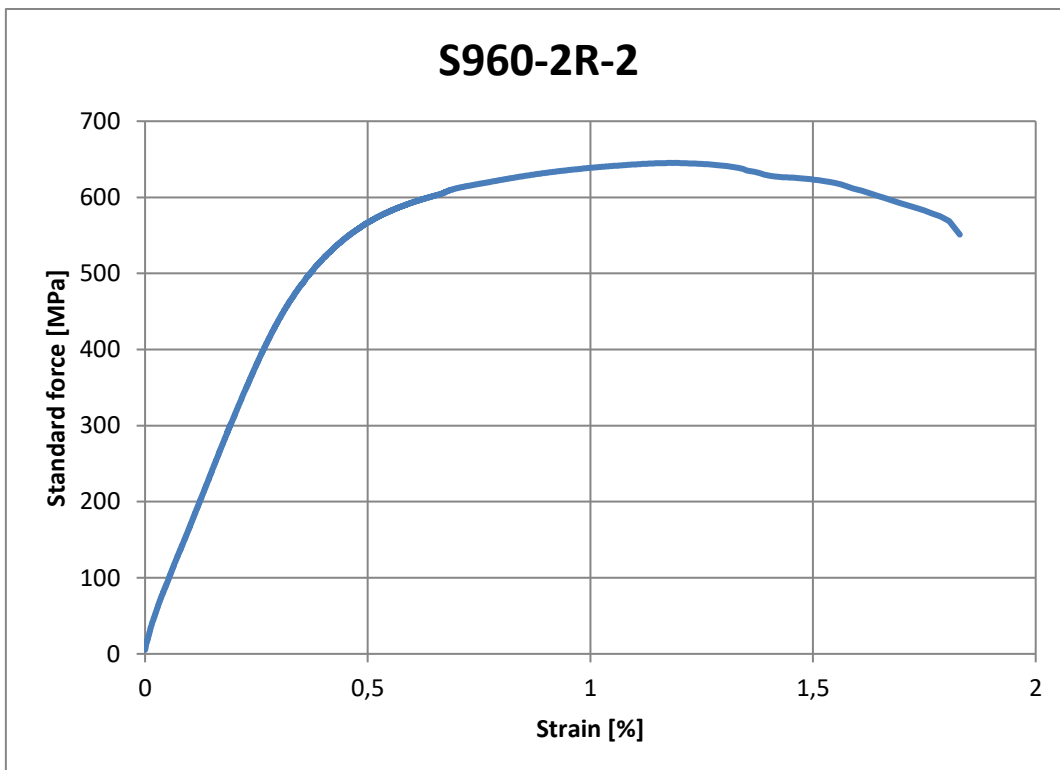
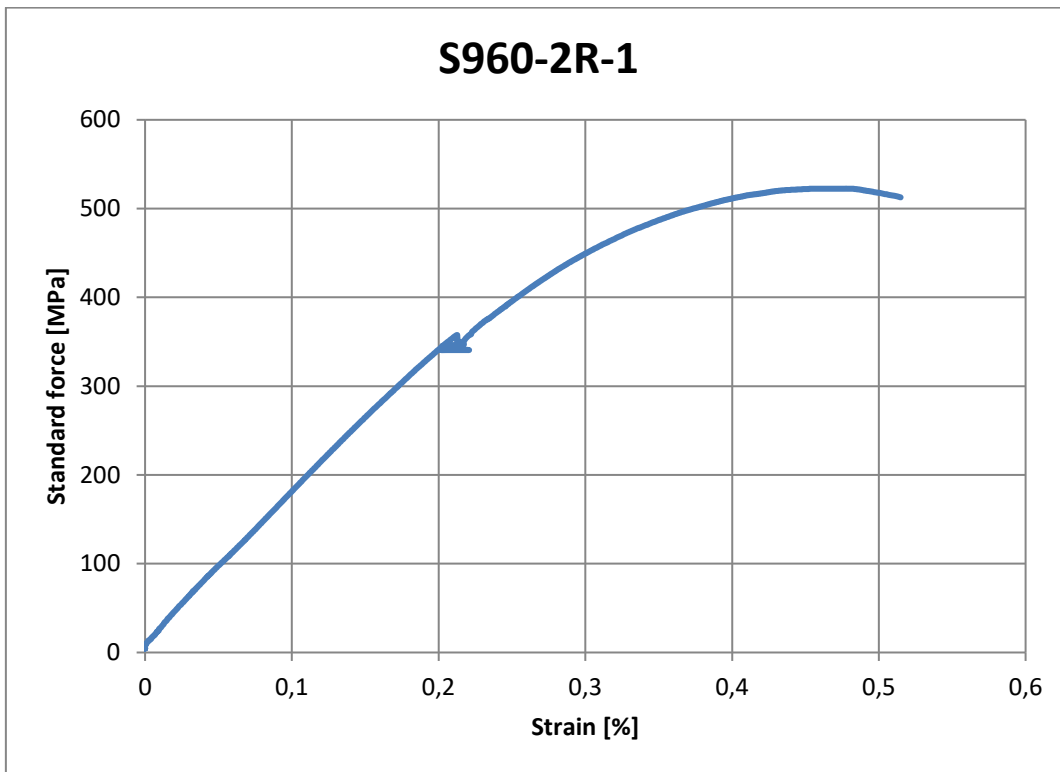


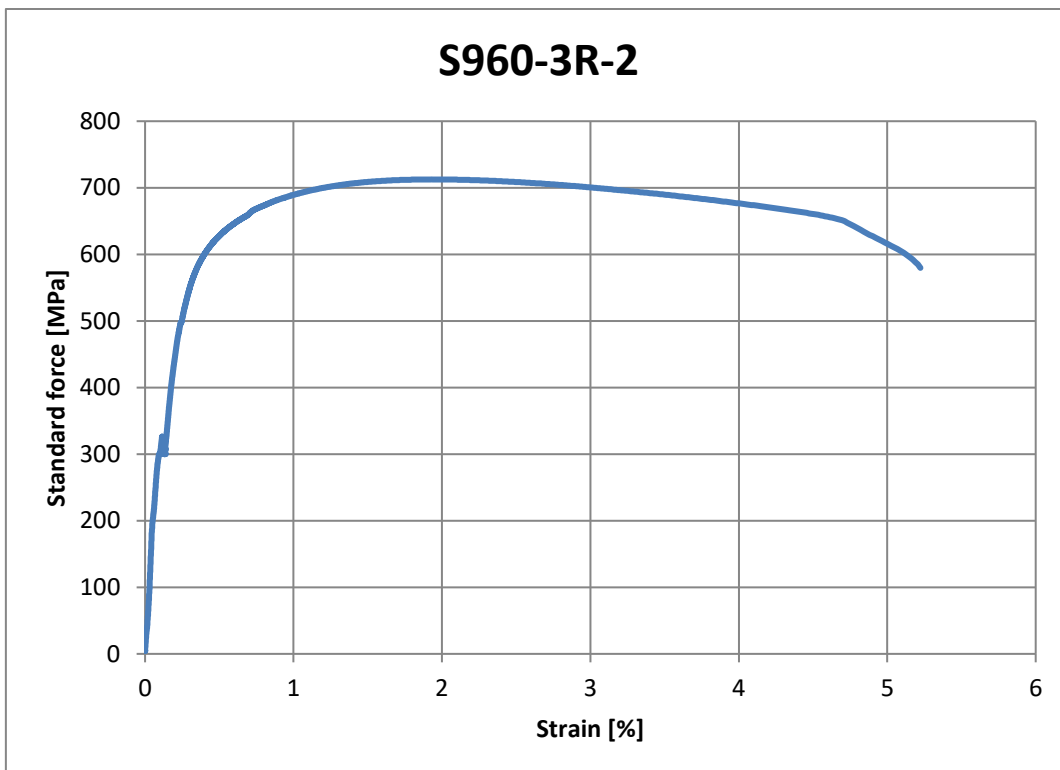
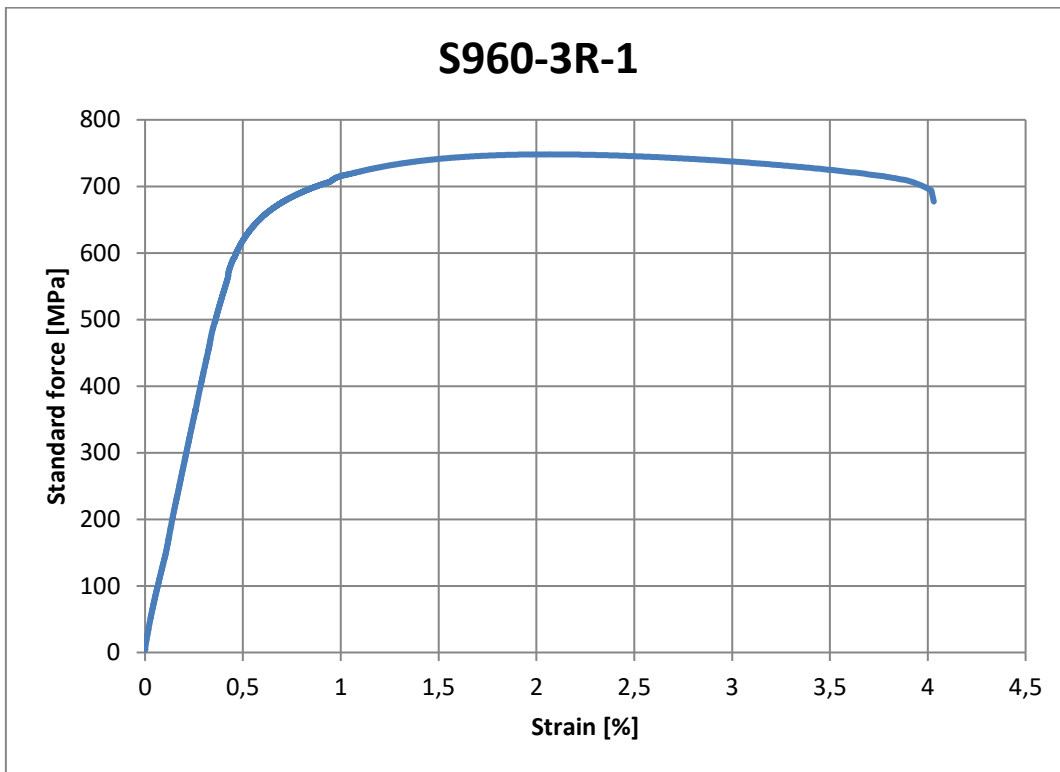












FAILURE MODES PHOTOGRAPHS



Figure 1. S420-1R-1 after the test



Figure 2. S420-1R-2 after the test



Figure 3. S420-2R-1 after the test



Figure 4. S420-2R-2 after the test



Figure 5. S420-3R-1 after the test



Figure 6. S420-3R-2 after the test



Figure 7. S500-1R-1 after the test



Figure 8. S500-1R-2 after the test



Figure 9. S500-2R-1 after the test



Figure 10. S500-2R-2 after the test



Figure 11. S500-3R-1 after the test



Figure 12. S500-3R-2 after the test





Figure 13. S700-1R-1 after the test



Figure 14. S700-1R-2 after the test



Figure 15. S700-2R-1 after the test

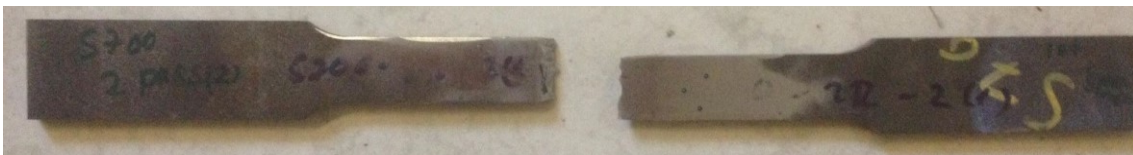


Figure 16. S700-2R-2 after the test



Figure 17. S700-3R-1 after the test



Figure 18. S700-3R-2 after the test



Figure 19. S960-1R-1 failure mode



Figure 20. S960-1R-2 failure mode

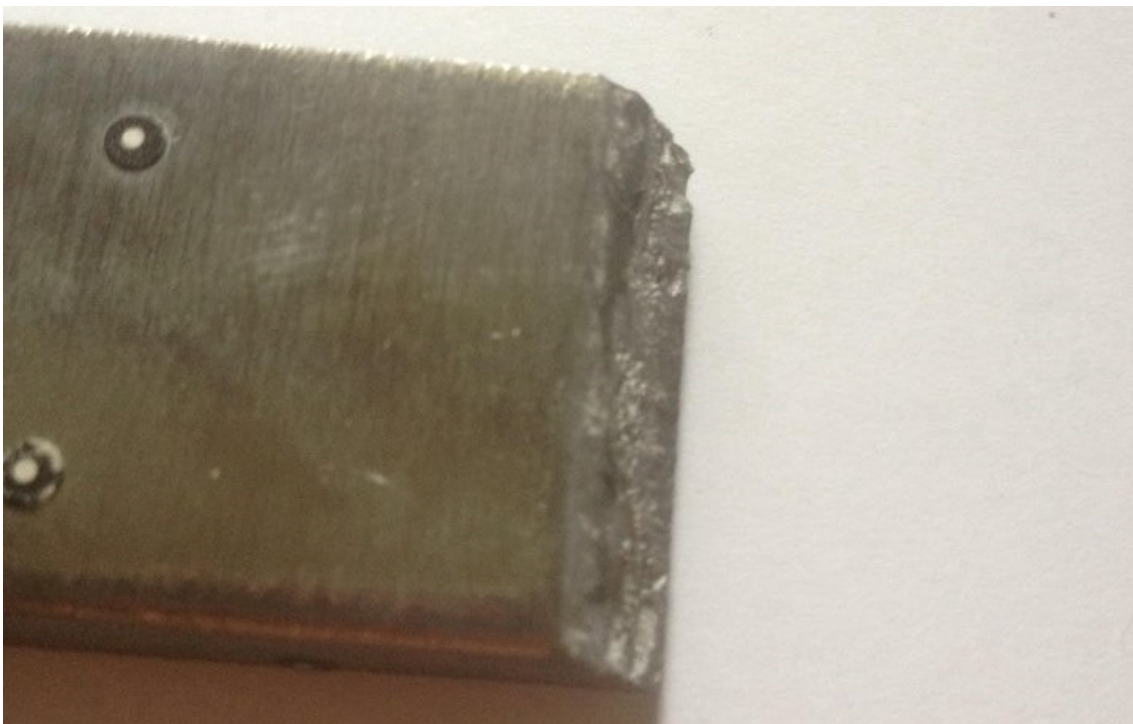


Figure 21. S960-2R-1 failure mode

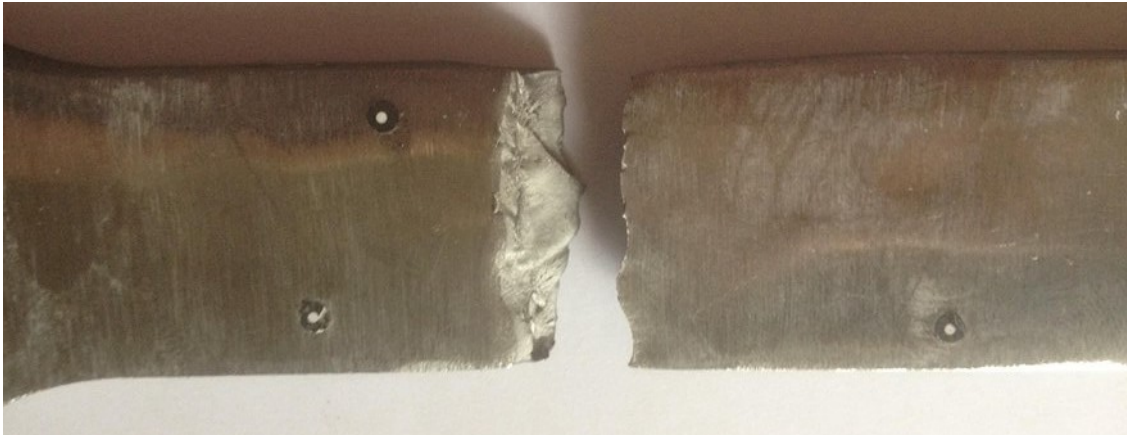


Figure 22. S960-2R-2 failure mode



Figure 23. S960-3R-1 failure mode



Figure 24. S960-3R-2 failure mode

